ISSN 2686-7575 (Online)

МИТХТ

ТОНКИЕ ХИМИЧЕСКИЕ ТЕХНОЛОГИИ

Fine Chemical Technologies

- Theoretical Bases of Chemical Technology
- Chemistry and Technology of Organic Substances
- Chemistry and Technology of Medicinal Compounds and Biologically Active Substances
- Synthesis and Processing of Polymers and Polymeric Composites
- Chemistry and Technology of Inorganic Materials
- Analytical Methods in Chemistry and Chemical Technology
- Mathematical Methods and Information Systems in Chemical Technology

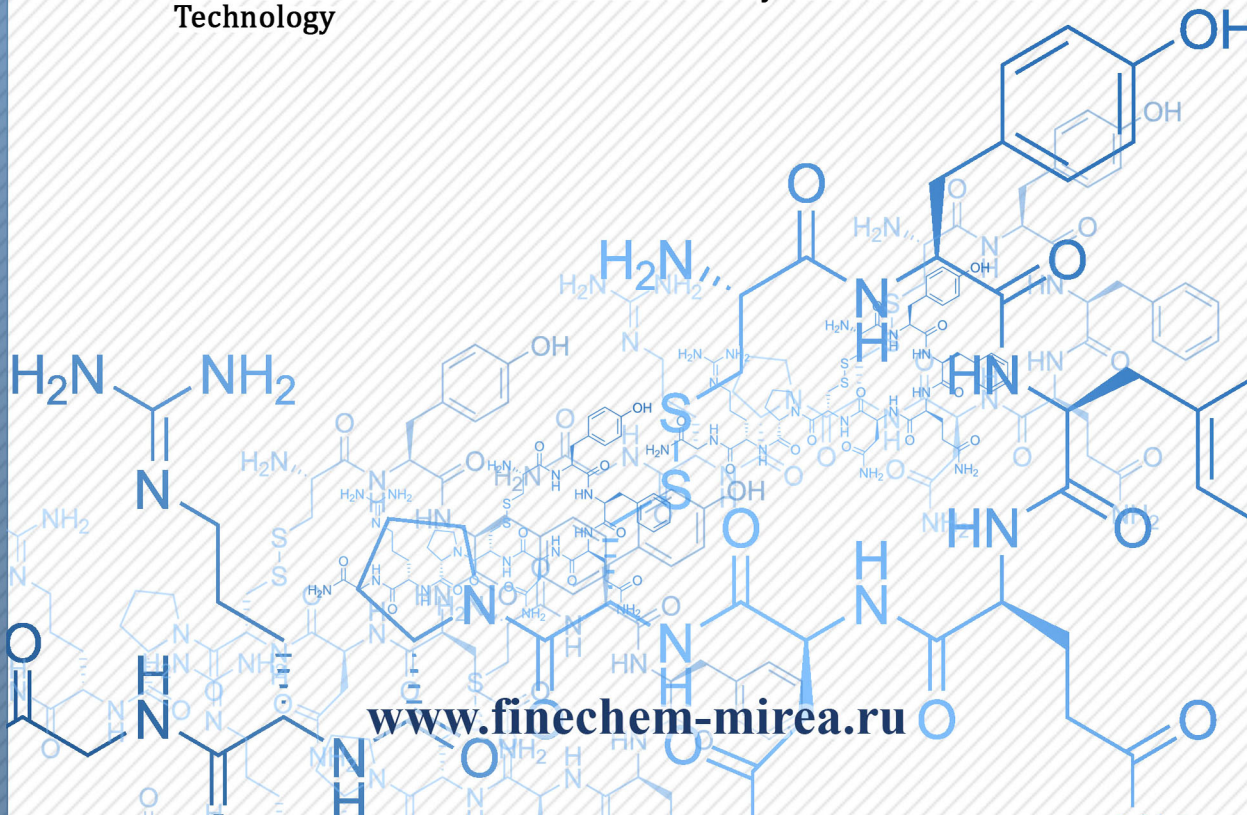

15(5)

2020

www.finechem-mirea.ru

ISSN 2686-7575 (Online)

ТОНКИЕ ХИМИЧЕСКИЕ ТЕХНОЛОГИИ

Fine Chemical Technologies

- Theoretical Bases of Chemical Technology
- Chemistry and Technology of Organic Substances
- Chemistry and Technology of Medicinal Compounds and Biologically Active Substances
- Synthesis and Processing of Polymers and Polymeric Composites
- Chemistry and Technology of Inorganic Materials
- Analytical Methods in Chemistry and Chemical Technology
- Mathematical Methods and Information Systems in Chemical Technology

Tonkie Khimicheskie Tekhnologii = Fine Chemical Technologies
Vol. 15, No. 5, 2020

Тонкие химические технологии = Fine Chemical Technologies
Том 15, № 5, 2020

https://doi.org/10.32362/2410-6593-2020-15-5
www.finechem-mirea.ru

https://doi.org/10.32362/2410-6593 ***www.finechem-mirea.ru***

Tonkie Khimicheskie Tekhnologii = Fine Chemical Technologies 2020, vol. 15, no. 5

The peer-reviewed scientific and technical journal Fine Chemical Technologies highlights the modern achievements of fundamental and applied research in the field of fine chemical technologies, including theoretical bases of chemical technology, chemistry and technology of medicinal compounds and biologically active substances, organic substances and inorganic materials, synthesis and processing of polymers and polymeric composites, analytical and mathematical methods and information systems in chemistry and chemical technology.

Founder and Publisher

Federal State Budget
Educational Institution
of Higher Education
"MIREA – Russian Technological University"
78, Vernadskogo pr., Moscow, 119454, Russian Federation.

Six issues a year are published.
The journal was founded in 2006. The name was Vestnik MITHT until 2015 (ISSN 1819-1487).

The journal is included into the List of peer-reviewed science press of the State Commission for Academic Degrees and Titles of the Russian Federation.
The journal is indexed:
DOAJ, Chemical Abstracts, Science Index, RSCI, Ulrich's International Periodicals Directory

86, Vernadskogo pr., Moscow, 119571, Russian Federation.
Phone: +7(495) 246-05-55 (#2-88)
E-mail: *seredina@mirea.ru*

Registration Certificate ПИ № ФС 77–74580, issued on December 14, 2018 by the Federal Service for Supervision of Communications, Information Technology, and Mass Media of Russia

The subscription index of *Pressa Rossii*: **36924**

Тонкие химические технологии = Fine Chemical Technologies 2020, том 15, № 5

Научно-технический рецензируемый журнал «Тонкие химические технологии» освещает современные достижения фундаментальных и прикладных исследований в области тонких химических технологий, включая теоретические основы химической технологии, химию и технологию лекарственных препаратов и биологически активных соединений, органических веществ и неорганических материалов, синтез и переработку полимеров и композитов на их основе, аналитические и математические методы и информационные системы в химии и химической технологии.

Учредитель и издатель

федеральное государственное бюджетное
образовательное учреждение
высшего образования
«МИРЭА – Российский технологический университет»
119454, РФ, Москва, пр-кт Вернадского, д. 78.

Периодичность: 6 раз в год.
Журнал основан в 2006 году. До 2015 года издавался под названием «Вестник МИТХТ» (ISSN 1819-1487).

Журнал входит в Перечень ведущих рецензируемых научных журналов ВАК РФ.
Индексируется:
DOAJ, Chemical Abstracts, РИНЦ (Science Index), RSCI, Ulrich's International Periodicals Directory

119571, Москва, пр. Вернадского, 86, оф. Л-119.
Тел.: +7(495) 246-05-55 (#2-88)
E-mail: *seredina@mirea.ru*

Свидетельство о регистрации СМИ: ПИ № ФС 77-74580 от 14.12.2018 г. выдано Федеральной службой по надзору в сфере связи, информационных технологий и массовых коммуникаций (Роскомнадзор)

Индекс по Объединенному каталогу «Пресса России»: **36924**

ТОНКИЕ ХИМИЧЕСКИЕ ТЕХНОЛОГИИ
Fine Chemical Technologies
15(5)
2020

CONTENTS

СОДЕРЖАНИЕ

Theoretical Bases of Chemical Technology

Nosov G.A., Uvarov M.E.
Contact crystallization of substances from solutions using evaporating refrigerants **7**

Chemistry and Technology of Organic Substances

Musin A.I. , Borisova Yu.G., Raskil'dina G.Z., Rabaev R.U., Daminev R.R., Zlotskii S.S.
Synthesis and reactions of alkenyl-*gem*-dichlorocyclopropanes obtained from piperylene **16**

Chemistry and Technology of Medicinal Compounds and Biologically Active Substances

Kuzmin I.S., Yuriev D.Yu., Toporkov G.A., Kalistratova A.V., Kovalenko L.V.
Synthesis and biological activity of *N*-phosphonacetyl-L-aspartate's structural analogs *N*-(α-dietoxyphosphorylcyclopropylcarbonyl)amino acids **26**

Теоретические основы химической технологии

Носов Г.А., Уваров М.Е.
Контактная кристаллизация веществ из растворов с применением испаряющегося хладагента **7**

Химия и технология органических соединений

Мусин А.И., Борисова Ю.Г., Раскильдина Г.З., Рабаев Р.У., Даминев Р.Р., Злотский С.С.
Синтез и реакции алкенил-*гем*-дихлорциклопропанов на основе пиперилена **16**

Химия и технология лекарственных препаратов и биологически активных соединений

Кузьмин И.С., Юрьев Д.Ю., Топорков Г.А., Калистратова А.В., Коваленко Л.В.
Синтез и биологическая активность *N*-(α-диэтоксифосфорилциклопропилкарбонил)аминокислот – структурных аналогов *N*-фосфонацетил-L-аспартата **26**

Romanova N.A., Budanova U.A., Sebyakin Yu.L.
Cationic amphiphiles based on malonic acid amides as transfection mediators **36**

Романова Н.А., Буданова У.А., Себякин Ю.Л.
Катионные амфифилы на основе амидов малоновой кислоты в качестве медиаторов трансфекции

Synthesis and Processing of Polymers and Polymeric Composites

Синтез и переработка полимеров и композитов на их основе

Khachaturov A.A., Potapov E.E., Reznichenko S.V., Kovaleva A.N.
Influence of iron ore concentrate (magnetite) on the kinetics of butadiene–styrene rubber-based blend curing in the presence of different accelerators **46**

Хачатуров А.А., Потапов Е.Э., Резниченко С.В., Ковалева А.Н.
Влияние железорудного концентрата (магнетита) на кинетику вулканизации резиновых смесей на основе бутадиен-стирольного каучука в присутствии различных ускорителей

Chemistry and Technology of Inorganic Materials

Химия и технология неорганических материалов

Get'man E.I., Oleksii Yu.A., Radio S.V., Ardanova L.I.
Determining the phase stability of luminescent materials based on the solid solutions of oxyorthosilicates $(Lu_{1-x}Ln_x)[(SiO_4)_{0.5}O_{0.5}]$, where Ln = La–Yb **54**

Get'man E.I., Oleksii Yu.A., Radio S.V., Ardanova L.I.
Determining the phase stability of luminescent materials based on the solid solutions of oxyorthosilicates $(Lu_{1-x}Ln_x)[(SiO_4)_{0.5}O_{0.5}]$, where Ln = La–Yb

THEORETICAL BASES OF CHEMICAL TECHNOLOGY

ТЕОРЕТИЧЕСКИЕ ОСНОВЫ ХИМИЧЕСКОЙ ТЕХНОЛОГИИ

ISSN 2686-7575 (Online)

https://doi.org/10.32362/2410-6593-2020-15-5-7-15

UDC 66.065.5:621.577

RESEARCH ARTICLE

Contact crystallization of substances from solutions using evaporating refrigerants

Gennadi A. Nosov, Mikhail E. Uvarov[@]

MIREA – Russian Technological University (M.V. Lomonosov Institute of Fine Chemical Technologies), Moscow, 119571 Russia

[@]*Corresponding author, e-mail: uvamikhail@yandex.ru*

Objectives. *The aim of this study was to analyze the possibility of using contact crystallization with evaporating refrigerants for the isolation of substances from their aqueous solutions using salts [KNO_3, NaI, and $(NH_2)_2CO$] as extraction examples and sucrose. Isobutane was used as a refrigerant.*

Methods. *The analysis of the influence of the main technological parameters (i.e., solution's cooling temperature, initial concentration, and compressed refrigerant vapor pressure) on the separation process and identification of its regularities was performed using mathematical dependencies previously developed by N.I. Gelperin and G.A. Nosov for each stage of the contact crystallization process. The authors studied the influence of these parameters on the yield of crystalline and liquid phases, refrigerant consumption, and compressor power.*

Results. *The study showed that the use of evaporating refrigerants can significantly intensify the process of separating the mixture and spent refrigerant from the resulting crystalline suspension. This occurs owing to the evaporation of the liquid refrigerant that is in contact with the solution, which is accompanied by intense cooling. This process can be carried out at the temperature difference between the refrigerant and crystallizing mixture in the range of 0.5–1.0°C.*

Conclusions. *Contact crystallization with evaporating refrigerants can be successfully applied to separate various substances from aqueous solutions. An important advantage of this process is the relatively low refrigerant consumption because heat removal from the solution is carried out as a result of changes in the aggregate state of the refrigerant. The use of contact crystallization can also considerably simplify the equipment.*

Keywords: *crystallization, contact cooling, evaporating refrigerants, aqueous solutions*

For citation: Nosov G.A., Uvarov M.E. Contact crystallization of substances from solutions using evaporating refrigerants. *Tonk. Khim. Tekhnol. = Fine Chem. Technol.* 2020;15(5):7-15 (Russ., Eng.). https://doi.org/10.32362/2410-6593-2020-15-5-7-15

НАУЧНАЯ СТАТЬЯ

Контактная кристаллизация веществ из растворов с применением испаряющегося хладагента

Г.А. Носов, М.Е. Уваров[@]

МИРЭА – Российский технологический университет (Институт тонких химических технологий им. М.В. Ломоносова), Москва, 119571 Россия
[@]*Автор для переписки, e-mail: uvamikhail@yandex.ru*

Цели. *Статья анализирует возможность применения контактной кристаллизации с использованием испаряющихся хладагентов для выделения веществ из их водных растворов на примере извлечения некоторых солей (KNO_3, NaI, $(NH_2)_2CO$) и сахарозы. В качестве хладагента использован изобутан.*
Методы. *Изучение влияния основных технологических параметров – температуры охлаждения раствора, его исходной концентрации и давления сжатых паров хладагента – на ход рассматриваемого процесса разделения, а также выявление закономерностей его протекания проводилось с помощью выведенных ранее Н.И. Гельперином и Г.А. Носовым математических зависимостей для каждой стадии процесса контактной кристаллизации. Авторы исследовали влияние указанных параметров на выход кристаллической и жидкой фаз, расход хладагента и мощность компрессора.*
Результаты. *Установлено, что применение испаряющихся хладагентов позволяет существенно интенсифицировать процесс кристаллизации и облегчает отделение отработанного хладагента от образующейся кристаллической суспензии. Это обусловлено тем, что при контакте жидкого хладагента с раствором происходит его испарение, которое сопровождается интенсивным охлаждением раствора. Установлено, что такой процесс может осуществляться при разности температур хладагента и кристаллизующейся смеси порядка 0.5–1.0 °C.*
Выводы. *Контактная кристаллизация с использованием испаряющихся хладагентов может быть успешно применена для выделения различных веществ из водных растворов. Важным преимуществом проведения подобного процесса является относительно небольшой расход хладагента, поскольку отвод теплоты из раствора осуществляется в результате изменения агрегатного состояния хладагента. Использование контактной кристаллизации позволяет также значительно упростить аппаратурное оформление процесса.*

Ключевые слова: *кристаллизация, контактное охлаждение, испаряющиеся хладагенты, водные растворы*

Для цитирования: Носов Г.А., Уваров М.Е. Контактная кристаллизация веществ из растворов с применением хладагента. *Тонкие химические технологии.* 2020;15(5):7-15. https://doi.org/10.32362/2410-6593-2020-15-5-7-15

INTRODUCTION

It is known that crystallization process is widely used to isolate substances from various solutions, purify substances from impurities by their recrystallization, and concentrate dilute solutions by freezing solvents [1–4]. The application of this process is not limited to the chemical industry. Crystallization is also used with great success in the food, pharmaceutical, petrochemical, and construction industry, and also in the production of radio electronics [5–13]. In most cases, this process is performed by cooling the solutions and melts. Evaporation, vacuum evaporation crystallization, and crystallization with salting-out agents are less commonly used.

In the case of crystallization by cooling, devices equipped with various cooling elements (e.g., jackets, coils, tubes, and hollow disks) are usually used. Heat removal from the crystallizing substance occurs

through the heat transfer walls of the above-mentioned devices [14]. Crystallization process is sometimes carried out by the direct contact of solutions with refrigerants [2, 4, 15, 16].

One of the significant advantages of the latter process is the absence of heat transfer surfaces to remove heat flux. This greatly simplifies the design of the apparatus and also removes the issue of encrustation. The possibility of achieving a more extended interphase surface, in contrast to the conventional contactless method of fractional crystallization, should be also attributed to the advantages of this process. Mixing of mass flows in a contact crystallizer is usually quite intensive. Carrying out the crystallization in this manner allows the process to occur at a relatively low-temperature difference between the incoming and crystallizing mixture refrigerant (approximately 0.5–2.0°C). This makes it possible not to be limited to expensive steel when choosing structural materials for crystallizers and to manufacture such devices from materials with low thermal conductivity (e.g., polymers, glass, and ceramics). In general, all of these advantages lower capital expenditures and operating costs.

When choosing a contact crystallization method, one should take into account the possibility of contamination of the target product with a refrigerant, which is a significant disadvantage of this process [2, 4]. Considering this, the stage of separating the spent refrigerant from the crystalline phase is necessary for this process.

It should be noted that various types of refrigerants can be used in the process of contact crystallization, differing from each other in thermophysical properties and state of aggregation. Chilled liquids, liquefied and nonliquefied gases can be used. The refrigerants entering the crystallizer upon contact with the crystallizing mixture pass into a gaseous state (evaporate) [2]. Contact crystallization can also be carried out by mixing the initial mixture (solution) with a highly supercooled solvent [17].

The contact crystallization process can occur both in continuous and dispersed phases. [2, 4, 16]. In this case, liquid refrigerants that do not mix with the original solution are used. The dispersion of cooled solution in the form of drops in the mass flow of the refrigerant forms a dispersed phase. When the refrigerant is dispersed in the crystallizing solution, the phase becomes continuous. Depending on the task that contact crystallization process needs to solve, it can be implemented in a batch or continuous mode. When choosing the contact crystallization method, it should be taken into account that with a small difference in the densities of the refrigerant, mother liquor, and crystalline phase, difficulties often arise in separating the resulting suspension, which can lead to contamination of the separation products with a refrigerant.

The use of gaseous refrigerants greatly facilitates their separation from suspensions. However, currently, they are rarely used in the industry because of their high consumption due to their low heat capacity.

The prospect of the industrial application of evaporating refrigerants in crystallization processes continues to be relevant. On one hand, they can significantly intensify the crystallization process because a significant amount of heat is absorbed during their evaporation, and on the other hand, there are no problems in separating the resulting refrigerant vapor from the suspension. Currently, this crystallization process is used mainly for desalination of water by freezing and concentrating dilute aqueous solutions [2, 5, 16]. This article presents the results of studies on contact crystallization concerning the isolation of potassium nitrate, carbamide, sodium iodide, and sucrose from their aqueous solutions.

DESCRIPTION OF THE CRYSTALLIZATION PROCESS INSTALLATION

A schematic diagram of the contact crystallization unit is shown in Fig. 1. Here the crystallizer Cryst (crystallization stage) continuously receives the initial solution in the amount F with the concentration of the dissolved substance x_F at the temperature t_F, which gradually cools down to the temperature t_{fr} below the point of its saturation. As a result, a crystalline phase of the target product is formed in solution. Liquid refrigerant, which is supplied to the crystallizer in the amount of G_R, is in contact with the cooled solution. This leads to gradual evaporation of the refrigerant, followed by cooling of the solution in the crystallizer. The suspension formed in the crystallizer consists of the crystalline phase C of the composition x_C and the mother liquor M of the composition x_M. Further, the C+M suspension is sent to Sep filtration (separation stage), where the crystalline phase is extracted in the amount of S from the mother liquor L. Of note, the suspension can be separated both by filtration and centrifugation [18].

In the process under consideration, a vapor compression refrigeration unit is used, in the circuit of which the G_R refrigerant circulates. In this case, crystallizer Cryst, which is continuously supplied with liquid refrigerant, is the evaporator of the refrigeration unit. The vapors of the G_R refrigerant, which are in a saturated state, are removed from the crystallizer and then they enter the Com compressor to compress them from pressure p_1 to pressure p_2. In this case, the temperature of the compressible vapors increases from Θ_1 to Θ_2, and the heat content

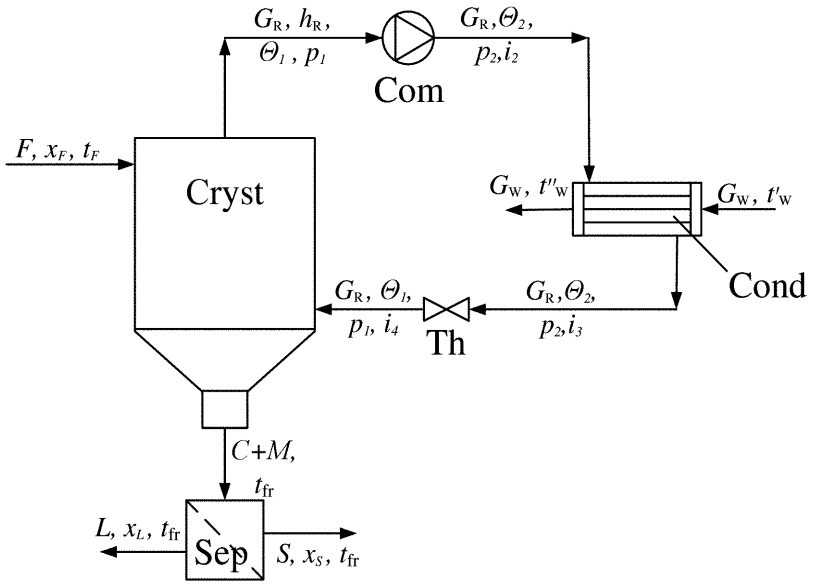

Fig. 1. Schematic diagram of contact crystallization with an evaporating refrigerant for the extraction of substances from aqueous solutions.

increases from i_1 to i_2. The change in the parameters of the refrigerant in the pressure–enthalpy diagram is shown in Fig. 2. In this diagram, the arrow *1–2* corresponds to the process of compressing the refrigerant by the compressor from pressure p_1 to p_2. Then, the compressed vapor of the G_R refrigerant enters the condenser of the Cond refrigeration unit, where it is cooled by the G_W water stream. In this case, the heat content of the refrigerant decreases from i_2 to i_3 (arrow *2–3*). A conventional shell and tube heat exchanger can be used as a condenser. Before supplying refrigerant to the crystallizer, it is necessary to reduce its pressure. Thus, it in condensed form passes through the throttle valve Th, which reduces the refrigerant pressure from p_2 to p_1. Then, the refrigerant returns to the crystallization stage Cryst in a liquid state. In the state diagram of the refrigerant, the arrow *3–4* shows the change in the parameters of the G_R flow when it is throttled. Of note, the throttling enthalpy remains constant $i_3 = i_4$ The arrow *4–1* corresponds to the evaporation of refrigerant at pressure p_1. In this case, the enthalpy of the refrigerant increases from i_4 to i_1.

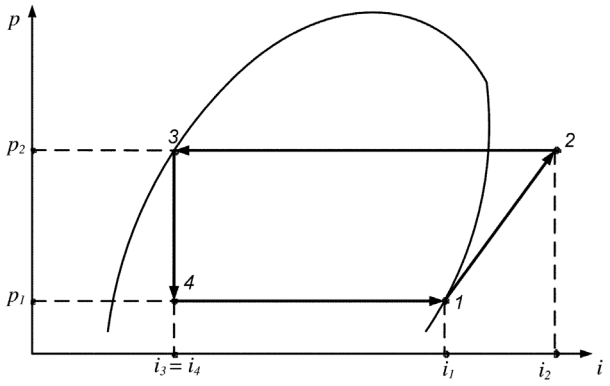

Fig. 2. Changes in the parameters of the refrigerant in the *p–i* state diagram during contact crystallization.

CALCULATION METHODS

To calculate the yield of the crystalline and liquid phases when carrying out the considered separation process, the same dependencies can be used as in the usual crystallization process. Thus, the yield of the crystalline phase can be established using the dependence [2]

$$C = F\frac{x_F - x_M}{x_C - x_M} \quad (1)$$

where x_C and x_M are the concentrations of solute in the crystalline phase C and mother liquor M.

The heat balance equation for the crystallization stage Cryst has the form

$$Fc_F t_F + Cr_{sub} + G_R i_4 = Cc_C t_{fr} + Mc_M t_{fr} + G_R i_1 \quad (2)$$

where c_C and c_M are the heat capacities of the crystalline phase of substance C and mother liquor M; r_{sub} is the heat of crystallization of the substance; i_4 and i_1 are the enthalpies of the refrigerant at the inlet and outlet of the crystallizer.

Using equation (2), it is possible to determine the amount of removed heat Q_{cool} and the flow rate of the refrigerant G_R at the crystallization stage Cryst:

$$Q_{cool} = G_R(i_1 - i_2) = Fc_F t_F + C(r_{sub} - c_C t_{fr}) - Mc_M t_{fr} \quad (3)$$

$$G_R = \frac{Q_{cool}}{i_1 - i_4} = \frac{Fc_F t_F + C(r_{sub} - c_C t_{fr}) - Mc_M t_{fr}}{i_1 - i_4} \quad (4)$$

The amount of removed heat energy Q_{cond} from the condensing compressed heat carrier in the condenser Cond can be determined using the dependence

$$Q_{cond} = G_R(i_2 - i_3) \quad (5)$$

where i_2 and i_3 are enthalpies of the refrigerant at the inlet and outlet of the condenser.

The power consumed by the turbocharger for the compression of refrigerant vapors from pressure p_1 to pressure p_2 is determined [19]

$$N_{real} = \frac{G_R(i_2 - i_1)}{\eta_A \eta_M} \quad (6)$$

where η_A and η_M are the adiabatic and mechanical efficiency coefficients of the compressor.

RESULTS AND DISCUSSION

The considered crystallization process was analyzed using the separation of KNO_3, $(NH_2)_2CO$, NaI, and sucrose from their aqueous solutions as an example. All of these substances do not form crystalline hydrates during crystallization. In the diagrams of their equilibrium with water, there are eutectic points, the parameters of which are provided in the table.

The separation process of the abovementioned binary systems was performed using isobutane as a refrigerant. The vapor pressure of isobutane after throttling was p_1 = 1 atm, and their compression in the compressor was carried out in the range up to p_2 = 2–5 atm depending on the cooling temperature of the solutions in the crystallizer t_{fr}.

As a result of the analysis, it was determined that cooling the solution to lower temperatures t_{fr} at the constant concentration of the initial solution x_F led to a regular increase in the yield of the crystalline phase of the isolated substance and to a corresponding decrease in the yield of the mother liquor (Fig. 3).

Of note, a change in the yield of the crystalline phase, in turn, affects the amount of heat released. Thus, a decrease in the solution cooling temperature t_{fr}, and, consequently, an increase in the yield of crystals leads to the corresponding increase in the amount of released thermal energy Q_{cool} (Fig. 4a) and an increase in the consumption of G_R refrigerant for the crystallization process (Fig. 4b). The power of compressor N_{real}, which is used to compress the vapor of the intermediate heat carrier, also increases (Fig. 5a) as well as the amount of heat Q_{cond}, which is removed during the condensation of the compressed heat carrier vapor in the condenser of the installation (Fig. 5b).

The efficiency of the considered separation process greatly depends on the concentration of the initial solution x_F. Its increase leads to a regular increase in the yield of the crystalline phase C (Fig. 3) and the amount of heat Q_{cool}, which is removed at the crystallization stage (Fig. 4). The flow rate of the refrigerant G_R and the compressor capacity N_{real} also increases (Fig. 5).

The analysis also showed that in addition to the fractionation temperature t_{fr} and concentration x_F, the refrigerant flow rate G_R and compressor power N_{real} are greatly affected by pressure p_2, to which the refrigerant vapor is compressed in the compressor. It is characteristic that during the separation of dilute solutions, the value of G_R slightly decreases with an increase in pressure p_2, and when fractionating concentrated solutions, it slightly increases (Fig. 6a); the compressor power always increases with an increase in p_2 (Fig. 6b).

Refrigerant consumption G_R and compressor power N_{real} can also depend on the physicochemical and thermophysical properties of crystallizing substances and their aqueous solutions [17]. Thus, for example, at the same yield of the crystalline phase for

Parameters of the eutectic point for some binary systems

System	x_F, wt %	t_F, °C
KNO_3–H_2O	11	−2
$(NH_2)_2CO$–H_2O	32	−12
NaI–H_2O	47	−32
$C_{12}H_{22}O_{11}$–H_2O	63	−14

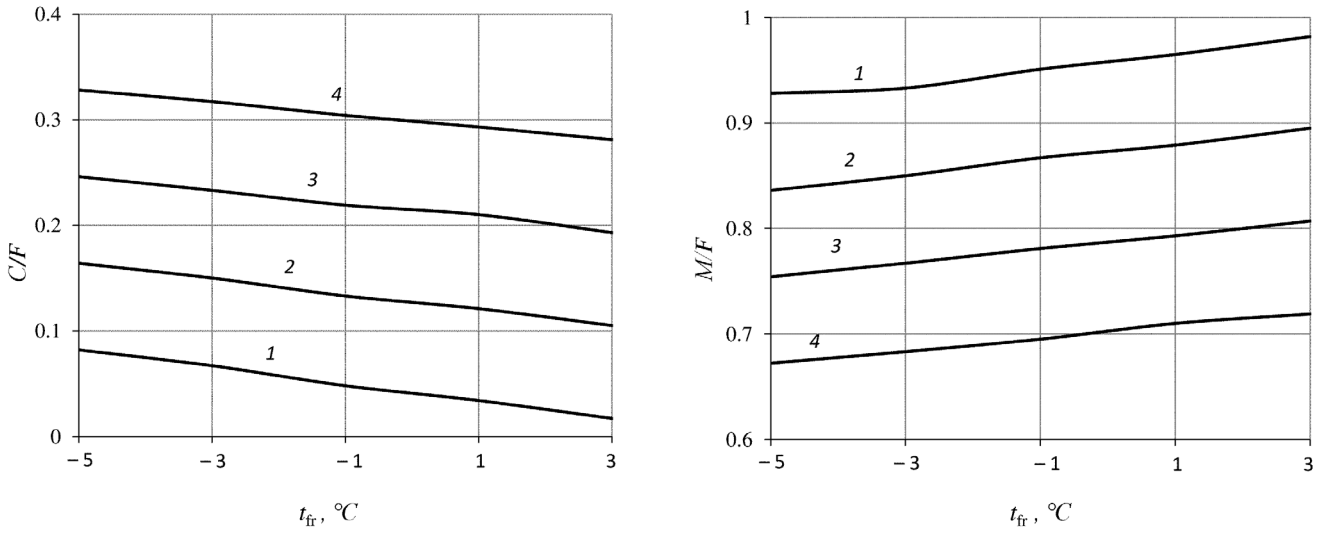

a b

Fig. 3. Influence of the cooling temperature t_{fr} on the yield of the crystal phase (a) and mother solution (b) (system $(NH_2)_2CO–H_2O$; p_2 = 2 atm): (1) x_F = 40% $(NH_2)_2CO$; (2) x_F = 45%; (3) x_F = 50%; (4) x_F = 55%.

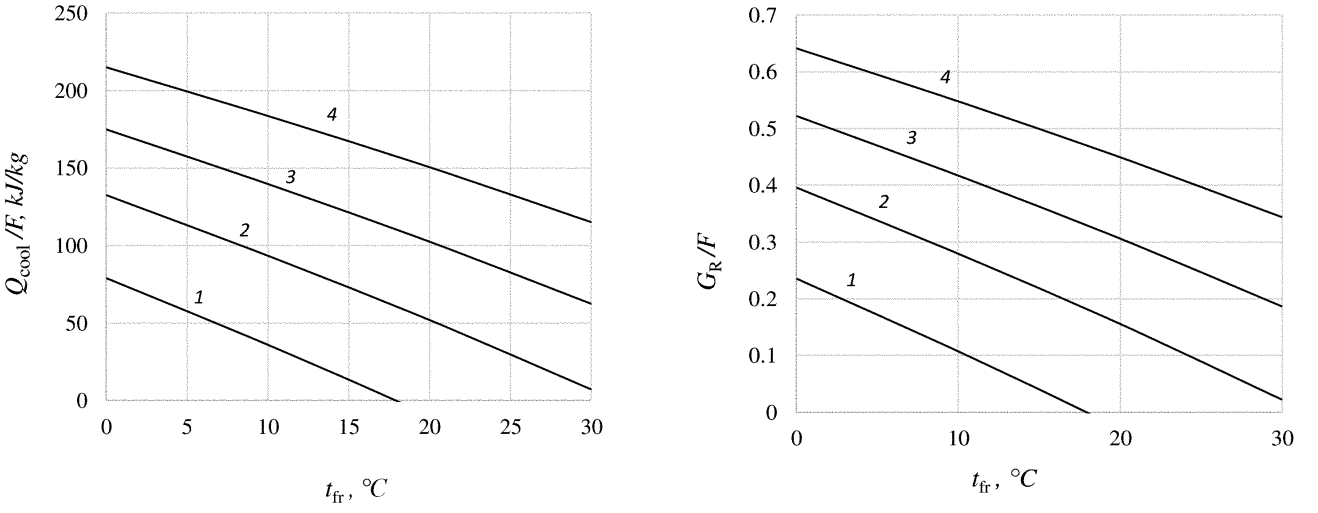

a b

Fig. 4. Dependence of the amount of heat removed from the crystallizer (a) and the refrigerant flow rate (b) on the fractionation temperature ($KNO_3–H_2O$ system; p_2 = 2 atm): (1) x_F = 20% KNO_3; (2) x_F = 30%; (3) x_F = 40%; (4) x_F = 50%.

NaI, the energy consumption for performing contact crystallization is 1.5–2.0 times higher than that for the crystallization of sucrose.

CONCLUSIONS

The analysis of data from previous studies and our research showed that contact crystallization using evaporating refrigerants can be successfully applied to isolate various substances from their aqueous solutions. It is especially advantageous to use it when the crystallization process is carried out at low temperatures. When using it, interfacial heat transfer is considerably intensified, and the instrumentation of the separation process is simplified.

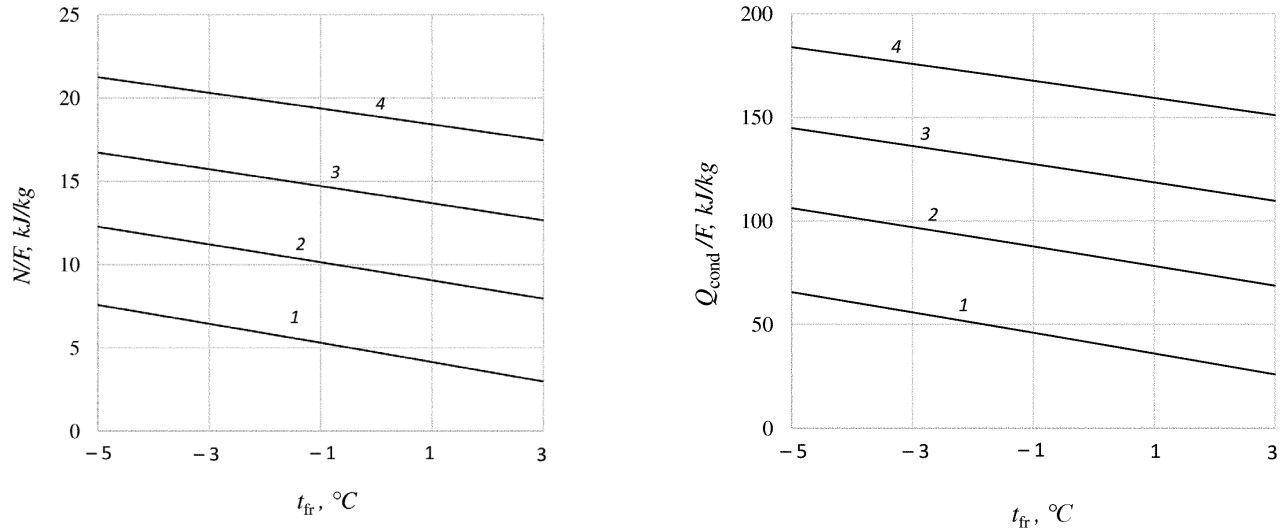

a b

Fig. 5. Dependence of the compressor power consumption (a) and the amount of heat removed during the condensation of refrigerant vapor (b) on the fractionation temperature (system $(NH_2)_2CO–H_2O$; p_2 = 2 atm): (1) x_F = 40% $(NH_2)_2CO$; (2) x_F = 45%; (3) x_F = 50%; (4) x_F = 55%.

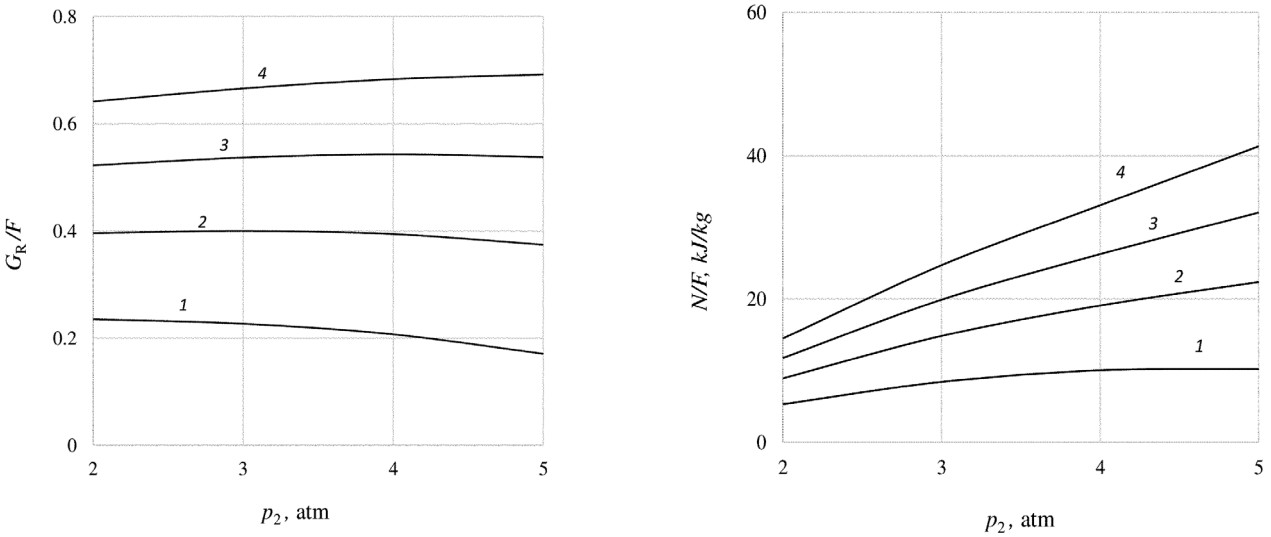

a b

Fig. 6. Dependence of the refrigerant flow (a) and compressor power (b) on the refrigerant pressure at the compressor outlet (NaI–H_2O system; t_{fr} = −28°C): (1) x_F = 60% NaI; (2) x_F = 63%; (3) x_F = 66%; (4) x_F = 69%.

Key
Cryst – crystallizer;
Sep – filter (separation);
Com – turbocharger;
Th – throttle valve;
Cond – refrigerant condenser;
F – mass flow of the initial solution;
C – output of the crystal phase;
M – output of the stock solution;
S – mass flow of the extracted crystal phase;
L – mass flow of the removed uterus;
G_R – refrigerant consumption;

G_W – water consumption;
x_F – concentration of the initial solution;
x_S – concentration of the extracted substance in the crystal phase;
x_L – concentration of the substance in the mother liquor;
t_{fr} – cooling temperature of the solution (fractionation);
Θ_1 – temperature of the refrigerant at the compressor input;
Θ_2 – temperature of the refrigerant compressed in the compressor;
t'_W – water temperature at the condenser input;
t''_W – water temperature at the condenser output;
p_1 – pressure of the refrigerant at the compressor input;
p_2 – pressure of the refrigerant compressed in the compressor;
h_R – enthalpy of the refrigerant at the compressor input;
i_2 – enthalpy of the refrigerant compressed in the compressor;
i_3 – enthalpy of the refrigerant at the condenser output;
i_4 – enthalpy of the refrigerant at the crystallizer input.

Financial support

This study did not have any financial support from outside organizations.

Authors' contribution

G.A. Nosov – research planning, analysis of scientific works, scientific editing, preparation of the list of references;

M.E. Uvarov – selection of model systems, conducting the study, writing the text of the article, technical editing, design of the list of references.

The authors declare no conflicts of interest.

REFERENCES

1. Matusevich L.N. *Kristallizatsiya iz rastvorov v khimicheskoi promyshlennosti* (Crystallization from solutions in the chemical industry). Moscow: Khimiya; 1968. 304 p. (in Russ.).

2. Gel'perin N.I., Nosov G.A. *Osnovy tekhniki fraktsionnoi kristallizatsii* (Fundamentals of fractional crystallization technique). Moscow: Khimiya; 1986. 304 p. (in Russ.).

3. Mullin J.W. Crystallization. Oxford: Butterworth-Heinemann, 2001. 594 p.

4. Mikhalev M.F., Schuplyak I.A. *Kontaktnaya kristallizatsiya* (Contact crystallization). Leningrad: LGU Publishing House; 1983. 190 p. (in Russ.).

5. Challener C.A. Considering continuous crystallization. *Pharm. Technol.* 2015;39(5):38-40.

6. Elfassy E., Basel Y., Mastai Y. Crystallization of amino acids at the chiral ionic liquid/water interface. *CrystEngComm.* 2016;18(45):8769-8775.
https://doi.org/10.1039/C6CE01726F

7. Kim H.J., Lee J. Novel porous materials prepared by repeated directional crystallization of solvent. *Polymer Korea.* 2015;9(1):151-156.
https://doi.org/10.7317/pk.2015.39.1.151

8. Liu S., Hao L., Rao Z., Zhang X. Experimental study on crystallization process and prediction for the latent heat of ice slurry generation based sodium chloride solution. *Appl. Energy.* 2017;185(2):1948-1953.
https://doi.org/10.1016/j.apenergy.2015.10.073

9. Stamenov L., Stefanova V., Petkov K., Iliev P. Study of the crystallization process of ferric sulfate hydrate from rich of Fe(III) waste solutions. *J. Chem. Technol. Metall.* 2017;52(2):333-339.

10. Rachah A., Noll D. Mathematical Analysis of a Continuous Crystallization Process. In: Anastassiou G., Duman O. (eds.). Intelligent Mathematics II: Applied Mathematics and Approximation Theory. Advances in Intelligent Systems and Computing. Springer, Cham. 2016;441:283-301.
https://doi.org/10.1007/978-3-319-30322-2_20

СПИСОК ЛИТЕРАТУРЫ

1. Матусевич Л.Н. Кристаллизация из растворов в химической промышленности. М.: Химия; 1968. 304 с.

2. Гельперин Н.И., Носов Г.А. Основы техники фракционной кристаллизации. М: Химия; 1986. 304 с.

3. Mullin J.W. Crystallization. Oxford: Butterworth-Heinemann; 2001. 594 p.

4. Михалёв М.Ф., Щупляк И.А. Контактная кристаллизация. Л.: Изд-во ЛГУ; 1983. 190 с.

5. Challener C.A. Considering continuous crystallization. *Pharm. Technol.* 2015;39(5):38-40.

6. Elfassy E., Basel Y., Mastai Y. Crystallization of amino acids at the chiral ionic liquid/water interface. *CrystEngComm.* 2016;18(45):8769-8775.
https://doi.org/10.1039/C6CE01726F

7. Kim H.J., Lee J. Novel porous materials prepared by repeated directional crystallization of solvent. *Polymer Korea.* 2015; 9(1):151-156.
https://doi.org/10.7317/pk.2015.39.1.151

8. Liu S., Hao L., Rao Z., Zhang X. Experimental study on crystallization process and prediction for the latent heat of ice slurry generation based sodium chloride solution. *Appl. Energy.* 2017;185(2):1948-1953.
https://doi.org/10.1016/j.apenergy.2015.10.073

9. Stamenov L., Stefanova V., Petkov K., Iliev P. Study of the crystallization process of ferric sulfate hydrate from rich of Fe(III) waste solutions. *J. Chem. Technol. Metall.* 2017;52(2):333-339.

10. Rachah A., Noll D. Mathematical Analysis of a Continuous Crystallization Process. In: Anastassiou G., Duman O. (eds.). Intelligent Mathematics II: Applied Mathematics and Approximation Theory. Advances in Intelligent Systems and Computing. Springer, Cham. 2016;441:283-301.
https://doi.org/10.1007/978-3-319-30322-2_20

11. Horst J.H., Schmidt C., Ulrich J. Fundamentals of Industrial Crystallization. In book: Handbook of Crystal Growth. Bulk Crystal Growth: Second Edition. 2015;2:1317-1349.
https://doi.org/10.1016/B978-0-444-63303-3.00032-8

11. Horst J.H., Schmidt C., Ulrich J. Fundamentals of Industrial Crystallization. In book: Handbook of Crystal Growth. Bulk Crystal Growth: Second Edition. 2015;2:1317-1349. https://doi.org/10.1016/B978-0-444-63303-3.00032-8

12. Price C.J. Continuous Pharmaceutical Crystallization from Solution. In: Roberts K., Docherty R., Tamura R. (eds.). Engineering Crystallography: From Molecule to Crystal to Functional Form. NATO Science for Peace and Security Series A: Chemistry and Biology. Springer, Dordrecht. 2017;1:315-329. https://doi.org/10.1007/978-94-024-1117-1_19

13. Mancigotti S., Hamilton A. Salt crystallisation in pores: The effect of crystal growth rate on damage. *WIT Trans. Built Environ.* 2017;171:207-214. https://doi.org/10.2495/STR170181

14. Harada R. Development of small continuous crystallizer. *J. Soc. Powder Technol. Japan.* 2017;54(7):478-482. https://doi.org/10.4164/sptj.54.478

15. Pap L. *Kontsentrirovanie vymorazhivaniem* (Freezing Concentration). Moscow: Light and Food Industry; 1982. 96 p. (in Russ.).

16. Filatkin V.N., Plotnikov V.T. *Razdelitel'nye vymorazhivayushchie ustanovki* (Separating freezing installations). Moscow: Agropromizdat; 1987. 352 p. (in Russ.).

17. Nosov G.A., Kesoyan G.A., Popov D.A. Contact crystallization with using of cooled solvents. *Tonkie khimicheskie tekhnologii = Fine Chemical Technologies.* 2008;3(2):40-44 (in Russ.).

18. Semenov E.V., Slavyanskiy A.A. Peculiarities of the process of suspensions separation in rotors of filtering centrifuges. *Khimicheskoe i Neftegazovoe Mashinostroenie.* 2017;5:7-12 (in Russ.).

19. Nosov G.A., Uvarov M.E. Two-stage recrystallization with the regeneration of the solvent. *Tonkie khimicheskie tekhnologii = Fine Chemical Technologies.* 2017;12(1):50-56 (in Russ.).

12. Price C.J. Continuous Pharmaceutical Crystallization from Solution. In: Roberts K., Docherty R., Tamura R. (eds.). Engineering Crystallography: From Molecule to Crystal to Functional Form. NATO Science for Peace and Security Series A: Chemistry and Biology. Springer, Dordrecht. 2017;1:315-329. https://doi.org/10.1007/978-94-024-1117-1_19

13. Mancigotti S., Hamilton A. Salt crystallisation in pores: The effect of crystal growth rate on damage. *WIT Trans. Built Environ.* 2017;171:207-214. https://doi.org/10.2495/STR170181

14. Harada R. Development of small continuous crystallizer. *J. Soc. Powder Technol. Japan.* 2017;54(7):478-482. https://doi.org/10.4164/sptj.54.478

15. Пап Л. Концентрирование вымораживанием. М.: Лёгкая и пищевая промышленность; 1982. 96 с.

16. Филаткин В.Н., Плотников В.Т. Разделительные вымораживающие установки. М.: Агропромиздат; 1987. 352 с.

17. Носов Г.А., Кесоян Г.А., Попов Д.А. Контактная кристаллизация с использованием охлажденных растворителей. *Тонкие химические технологии.* 2008;3(2):40-44.

18. Семенов Е.В., Славянский А.А. Особенности процесса разделения суспензий в роторах фильтрующих центрифуг. *Химическое и нефтегазовое машиностроение.* 2017;5:7-12.

19. Носов Г.А., Уваров М.Е. Двухстадийная перекристаллизация с регенерацией растворителя. *Тонкие химические технологии.* 2017;12(1):50-56. https://doi.org/10.32362/2410-6593-2017-12-1-50-56

About the authors:

Gennadi A. Nosov, Dr. of Sci. (Engineering), Professor, N.I. Gel'perin Department of Processes and Apparatus of Chemical Technologies, M.V. Lomonosov Institute of Fine Chemical Technologies, MIREA – Russian Technological University (86, Vernadskogo pr., Moscow, 119571, Russia). E-mail: nosovga@mail.ru. Scopus Author ID 7003643516

Mikhail E. Uvarov, Senior Teacher, N.I. Gel'perin Department of Processes and Apparatus of Chemical Technologies, M.V. Lomonosov Institute of Fine Chemical Technologies, MIREA – Russian Technological University (86, Vernadskogo pr., Moscow, 119571, Russia). E-mail: uvamikhail@yandex.ru. http://orcid.org/0000-0003-3184-8496

Об авторах:

Носов Геннадий Алексеевич, доктор технических наук, профессор кафедры процессов и аппаратов химических технологий имени Н.И. Гельперина Института тонких химических технологий имени М.В. Ломоносова ФГБОУ ВО «МИРЭА – Российский технологический университет» (119571, Россия, Москва, пр-т Вернадского, д. 86). E-mail: nosovga@mail.ru. Scopus Author ID 7003643516

Уваров Михаил Евгеньевич, старший преподаватель кафедры процессов и аппаратов химических технологий имени Н.И. Гельперина Института тонких химических технологий имени М.В. Ломоносова ФГБОУ ВО «МИРЭА – Российский технологический университет» (119571, Россия, Москва, пр-т Вернадского, д. 86). E-mail: uvamikhail@yandex.ru. http://orcid.org/0000-0003-3184-8496

The article was submitted: December 27, 2019; approved after reviewing: April 02, 2020; accepted for publication: July 30, 2020.

Translated from Russian into English by S. Durakov
Edited for English language and spelling by Enago, an editing brand of Crimson Interactive Inc.

CHEMISTRY AND TECHNOLOGY OF ORGANIC SUBSTANCES

ХИМИЯ И ТЕХНОЛОГИЯ ОРГАНИЧЕСКИХ ВЕЩЕСТВ

ISSN 2686-7575 (Online)

https://doi.org/10.32362/2410-6593-2020-15-5-16-25

UDC 547.464.7

RESEARCH ARTICLE

Synthesis and reactions of alkenyl-*gem*-dichlorocyclopropanes obtained from piperylene

Airat I. Musin[1], Yulianna G. Borisova[2,@], Gul'nara Z. Raskil'dina[2], Ruslan U. Rabaev[2], Rustem R. Daminev[1], Simon S. Zlotskii[2]

[1]Ufa State Petroleum Technological University, Branch in Sterlitamak, Sterlitamak, 453118 Russia
[2]Ufa State Petroleum Technological University, Ufa, 450062 Russia
[@]Corresponding author, e-mail: yulianna_borisova@mail.ru

Objectives. *This study aims to obtain alkenyl-gem-dichlorocyclopropanes from piperylene. The products are then subjected to thermocatalytic isomerization and hydrogenation.*
Methods. *To determine the qualitative and quantitative composition of the reaction crudes, the following analytical methods were used: gas-liquid chromatography using the Crystal 2000 hardware complex, mass spectrometry using a Chromatec-Crystal 5000M device with the NIST 2012 database, and nuclear magnetic resonance (NMR) spectroscopy using a Bruker AM-500 device at operating frequencies of 500 and 125 MHz.*
Results. *Alkenyl-gem-dichlorocyclopropanes were synthesized in the presence of triethylbenzyl ammonium chloride as catalyst. Their isomerization and hydrogenation gave the corresponding gem-dichlorocyclopentene and isomers of alkyl-gem-dichlorocyclopropanes. The structure of synthesized substances were analyzed by gas-liquid chromatography, mass spectrometry, and NMR spectroscopy.*
Conclusions. *The results show that formation of four isomeric substituted gem-dichlorocyclopropanes occurs in high yield during incomplete dichlorocyclopropanation of piperylene. The thermocatalytic isomerization of substituted gem-dichlorocyclopropanes in the presence of SAPO-34 zeolite leads to the formation of one product, i.e., gem-dichlorocyclopentene, and hydrogenation of substituted gem-dichlorocyclopropanes in the presence of Pd/C catalyst gives three isomeric alkyl-gem-dichlorocyclopropanes.*

Keywords: *alkenyl-gem-dichlorocyclopropane, isomerization, hydrogenation, SAPO-34 zeolite, Pd/C catalyst*

For citation: Musin A.I., Borisova Yu.G., Raskil'dina G.Z., Rabaev R.U., Daminev R.R., Zlotskii S.S. Synthesis and reactions of alkenyl-*gem*-dichlorocyclopropanes obtained from piperylene. *Tonk. Khim. Tekhnol. = Fine Chem. Technol.* 2020;15(5):16-25 (Russ., Eng.). https://doi.org/10.32362/2410-6593-2020-15-5-16-25

НАУЧНАЯ СТАТЬЯ

Синтез и реакции алкенил-*гем*-дихлорциклопропанов на основе пиперилена

А.И. Мусин[1], Ю.Г. Борисова[2,@], Г.З. Раскильдина[2], Р.У. Рабаев[2], Р.Р. Даминев[1], С.С. Злотский[2]

[1]Уфимский государственный нефтяной технический университет, филиал в г. Стерлитамак, Стерлитамак, 453118 Россия
[2]Уфимский государственный нефтяной технический университет, Уфа, 450064 Россия
[@]Автор для переписки, e-mail: yulianna_borisova@mail.ru

Цели. *Получить алкенил-гем-дихлорциклопропаны на основе пиперилена, провести их термокаталитическую изомеризацию и гидрирование.*
Методы. *Для определения качественного и количественного состава реакционных масс использованы следующие методы анализа: газожидкостная хроматография (на аппаратно-программном комплексе «Кристалл 2000»), хроматомасс-спектрометрия (на приборе «Хроматэк-Кристалл 5000М» с базой NIST 2012) и спектроскопия ядерного магнитного резонанса (ЯМР) (на приборе «Bruker AM-500» с рабочими частотами 500 и 125 МГц).*
Результаты. *Алкенил-гем-дихлорциклопропаны синтезированы в присутствии катализатора триэтилбензиламмоний хлористый. Дальнейшей их изомеризацией и восстановлением получены соответствующие гем-дихлорциклопентен и изомеры алкил-гем-дихлорциклопропанов. Строение синтезированных веществ проанализировано и доказано методами газожидкостной хроматографии, масс-спектрометрии и ЯМР-спектроскопии.*
Выводы. *Установлено, что неполное дихлорциклопропанирование пиперилена протекает количественно с образованием четырех изомерных замещенных гем-дихлорциклопропанов, при термокаталитической изомеризации которых в присутствии цеолита SAPO-34 происходит образование одного продукта – гем-дихлорциклопентена, а при их восстановлении с помощью катализатора Pd/C наблюдается образование трех изомерных алкил-гем-дихлорциклопропанов.*

Ключевые слова: *алкенил-гем-дихлорциклопропаны, изомеризация, гидрирование, SAPO-34, Pd/C*

Для цитирования: Мусин А.И., Борисова Ю.Г., Раскильдина Г.З., Рабаев Р.У., Даминев Р.Р., Злотский С.С. Синтез и реакции алкенил-*гем*-дихлорциклопропанов на основе пиперилена. *Тонкие химические технологии.* 2020;15(5):16-26. https://doi.org/10.32362/2410-6593-2020-15-5-16-25

INTRODUCTION

Substituted three-membered carbocycles, in particular, *gem*-dichlorocyclopropanes, are widely used in the chemistry of natural and medicinal substances [1–8]. The most effective route for the synthesis of *gem*-dihalocyclopropanes is based on the [2 + 1]-cycloaddition of dichlorocarbenes at multiple bonds [9–18]. Following this method, from industrial dienes such as divinyl, isoprene, and 2,3-dimethyl-butadiene, the corresponding alkenyl-*gem*-dichlorocyclopropanes are obtained, which are used in fine organic synthesis [19, 20]. In this context, the purpose of this study is to perform the dichlorocarbenation of piperylene as a large-tonnage diene and to conduct a series of conversions of the corresponding alkenyl-*gem*-dichlorocyclopropanes.

MATERIALS AND METHODS

Analysis of the reaction crudes was performed using gas-liquid chromatography on the hardware-software complex Crystal 2000, *NPF Meta-khrom*, Russia. Mass spectra were obtained using a *Chromatec-Crystal 5000M* instrument (*Chromatec*, Russia) with the NIST 2012 database (*National Institute of Standards and Technology*, USA). ^{1}H and ^{13}C nuclear magnetic resonance (NMR) spectra were recorded on a Bruker AM-500 spectrometer (*Bruker Corporation*, USA) at operating frequencies

of 500 and 125 MHz, respectively, using $CDCl_3$ as solvent. Chemical shifts are reported in δ (ppm) relative to tetramethylsilane as internal standard. Spin–spin coupling constants (*J*) are given in Hz.

Substituted vinyl-*gem*-dichlorocyclopropanes **2a,b** and **3a,b** were obtained following a reported procedure [19], using chloroform, 50% alkali solution, and triethylbenzylammonium chloride as an interphase catalyst.

1,1-Dichloro-2-((1-*Z*)-prop-1-en-1-yl)-cyclopropane (2a). Colorless liquid. Yield (**2** + **3**): 95%, T_{boil} = 48–50°C (35 mm Hg). ^{1}H NMR spectrum ($CDCl_3$), δ (ppm), *J* (Hz): 1.20 d (1H, CHa, *J* = 5.3), 1.72 d (1H, CHb *J* = 5.3), 1.75 t (3H, CH_3, *J* = 3.1), 2.38–2.43 m (1H, CH), 5.15 t (1H, CH, *J* = 6), 5.20–5.25 m (1H, CH). ^{13}C NMR ($CDCl_3$), δ_C (ppm): 14.39 (CH_3), 27.42 (CH_2), 28.72 (CH), 61.09 (C), 126.11 (CH), 128.97 (CH). Mass spectrum, *m/e* (I_{rel}, %): 150/152/154 (≤3) [M^+], 135/137/139 (≤5), 115/117 (44/12), 99/101 (22/8), 79/100, 77/65.

1,1-Dichloro-2-((1-*E*)-prop-1-en-1-yl)-cyclopropane (2b). Colorless liquid. Yield (**2** + **3**): 95%, T_{boil} = 48–50°C (35 mm Hg). ^{1}H NMR ($CDCl_3$), δ (ppm), *J* (Hz): 1.20 d (1H, CHa, *J* = 5.3), 1.72 d (1H, CHb, *J* = 5.3), 1.75 t (3H, CH_3, *J* = 3.1), 2.08–2.12 m (1H, CH), 5.28–5.35 m (1H, CH), 5.37 d (1H, CH, *J* = 13.7). ^{13}C NMR ($CDCl_3$), δ_C (ppm): 18.03 (CH_3), 28.39 (CH), 27.69 (CH_2), 61.09 (C), 126.63 (CH), 130.12 (CH). Mass spectrum, *m/e* (I_{rel}, %): 150/152/154 (≤4) [M^+], 135/137.139 (≤5), 115/117 (42/12), 99/101 (20/10), 79/100, 77/72.

***cis*-1,1-Dichloro-2-vinyl-3-methylcyclopropane (3a).** Colorless liquid. Yield (**2** + **3**): 95%, T_{boil} = 48–50°C (35 mm Hg). ^{1}H NMR ($CDCl_3$), δ (ppm), *J* (Hz): 1.42 s (1H, CH), 1.35 t (3H, CH_3, *J* = 7.8), 2.20–2.30 m (1H, CH), 5.45–5.60 m (2H, CH_2), 5.75 dd (1H, CH, *J* = 10, 13). ^{13}C NMR ($CDCl_3$), δ_C (ppm): 9.68 (CH_3), 31.90 (CH), 35.91 (CH), 61.09 (C), 120.11 (CH_2), 134.32 (CH). Mass spectrum, *m/e* (I_{rel}, %): 150/152/154 (≤4) [M^+], 135/137/139 (≤5), 115/117 (36/12), 99/101 (20/8), 79/100, 77/70.

***trans*-1,1-Dichloro-2-vinyl-3-methyl-cyclopropane (3b).** Colorless liquid. Yield (**2** + **3**): 95%, T_{boil} = 48–50°C (35 mm Hg). ^{1}H NMR ($CDCl_3$), δ (ppm), *J* (Hz): 1.11 d (1H, CH, *J* = 10), 1.52 t (3H, CH_3, *J* = 6.8), 2.20–2.30 m (1H, CH), 5.45–5.60 m (2H, CH_2), 5.75 dd (1H, CH, *J* = 10, 13). ^{13}C NMR ($CDCl_3$), δ_C (ppm): 9.68 (CH_3), 33.15 (CH), 40.19 (CH), 61.09 (C), 118.29 (CH_2), 134.32 (CH). Mass spectrum, *m/e* (I_{rel}, %): 150/152/154 (≤8) [M^+], 135/137/139 (≤8), 115/117 (46/26), 99/101 (22/10), 79/100, 77/72.

Isomerization was conducted in a fixed-bed flow-through unit in a reactor with a volume of 15 cm^3, at atmospheric pressure, and at a temperature ranging from 130 to 280°C. SAPO-34 zeolite (made in China) was used as a catalyst, which was activated in a flow of hydrogen at 550°C for 5 h before use. Raw materials (50 mL of a mixture of vinyl-*gem*-dichlorocyclopropane : decane in a 1 : 2 volume ratio) were supplied using a pump. The product of the catalysis was dried with freshly calcined calcium chloride and evaporated under a weak vacuum after filtering off the salt to give 4.

4,4-Dichloro-3-methylcyclopentene (4). Colorless liquid. Yield: 94%, T_{boil} = 57°C (35 mm Hg). ^{1}H NMR ($CDCl_3$), δ (ppm), *J* (Hz): 1.35 t (3H, CH_3, *J* = 7.0), 2.53 d (1H, CHa, *J* = 3.9), 2.85 t (1H, CHb, *J* = 3.6), 5.56 t (1H, CH, *J* = 6), 5.88 d (1H, CH, *J* = 5.9). ^{13}C NMR ($CDCl_3$), δ_C (ppm): 14.99 (CH_3), 53.22 (CH_2), 62.68 (CH_2), 81.16 (C), 124.92 (CH=), 141.06 (C=). Mass spectrum, *m/e* (I_{rel}, %): (150/152/154)/35/16/5 [M^+], (115/117)/(100/34), (77/79)/(89/55), 51/27.

For *hydrogenation*, palladium on carbon (Pd/C), granular, TU 2170-300-29131036-97[1], was used as a catalyst. The catalyst was ground in a mortar before use, sieved, and stored in a box in an extractor. A calculated amount of Pd/C catalyst, which was finely ground in a mortar and weighed on an analytical balance, was loaded into the reactor (Fig. 1). A solution containing a mixture of dichlorocyclopropanes **2a,b** and **3a,b** in ethyl-acetate (20 mL) with a mass concentration of 50 g/L was added. From hydrogen generator 6, buffer tank 7 was filled with hydrogen by opening valve 1 and closing valve 2. Valve 1 was then closed, and valves 2–4 were open, while maintaining mixing device 11 turned off and vessel 10 completely filled with liquid. Thus, the system was purged with hydrogen. Then, valves 4 and 3 were sequentially closed, and with valve 5 open, cylindrical vessel 8 was filled with hydrogen from the buffer tank to the lower mark, creating a slight excess pressure of the water column from pressure reservoir 9. Then, valve 2 was closed, valve 3 was open, and the stirring device was turned on, setting the preset mixing speed. The progress of the reaction was monitored by determining the volume of absorbed hydrogen. The experiment was continued until a noticeable decrease in the rate of hydrogen absorption was observed.

After hydrogenation, the following products were obtained:

1,1-Dichloro-2-propylcyclopropane (5). Colorless liquid. Yield (**5** + **6**): 95%, T_{boil} = 54°C (35 mm Hg). ^{1}H NMR ($CDCl_3$), δ (ppm), *J* (Hz): 0.95 t (3H, CH_3, *J* = 7), 1.20–1.25 m (6H, 3 CH_2), 1.36–1.55 m (1H, CH). ^{13}C NMR ($CDCl_3$), δ_C (ppm): 15.03 (CH_3), 23.99 (CH_2), 27.06 (CH_2), 31.09 (CH_2), 38.44 (CH), 65.44 (C). Mass spectrum, *m/e* (I_{rel}, %): 152/154/156 (7) [M^+], 123/49, 110/66, 75/5, 87/37, 51/100.

[1] Information about the catalyst is available on the manufacturer's website https://www.kazanorgsintez.ru.

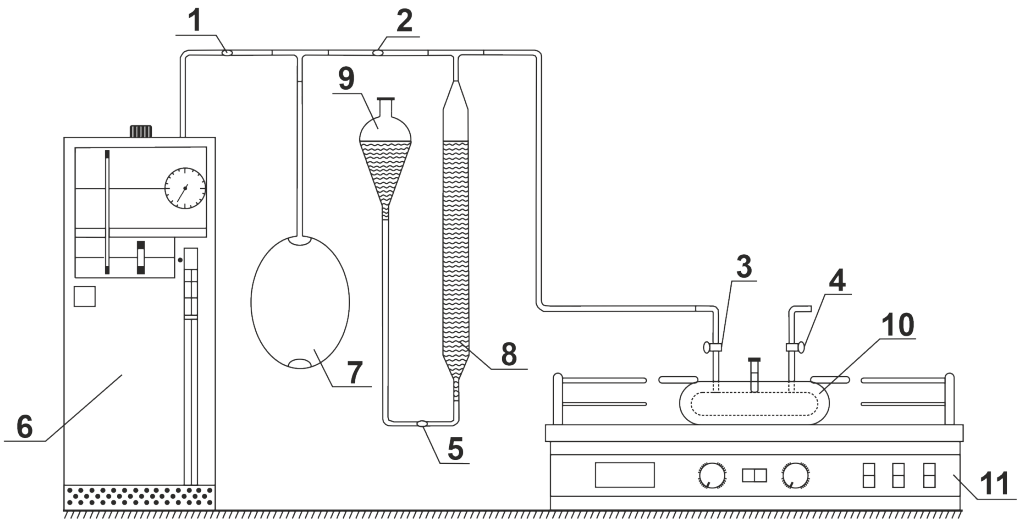

Schematic representation of the installation for hydrogenation at atmospheric pressure. Valves (1–5), hydrogen generator (6), buffer tank (7), cylindrical vessel (8), pressure tank (9), hydrogenation reactor (10), stirring device (11).

***cis*-1,1-Dichloro-2-methyl-3-ethylcyclopropane (6a).** Colorless liquid. Yield (**5** + **6**): 95%, T_{boil} = 54°C (35 mm Hg). ^{1}H NMR ($CDCl_3$), δ (ppm), *J* (Hz): 0.90 d (1H, 1 CH, *J* = 7), 1.02 t (3H, CH_3, *J* = 5), 1.45 t (3H, CH_3, *J* = 3), 1.61–1.66 m (1H, CH), 1.78–1.83 m (2H, CH_2). ^{13}C NMR ($CDCl_3$), δ_C (ppm): 10.55 (CH_3), 14.09 (CH_3), 19.44 (CH_2), 32.94 (CH), 34.01 (CH), 67.55 (C). Mass spectrum, *m/e* (I_{rel}, %): 152/154/156 (9) [M^+], 123/59, 110/30, 75/15, 87/67, 51/100.

***trans*-1,1-Dichloro-2-methyl-3-ethylcyclopropane (6b).** Colorless liquid. Yield (**5** + **6**): 95%, T_{boil} = 54°C (35 mm Hg). ^{1}H NMR ($CDCl_3$), δ (ppm), *J* (Hz): 1.05–1.15 m (1H, CH), 1.02 t (3H, CH_3, *J* = 5), 1.45 t (3H, CH_3, *J* = 3), 1.61–1.66 m (1H, CH), 1.78–1.83 m (2H, CH_2). ^{13}C NMR ($CDCl_3$), δ_C (ppm): 11.01 (CH_3), 15.88 (CH_3), 19.44 (CH_2), 34.71 (CH), 41.39 (CH), 67.67 (C). Mass spectrum, *m/e* (I_{rel}, %): 152/154/156 (7) [M^+], 123/49, 110/66, 75/5, 87/37, 51/100.

RESULTS AND DISCUSSION

At the initial stage of the dichlorocarbenation of commercial piperylene (*cis*-**1a** : *trans*-**1b** = 1 : 4), which was performed according to the Makoshi method [21], carbenes attach to nonequivalent terminal and internal double C=C bonds at different rates, leading to the formation of a mixture of propenyl derivatives **2a,b** and vinyl derivatives **3a,b** in a ratio of 1 : 3, respectively (Scheme 1). This is due to the fact that the methyl substituent located in the α-position activates the double bond with respect to the electron-withdrawing :CCl_2 carbene. Note that the 2,2-disubstituted double bond in isoprene is one order of magnitude more active than the unsubstituted one [19].

The observed ratio of stereoisomers **2a** : **2b** = 1 : 4 coincides with the content of *cis*- and *trans* forms in the initial diene **1a,b**. The addition of dichlorocarbene to the

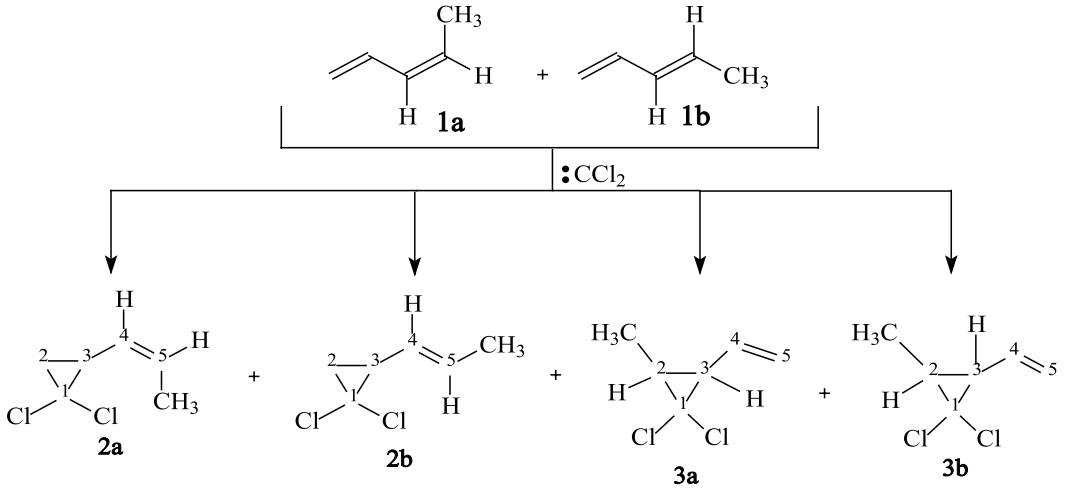

Scheme 1. Carbenation of piperylene **1a,b**.

substituted double bond proceeds nonstereoselectively, and isomers **3a,b** are formed in similar amounts (**3a** : **3b** = 1 : 1.5).

Next, the thermocatalytic isomerization (Scheme 2) of the obtained alkenyl-*gem*-dichlorocyclopropanes **2a,b** and **3a,b** was performed at 230°C according to a previously described method [22] using commercially available SAPO-34 zeolite as a catalyst [23].

4,4-Dichloro-3-methylcyclopentene **4** was obtained in a yield of more than 90% as a result of the opening of the three-membered carbocycles at the C^1–C^3 bonds on the catalyst. No products resulting from the cleavage of the C^2–C^3 bonds were detected.

Hydrogenation (Scheme 3) of alkenyl-*gem*-dichlorocyclopropanes **2a,b** and **3a,b** was conducted using commercial Pd/C catalyst [24, 25] at a temperature of 22–24°C and atmospheric pressure for 3.5–4 h.

Under these conditions, a mixture of propyl-*gem*-dichlorocyclopropane **5**, *cis*-2-methyl-3-ethyl-*gem*-dichlorocyclopropane **6a**, and *trans*-2-methyl-3-ethyl-*gem*-dichlorocyclopropane **6b** was obtained quantitatively. The ratio of the latter compounds corresponds to the starting content in the initial mixture of vinyl derivatives (**6a** : **6b** = **3a** : **3b** = 1 : 1.5).

The method of competitive kinetics [26] (maximum conversion of 30%) was used to determine the relative reactivity of propenyl **2a,b** and vinyl derivatives **3a,b** in the hydrogenation reaction. Under the studied conditions[2], judging by the rate of accumulation of products **5** and **6a,b**, vinyl derivatives **3a,b** are two times more active than propenyl derivatives **2a,b**.

The composition of the obtained products **2a,b**, **3a,b**, **5**, **6a,b**, and the isolated compound **4** was established by NMR spectroscopy and gas chromatography–mass spectrometry.

The ^{1}H NMR spectrum of the mixture of carbenation products **2a,b** and **3a,b** shows the presence of signals of multiple bonds of protons at C^4 and C^5 carbon atoms. For molecule **2a**, the proton at the C^4 carbon atom gives rise to a triplet at 5.15 ppm (^3J = 6 Hz), and that at the C^5 carbon atom affords a

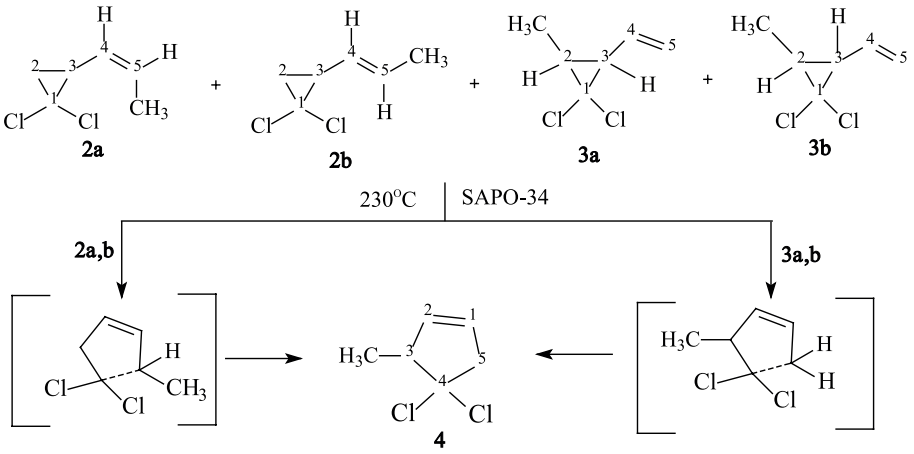

Scheme 2. Isomerization of alkenyl-*gem*-dichlorocyclopropanes **2a,b** and **3a,b.**

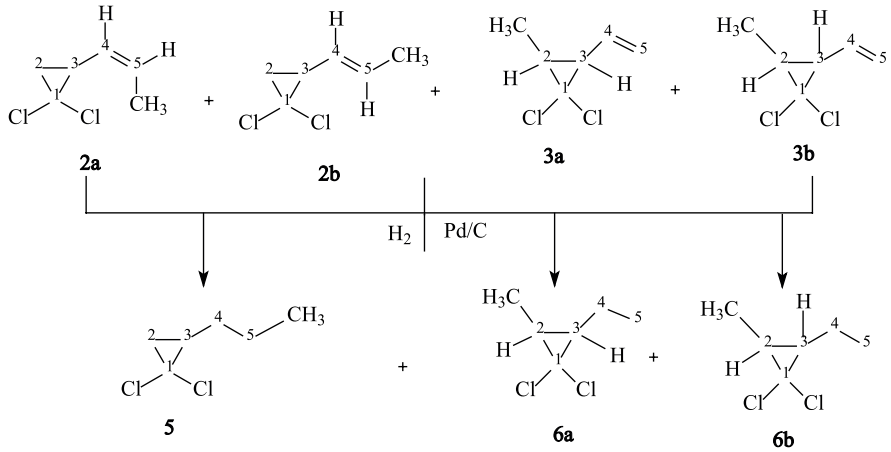

Scheme 3. Reduction of alkenyl-*gem*-dichlorocyclopropanes **2a,b** and **3a,b.**

[2] The starting ratio **2a,b** : **3a,b** = 1 : 3.

multiplet in the range 5.20–5.25 ppm, which is typical for the *cis*-isomer. Meanwhile, for the *trans*-**2b** isomer, the signal of the proton at the C^4 carbon atom appears at 5.28–5.35 ppm, and the proton at C^5 resonates as a doublet at 5.37 ppm (^3J = 13.7 Hz), which confirms the *trans*-configuration of the double bond. In a mixture of compounds **3a** and **3b**, analogous signals of protons at C^4 and C^5 appear as doublet of doublets at 5.75 ppm (^3J = 10 and 13 Hz) and a multiplet at 5.45–5.60 ppm. The protons of the cyclopropane ring at the C^2 the carbon atom for the *cis*-**2a** and *trans*-**2b** isomers appear as two identical doublets at 1.20 ppm (^2J = 5.3 Hz) and 1.72 ppm (^2J = 5.3 Hz). A similar proton signal at the C^2 carbon atom of molecules **3a** and **3b** affords a multiplet at 2.20–2.30 ppm. The proton at the C^3 carbon atom for compound **3a** appears as a singlet at 1.42 ppm, which indicates its *cis*-arrangement, whereas it is high-field shifted to 1.11 ppm and appears as a doublet (^3J = 10 Hz) for compound **3b**, which is typical for the *trans*-configuration of the proton.

In the ^{1}H NMR spectrum of a mixture of hydrogenation products **5** and **6a,b**, the presence of propyl-*gem*-dichlorocyclopropane **5** is evidenced by a triplet signal of the methyl group in the high-field region at 0.95 ppm (^3J = 7 Hz) and a multiplet for two methylene groups of the propyl fragment in the range 1.20–1.25 ppm. The geometric isomers **6a,b** are characterized by the presence of signals attributable to the proton at the C^3 carbon atom conjugated with the ethyl group. Thus, for *cis*-1,1-dichloro-2-methyl-3-ethylcyclopropane **6a**, the proton at the C^3 carbon atom of cyclopropane gives rise to a doublet in the high-field region at 0.90 ppm (^3J = 7 Hz), and for *trans*-1,1-dichloro-2-methyl-3-ethylcyclopropane **6b**, a similar signal appears as a multiplet in the lower region at 1.05–1.10 ppm.

In the ^{13}C NMR spectra of the mixture of alkenyl-*gem*-dichlorocyclopropanes **2a,b** and **3a,b**, the most representative feature is the C^1 signal of the carbon atom at 61.09 ppm. For the *cis*-**2a** isomer, the C^4 and C^5 carbon atoms of the double bond resonate at 126.11 and 128.97 ppm, respectively, whereas for the *trans*-**2b** isomer they appear in lower field, at 126.63 and 130.12 ppm, respectively. For compound **3a**, the presence of high-field signals for the C^2 and C^3 carbon atoms of the cyclopropane ring (31.90 and 35.91 ppm) confirms the *cis*-configuration, whereas the signals at lower field for C^2 and C^3 (33.15 and 40.19 ppm) of molecule **3b** are indicative of the *trans*-configuration of this isomer.

The ^{13}C NMR spectra of a mixture of alkyl derivatives **5** and **6a,b** are characterized by the signals ascribed to the C^1 carbon atoms in the range of 65–67 ppm. The signal of the methyl group of 1,1-dichloro-2-propylcyclopropane **5** appears at 15.03 ppm, whereas those of molecules **6a,b** are high-field shifted to 10.55 and 11.01 ppm, respectively. For compound **6a**, the presence of signals of the C^2 and C^3 carbons of the cyclopropane ring at 32.94 and 34.01 ppm confirms the *cis*-configuration. For molecule **3b**, the signals of C^2 and C^3 atoms appear at lower field (34.71 and 41.39 ppm), indicating the trans configuration of this isomer.

Several pathways can be proposed for the dissociative ionization of a mixture of *gem*-dichlorocyclopropanes **2a,b** and **3a,b**. Thus, the molecule decomposes into a dichlorocyclopropane fragment and the substituent or the molecule loses chlorine atoms while the main carbon skeleton is preserved.

The table shows the values of fission ion mass *m* and the relative intensity of ion peaks *e*, (% of the maximum) for compounds **2a,b** and **3a,b**.

The dissociative ionization of *gem*-dichlorocyclopropanes **6** and **7a,b** and alkenyl-*gem*-dichlorocyclopropanes **2a,b** and **3a,b**, can proceed as follows: the molecule decomposes into a dichlorocyclopropane fragment and a substituent R; alternatively, the molecule loses chlorine atoms while preserving the carbon skeleton.

CONCLUSIONS

The dichlorocarbenation of piperylene by the Makoshi method proceeds quantitatively yielding a mixture of *cis*-, *trans*-1,1-dichloro-2-(prop-1-en-1-yl)cyclopropanes and

Values of fission ion mass *m* and relative intensity of ion peaks *e* (% of maximum) for compounds **2a,b** and **3a,b**

Compound	*m/e* (%)					
	M+ 150/152/154	79	77	115/117	99/101	135/137/139
2a	≤3	100	65	44/12	22/8	≤5
2b	≤4		72	42/12	20/10	≤5
3a	≤4		70	36/12	20/8	
3b	≤8		72	46/26	22/10	≤8

cis-, *trans*-1,1-dichloro-2-vinyl-3-methylcyclopropanes. Hydrogenation of the obtained isomeric alkenyl-*gem*-dichlorocyclopropanes over a palladium catalyst (Pd/C) gives 1,1-dichloro-2-propylcyclopropane and *cis*-, *trans*-1,1-dichloro-2-methyl-3-ethylcyclopropanes. *Cis*-, *trans*-1,1-dichloro-2-(prop-1-en-1-yl)cyclopropanes and *cis*-, *trans*-1,1-dichloro-2-vinyl-3-methylcyclopropanes are converted via thermocatalytic isomerization in the presence of SAPO-34 zeolite to 4,4-dichloro-3-methylcyclopentene in a yield of more than 90%.

Financial support

This research was carried out with the financial support of the grant of the President of the Russian Federation for state support of young Russian scientists—candidates of sciences and doctors of sciences under No. MK-1689.2020.3.

Authors' contribution

A.I. Musin – conducting research, literature analysis;
Y.G. Borisova – collection and processing of the material, writing the text of the article;
G.Z. Raskil'dina – collection and processing of the material, statistical processing;
R.U. Rabaev – consultation on conducting individual stages of the study;
R.R. Daminev – consultation on planning, methodology and implementation of the study;
S.S. Zlotskii – development of the concept of scientific work, critical revision with the introduction of valuable intellectual content.

The authors declare no conflicts of interest.

REFERENCES

1. Kuznetsova T.S., Averina E.B., Yashin N.V., Sedenkova K.N. *Khimiya tsiklopropanovykh soedinenii: dostizheniya i perspektivy. Organicheskaya khimiya v rabotakh N.S. Zefirova: sbornik obzorov* (Chemistry of cyclopropane compounds: achievements and prospects. In: Organic chemistry in the works of N.S. Zefirov: collection of reviews). Ufa: Gilem; 2012. P. 31-71 (in Russ.).

2. Ebner C., Carreira E.M. Cyclopropanation strategies in recent total syntheses. *Chem. Rev.* 2017;117:11651-11679.
https://doi.org/10.1021/acs.chemrev.6b00798

3. Batista G.M.F., De Castro P.P., Carpanez A.G., Horta B.A.C., Amarante G.W. *Gem*-Dichlorocyclopropanation of dicarbonyl derivatives. *Chem. Eur. J.* 2019;25(72):16555-16563.
https://doi.org/10.1002/chem.201904149

4. Stanislawski P.C., Willis A.C., Banwell M.G. *Gem*-dihalocyclopropanes as building blocks in natural-product synthesis: enantioselective total syntheses of *ent*-erythramine and 3-*epi*-erythramine. *Chem. Asian J.* 2007;2:1127-1136.
https://doi.org/10.1002/asia.200700155

5. Liu L.J., Kim E., Hong J.H. Synthesis of novel 6′-spirocyclopropyl-5′-norcarbocyclic adenosine phosphonic acid analogues as potent anti-hiv agents. *Nucleos. Nucleot. Nucls.* 2011;30(10):784-797.
https://doi.org/10.1080/15257770.2011.602656

6. Thankachan A.P., Sindhu K.S., Krishnan K.K., Anilkumar G. Recent advances in the syntheses, transformations and applications of 1,1-dihalocyclopropanes. *Org. Biomol. Chem.* 2015;13(33):8780-8802.
https://doi.org/10.1039/C5OB01088H

7. Kailania M.H., Al-Bakrib A.G., Saadeha H., Al-Hiari Y.M. Preparation and antimicrobial screening of novel 2,2-dichlorocyclopropane–*cis*-dicarbamates and comparison to their alkane and *cis*-alkene analogs. *Jordan Journal of Chemistry.* 2012;7(3):239-252.

СПИСОК ЛИТЕРАТУРЫ

1. Кузнецова Т.С., Аверина Е.Б., Яшин Н.В., Седенкова К.Н. Химия циклопропановых соединений: достижения и перспективы. Органическая химия в работах Н.С. Зефирова: сборник обзоров. Уфа: Гилем; 2012. С. 31-71.

2. Ebner C., Carreira E.M. Cyclopropanation strategies in recent total syntheses. *Chem. Rev.* 2017;117:11651-11679.
https://doi.org/10.1021/acs.chemrev.6b00798

3. Batista G.M.F., De Castro P.P., Carpanez A.G., Horta B.A.C., Amarante G.W. *Gem*-Dichlorocyclopropanation of dicarbonyl derivatives. *Chem. Eur. J.* 2019;25(72):16555-16563.
https://doi.org/10.1002/chem.201904149

4. Stanislawski P.C., Willis A.C., Banwell M.G. *Gem*-dihalocyclopropanes as building blocks in natural-product synthesis: enantioselective total syntheses of *ent*-erythramine and 3-*epi*-erythramine. *Chem. Asian J.* 2007;2:1127-1136.
https://doi.org/10.1002/asia.200700155

5. Liu L.J., Kim E., Hong J.H. Synthesis of novel 6′-spirocyclopropyl-5′-norcarbocyclic adenosine phosphonic acid analogues as potent anti-hiv agents. *Nucleos. Nucleot. Nucls.* 2011;30(10):784-797.
https://doi.org/10.1080/15257770.2011.602656

6. Thankachan A.P., Sindhu K.S., Krishnan K.K., Anilkumar G. Recent advances the syntheses, transformations and applications of 1,1-dihalocyclopropanes. *Org. Biomol.* Chem. 2015;13(33):8780-8802.
https://doi.org/10.1039/C5OB01088H

7. Kailania M.H., Al-Bakrib A.G., Saadeha H., Al-Hiari Y.M. Preparation and antimicrobial screening of novel 2,2-dichlorocyclopropane–*cis*-dicarbamates and comparison to their alkane and *cis*-alkene analogs. *Jordan Journal of Chemistry.* 2012;7(3):239-252.

8. Harvey J.E., Hewitt R.J., Moore P.W., Somarathne K.K. Reactions of 1,2-cyclopropyl carbohydrates. *Pure Appl. Chem.* 2014;86(9):1377-1399.
https://doi.org/10.1515/pac-2014-0403

8. Harvey J.E., Hewitt R.J., Moore P.W., Somarathne K.K. Reactions of 1,2-cyclopropyl carbohydrates. *Pure Appl. Chem.* 2014;86(9):1377-1399.
https://doi.org/10.1515/pac-2014-0403

9. Fedorynski M. Syntheses of *gem*-dihalocyclopropanes and their use in organic synthesis. *Chem. Rev*. 2003;103(4):1099-1132.
https://doi.org/10.1021/cr0100087

10. Dolbier Jr.W.R., Battiste M.A. Structure synthesis, and chemical reactions of fluorinated cyclopropanes and cyclopropenes. *Chem. Rev.* 2003;103(4):1071-1098.
https://doi.org/10.1021/cr010023b

11. Le N.N.T., Klinkerch E.J., Thamattoor D.M. Stereochemistry of dichlorocarbene addition to alkenes: A Collaborative, Discovery-Based Experiment for the Organic Chemistry Laboratory. *J. Chem. Educ.* 2019;96(8):1727-1730.
https://doi.org/10.1021/acs.jchemed.8b00758

12. Komissarova N.G., Belenkova N.G., Shitikova O.V., Spirikhin L.V., Yunusov M.S. Cyclopropanation of betulin and its diacetate with dihalocarbenes. *Russ. J. Org. Chem.* 2004;40(10):1462-1468.
https://doi.org/10.1007/s11178-005-0041-1

13. Merrer D.C., Doubleday C. Dynamic control of dichlorocarbene addition to cyclopropene. *J. Phys. Org. Chem.* 2011;24(10):947-951
https://doi.org/10.1002/poc.1883

14. Lenhardt J.M., Black A.L., Craig S.L. *Gem*-dichlorocyclopropanes as abundant and efficient mechanophores in polybutadiene copolymers under mechanical stress. *J. Am. Chem. Soc*. 2009;131(31):10818-10819.
https://doi.org/10.1021/ja9036548

15. Mahdavi H., Amirsadeghi M. Kinetic study of dichlorocarbene addition to olefins via a quaternized highly branched polyacrylamide as a new multi-site phase transfer catalyst. *Iran. Polym. J.* 2012;21:641-649.
https://doi.org/10.1007/s13726-012-0070-x

16. Makosha M., Fedoryński M. Phase transfer catalysis in dichlorocarbene chemistry: basic principles and specific features. *Rus. Chem. Bul.* 2011;60(11):2141-2146.
https://doi.org/10.1007/s11172-011-0332-3

17. Vikhareva I.N., Shavshukova S.Yu., Udalova E.A. Cyclization reactions using microwave radiation. *Bashkirskii khimicheskii zhurnal = Bashkir Chemical Journal.* 2009;16(3):34-39 (in Russ.).

18. Gordeev E.G., Shkulipa A.Yu., Kirilin A.D. Reactions of dichlorocarbene, dichlorosilylene, and dichlorogermylene with carboranes(12). A theoretical study. *Russ. J. Gen. Chem.* 2014;84(7):1330-1338.
https://doi.org/10.1134/S1070363214070147

19. Raskil'dina G.Z., Borisova Yu.G., Zlotskii S.S. Dichlorocarbenation of conjugated diene hydrocarbons. *Neftekhimiya = Pet. Chem.* 2017;57:278-283.
https://doi.org/10.1134/S0965544117020219

20. Arbuzova T.V., Khamidullina A.R., Zlotsky S.S. Syntheses based on vinil-gem-dichlorcyclopropanes. *Izv. Vyssh. Ucheb. Zaved. Khim. Khim. Tekhnol.* 2007;50(6):15-17 (in Russ.).

21. Demlov E., Demlov Z. *Mezhfaznyi kataliz* (Interphase catalysis). Moscow: Mir; 1987. 485 p. (in Russ.).

22. Raskil'dina G.Z., Borisova Y.G., Davletshin A.R., *et al.* Catalytic Isomerization of substituted vinylcyclopropanes. *Doklady Akademii Nauk = Doklady Chemistry.* 2019;487(1):192-194.
https://doi.org/10.1134/S0012500819070115

9. Fedorynski M. Syntheses of *gem*-dihalocyclopropanes and their use in organic synthesis. *Chem. Rev.* 2003;103(4):1099-1132.
https://doi.org/10.1021/cr0100087

10. Dolbier Jr.W.R., Battiste M.A. Structure synthesis, and chemical reactions of fluorinated cyclopropanes and cyclopropenes. *Chem. Rev.* 2003;103(4):1071-1098.
https://doi.org/10.1021/cr010023b

11. Le N.N.T., Klinkerch E.J., Thamattoor D.M. Stereochemistry of dichlorocarbene addition to alkenes: A Collaborative, Discovery-Based Experiment for the Organic Chemistry Laboratory. *J. Chem. Educ.* 2019;96(8):1727-1730.
https://doi.org/10.1021/acs.jchemed.8b00758

12. Komissarova N.G., Belenkova N.G., Shitikova O.V., Spirikhin L.V., Yunusov M.S. Cyclopropanation of betulin and its diacetate with dihalocarbenes. *Russ. J. Org. Chem.* 2004;40(10):1462-1468.
https://doi.org/10.1007/s11178-005-0041-1

13. Merrer D.C., Doubleday C. Dynamic control of dichlorocarbene addition to cyclopropene. *J. Phys. Org. Chem.* 2011;24(10):947-951.
https://doi.org/10.1002/poc.1883

14. Lenhardt J.M., Black A.L., Craig S.L. *Gem*-dichlorocyclopropanes as abundant and efficient mechanophores in polybutadiene copolymers under mechanical stress. *J. Am. Chem. Soc.* 2009;131(31):10818-10819.
https://doi.org/10.1021/ja9036548

15. Mahdavi H., Amirsadeghi M. Kinetic study of dichlorocarbene addition to olefins via a quaternized highly branched polyacrylamide as a new multi-site phase transfer catalyst. *Iran. Polym. J.* 2012;21:641-649.
https://doi.org/10.1007/s13726-012-0070-x

16. Макоша М., Федорыньски М. Межфазный катализ в химии дихлоркарбена: основные принципы и характерные особенности. *Известия Академии наук. Серия химическая.* 2011;11:2101-2101.

17. Вихарева И.Н., Шавшукова С.Ю., Удалова Е.А. Реакции циклизации с использованием микроволнового излучения. *Баш. хим. журнал.* 2009;16(3):34-39.

18. Gordeev E.G., Shkulipa A.Yu., Kirilin A.D. Reactions of dichlorocarbene, dichlorosilylene, and dichlorogermylene with carboranes(12). A theoretical study. *Russ. J. Gen. Chem.* 2014;84(7):1330-1338.
https://doi.org/10.1134/S1070363214070147

19. Раскильдина Г.З., Борисова Ю.Г., Злотский С.С. Дихлоркарбенирование сопряженных диеновых углеводородов. *Нефтехимия.* 2017;57(2):220-225.
https://doi.org/10.7868/S0028242117020149

20. Арбузова Т.В., Хамидуллина А.Р., Злотский С.С. Синтезы на основе винил-*гем*-дихлорцилопропанов. Изв. вузов. *Химия и хим. технология.* 2007;50(6):15-17.

21. Демлов Э., Демлов З. Межфазный катализ. М.: Мир; 1987. 485 с.

22. Раскильдина Г.З., Борисова Ю.Г., Давлетшин А.Р., Злотский С.С. Каталитическая изомеризация замещенных винилциклопропанов. *ДАН.* 2019;487(3):266-269.
https://doi.org/10.31857/S0869-56524873266-269

23. Трегер Ю.А., Розанов В.Н., Соколова С.В., Мурашева О.П. Получение этилена и пропилена из природного газа через промежуточный синтез хлористого метила и последующий его каталитический пиролиз. *Катализ в промышленности.* 2012;3:15а-20.

24. Oosthuizen R.S., Nyamori V.O. Carbon Nanotubes as Supports for Palladium and Bimetallic Catalysts for Use in Hydrogenation Reactions. *Platinum Metals Rev.* 2011;55(3):154-169.
https://doi.org/10.1595/147106711X577274

23. Treger Y.A., Rozanov V.N., Sokolova S.V., Murasheva O.P. Proceeding of ethylene and propylene from natural gas via the intermediate synthesis of methyl choride and its subsequent catalytic pyrolysis. *Kataliz v promyshlennosti = Catalysis in Industry.* 2012;3:15a-20 (in Russ.).

24. Oosthuizen R.S., Nyamori V.O. Carbon Nanotubes as Supports for Palladium and Bimetallic Catalysts for Use in Hydrogenation Reactions. Platinum Metals Rev. 2011;55(3):154-169. https://doi.org/10.1595/147106711X577274

25. Ilyin S.O., Petrukhina N.N., Kostyuk A.V., Filatova M.P., Antonov S.V., Maksimov A.L., Dzhabarov E.G. Hydrogenation of indene-coumarone resin on palladium catalysts for use in polymer adhesives. *Russ. J. Appl. Chem.* 2019;92(8):1143-1152. https://doi.org/10.1134/S1070427219080135

26. Brusentsova E.A., Zlotskii S.S., Kutepov B.I., Khazipova A.N. Relative activity of alkenyl-*gem*-dichlorocyclopropanes in the reactions of hydrogenation and alkylation. *Russ. J. Appl. Chem.* 2009;82(6):1029-1032. https://doi.org/10.1134/S1070427209060196

23. Treger Y.A., Rozanov V.N., Sokolova S.V., Murasheva O.P. Proceeding of ethylene and propylene from natural gas via the intermediate synthesis of methyl choride and its subsequent catalytic pyrolysis. *Kataliz v promyshlennosti = Catalysis in Industry.* 2012;3:15a-20 (in Russ.).

24. Oosthuizen R.S., Nyamori V.O. Carbon Nanotubes as Supports for Palladium and Bimetallic Catalysts for Use in Hydrogenation Reactions. Platinum Metals Rev. 2011;55(3):154-169. https://doi.org/10.1595/147106711X577274

25. Ilyin S.O., Petrukhina N.N., Kostyuk A.V., Filatova M.P., Antonov S.V., Maksimov A.L., Dzhabarov E.G. Hydrogenation of indene-coumarone resin on palladium catalysts for use in polymer adhesives. *Russ. J. Appl. Chem.* 2019;92(8):1143-1152. https://doi.org/10.1134/S1070427219080135

26. Brusentsova E.A., Zlotskii S.S., Kutepov B.I., Khazipova A.N. Relative activity of alkenyl-*gem*-dichlorocyclopropanes in the reactions of hydrogenation and alkylation. *Russ. J. Appl. Chem.* 2009;82(6):1029-1032. https://doi.org/10.1134/S1070427209060196

About the authors:

Airat I. Musin, Postgraduate Student, Department of General, Analytical and Applied Chemistry, Ufa State Petroleum Technological University, Branch in Sterlitamak (2, Oktyabrya pr., Sterlitamak, 453118, Russia). E-mail: musin_1995@list.ru. ResearcherID R-9142-2016, https://orcid.org/0000-0002-8662-9680

Yulianna G. Borisova, Cand. of Sci. (Chemistry), Teacher, Department of General, Analytical and Applied Chemistry, Ufa State Petroleum Technological University, Branch in Sterlitamak (2, Oktyabrya pr., Sterlitamak, 453118, Russia). E-mail: yulianna_borisova@mail.ru. ResearcherID P-9744-2017, Scopus Author ID 56526865000, https://orcid.org/0000-0001-6452-9454

Gul'nara Z. Raskil'dina, Cand. of Sci. (Chemistry), Associate Professor, Department of General, Analytical and Applied Chemistry, Ufa State Petroleum Technological University (1, Kosmonavtov ul., Ufa, 450064, Russia). E-mail: graskildina444@mail.ru. ResearcherID F-1619-2017, Scopus Author ID 56069888400, https://orcid.org/0000-0001-9770-5434

Ruslan U. Rabaev, Cand. of Sci. (Engineering), Vice Rector for Innovation and Scientific Work, Ufa State Petroleum Technological University (1, Kosmonavtov ul., Ufa, 450064, Russia). E-mail: nauka_ugntu@mail.ru. Scopus Author ID 57207916610.

Rustem R. Daminev, Dr. of Sci. (Engineering), Professor, Director of Branch in Sterlitamak, Ufa State Petroleum Technological University, Branch in Sterlitamak (2, Oktyabrya pr., Sterlitamak, 453118, Russia). E-mail: daminew@mail.ru. Scopus Author ID 15026168000, https://orcid.org/0000-0001-8673-5240

Simon S. Zlotskii, Dr. of Sci. (Chemistry), Professor, Head of Department of General, Analytical and Applied Chemistry, Ufa State Petroleum Technological University (1, Kosmonavtov ul., Ufa, 450064, Russia). E-mail: nocturne@mail.ru. ResearcherID W-6564-2018, Scopus Author ID 6701508202, https://orcid.org/0000-0001-6365-5010

Об авторах:

Мусин Айрат Ильдарович, аспирант кафедры общей, аналитической и прикладной химии, ФГБОУ ВО «Уфимский государственный нефтяной технический университет», филиал в г. Стерлитамак (453118, Россия, г. Стерлитамак, пр-т Октября, д. 2). E-mail: musin_1995@list.ru. ResearcherID R-9142-2016, https://orcid.org/0000-0002-8662-9680

Борисова Юлианна Геннадьевна, кандидат химических наук, преподаватель кафедры общей, аналитической и прикладной химии, филиал ФГБОУ ВО «Уфимский государственный нефтяной технический университет», филиал в г. Стерлитамак (453118, Россия, г. Стерлитамак, пр-т Октября, д. 2). E-mail: yulianna_borisova@mail.ru. ResearcherID P-9744-2017, Scopus Author ID 56526865000, https://orcid.org/0000-0001-6452-9454

Раскильдина Гульнара Зинуровна, кандидат химических наук, доцент кафедры общей, аналитической и прикладной химии, ФГБОУ ВО «Уфимский государственный нефтяной технический университет» (450064, Россия, г. Уфа, ул. Космонавтов, д. 1). E-mail: graskildina444@mail.ru. ResearcherID F-1619-2017, Scopus Author ID 56069888400, https://orcid.org/0000-0001-9770-5434

Рабаев Руслан Уралович, кандидат технических наук, проректор по инновационной и научной работе ФГБОУ ВО «Уфимский государственный нефтяной технический университет» (450064, Россия, г. Уфа, ул. Космонавтов, д. 1). E-mail: nauka_ugntu@mail.ru. Scopus Author ID 57207916610.

Даминев Рустем Рифович, доктор технических наук, профессор, директор филиала в г. Стерлитамак ФГБОУ ВО «Уфимский государственный нефтяной технический университет», филиал в г. Стерлитамак (453118, Россия, г. Стерлитамак, Октября пр-т, д. 2). E-mail: daminew@mail.ru. Scopus Author ID 15026168000. https://orcid.org/0000-0001-8673-5240

Злотский Семен Соломонович, доктор химических наук, заведующий кафедрой общей, аналитической и прикладной химии, ФГБОУ ВО «Уфимский государственный нефтяной технический университет» (450064, Россия, г. Уфа, ул. Космонавтов, д. 1). E-mail: nocturne@mail.ru. ResearcherID W-6564-2018, Scopus Author ID 6701508202, https://orcid.org/0000-0001-6365-5010

The article was submitted: August 10, 2020; approved after reviewing: August 24, 2020; accepted for publication: September 13, 2020.

Translated from Russian into English by H. Moshkov
Edited for English language and spelling by Enago, an editing brand of Crimson Interactive Inc.

CHEMISTRY AND TECHNOLOGY OF MEDICINAL COMPOUNDS AND BIOLOGICALLY ACTIVE SUBSTANCES
ХИМИЯ И ТЕХНОЛОГИЯ ЛЕКАРСТВЕННЫХ ПРЕПАРАТОВ И БИОЛОГИЧЕСКИ АКТИВНЫХ СОЕДИНЕНИЙ

ISSN 2686-7575 (Online)

https://doi.org/10.32362/2410-6593-2020-15-5-26-35

UDC 547.1

RESEARCH ARTICLE

Synthesis and biological activity of *N*-phosphonacetyl-L-aspartate's structural analogs *N*-(α-dietoxyphosphorylcyclopropylcarbonyl)-amino acids

Ivan S. Kuzmin[@], Danil Yu. Yuriev, Grigorii A. Toporkov, Antonida V. Kalistratova, Leonid V. Kovalenko

D.I. Mendeleev University of Chemical Technology of Russia, Moscow, 125047 Russia
[@]Corresponding author, e-mail: kyzka06@mail.ru

Objectives. *With the development and improvement of new delivery systems for substances of various natures, organophosphorus compounds with an antimetabolic mechanism of action have become relevant again. A few examples of them are organophosphorus analogs of carboxylic acids, such as N-phosphonacetyl-L-aspartate (PALA) and N-phosphonacetyl-L-isoasparagine, both of which are bio-rationally developed analogs of the transition state of carbamoylaspartate in the biosynthesis of pyrimidine bases, which is catalyzed by the enzyme aspartate transcarbamoylase (ATCase). Despite their high activity, these compounds have not found widespread use as anticancer agents due to a large number of side-effects and low bioavailability. Given the emerging opportunities for the delivery of phosphate and phosphonate derivatives into target cells, obtaining more effective analogs of PALA seems to be an interesting and promising research objective. The goal of the present study was thus to synthesize and study the biological activities of novel PALA analogs that are derivatives of phosphonacetic acid.*

Methods. *For directed work within the framework of the study, we used the molecular docking method, which allowed us to simulate the binding of N-(a-diethoxyphosphorylcyclopropylcarbonyl)-substituted amino acids to ATCase. The target compounds were synthesized using classical methods of organic synthesis. The obtained compounds' cytotoxicity was probed in relation to cell lines of human breast cancer (MDA-MB-231), skin cancer (A-375), and glioblastoma (U-87 MG).*

Results. *The synthesis of eight novel N-(a-diethoxyphosphorylcyclopropylcarbonyl)-substituted amino acids was carried out. A few of the synthesized derivatives were tested for anticancer activity, but none displayed significant cytotoxicity.*

Conclusions. *N-(α-diethoxyphosphorylcyclopropylcarbonyl)-substituted amino acids are synthetically available analogs of PALA, a compound capable of strong interaction with ATCase. However, the compounds synthesized in this work did not display any pronounced anticancer properties. One of the reasons for the observed low activity may be the presence of ether groups in the phosphonate building block.*

Keywords: *phosphonocarboxylic acids, N-phosphonacetyl-L-aspartate (PALA), aspartate transcarbamylase (ATCase), α-diethoxyphosphonacetic acid, α-diethoxyphosphorylcyclopropylcarboxylic acid, N-(α-diethoxyphosphorylcyclopropylcarbonyl)amino acids.*

For citation: Kuzmin I.S., Yuriev D.Yu., Toporkov G.A., Kalistratova A.V., Kovalenko L.V. Synthesis and biological activity of *N*-phosphonacetyl-L-aspartate's structural analogs *N*-(α-dietoxyphosphorylcyclopropylcarbonyl)amino acids. *Tonk. Khim. Tekhnol. = Fine Chem. Technol.* 2020;15(5):26-35 (Russ., Eng.). https://doi.org/10.32362/2410-6593-2020-15-5-26-35

НАУЧНАЯ СТАТЬЯ

Синтез и биологическая активность *N*-(α-диэтоксифосфорилциклопропилкарбонил)аминокислот – структурных аналогов *N*-фосфонацетил-L-аспартата

И.С. Кузьмин[@], Д.Ю. Юрьев, Г.А. Топорков, А.В. Калистратова, Л.В. Коваленко

Российский химико-технологический университет им. Д.И. Менделеева, Москва, 125047 Россия

[@]Автор для переписки, e-mail: kyzka06@mail.ru

Цели. *С развитием и совершенствованием новых систем доставки для веществ различного характера, вновь приобретают актуальность фосфорорганические соединения с антиметаболитным механизмом действия. К ним можно отнести, например, фосфорорганические аналоги карбоновых кислот, такие как N-фосфонацетил-L-аспартат (PALA) и N-фосфонацетил-L-изоаспарагин, являющиеся биорационально разработанными аналогами переходного состояния карбамоиласпартата в реакции биосинтеза пиримидиновых оснований, которая катализируется ферментом аспартат-транскарбамоилазой (ATCase). Несмотря на высокую активность эти соединения не нашли широкого применения из-за большого количества побочных эффектов и низкой биодоступности. С учетом открывающихся возможностей по доставке фосфатных и фосфонатных производных в клетки-мишени, получение более эффективных аналогов PALA кажется интересной и перспективной задачей. Поэтому целью данной работы являлись синтез и исследование биологической активности новых производных фосфонуксусной кислоты – N-(α-диэтоксифосфорилциклопропилкарбонил)-замещенных аминокислот – аналогов N-фосфоноацетил-L-аспартата (PALA).*

Методы. *Для направленной работы в рамках исследования применяли метод молекулярного докинга, который позволяет смоделировать связывание N-(α-диэтоксифосфорилциклопропилкарбонил)-замещенных аминокислот с аспартат-транскарбамоилазой. Целевые соединения были синтезированы с использованием классических методов органического синтеза. Исследование цитотоксичности проводили по отношению к клеточным линиям рака молочной железы человека (MDA-MB-231), рака кожи (A-375) и глиобластомы (U-87 MG).*

Результаты. *В рамках работы был осуществлен синтез восьми новых N-(α-диэтоксифосфорилциклопропилкарбонил)-замещенных аминокислот. Исследование ряда синтезированных производных на противораковую активность не выявило значимого проявления цитотоксичности.*

Выводы. *N-(α-диэтоксифосфорилциклопропилкарбонил)-замещенные аминокислоты представляют собой синтетически доступные аналоги PALA, способные к более сильному взаимодействию с ATCase. Тем не менее синтезированные в данной работе соединения не проявили выраженных противораковых свойств. Одной из причин низкой активности может быть наличие эфирных групп в фосфонатном структурном элементе.*

Ключевые слова: *фосфонкарбоновые кислоты, N-фосфонацетил-L-аспартат (PALA), аспартат-транскарбомоилаза (ATCase), диэтоксифосфорилуксусная кислота, α-диэтоксифосфорилциклопропанкарбоновая кислота, N-(α-диэтоксифосфорилциклопропилкарбонил)-замещенные аминокислоты.*

Для цитирования: Кузьмин И.С., Юрьев Д.Ю., Топорков Г.А., Калистратова А.В., Коваленко Л.В. Синтез и биологическая активность *N*-(α-диэтоксифосфорилциклопропилкарбонил)аминокислот – структурных аналогов *N*-фосфонацетил-L-аспартата. 2020;15(5):26-35. https://doi.org/10.32362/2410-6593-2020-15-5-26-35

INTRODUCTION

Antineoplastic drugs with an antimetabolic mechanism of activity have become established in the practice of oncological disease treatment. Although these drugs differ in structure, intracellular metabolism, and mechanism of cytotoxic action, all of them, in one way or another, are analogs of natural metabolites, and they are able to compete with these metabolites, both with respect to transport pathways into the cell and participation in key enzymatic processes. Antimetabolites of nucleic acid biosynthesis are especially relevant for the treatment of oncological diseases.

A promising anticancer drug identified in the 1980s was *N*-phosphonacetyl-L-aspartate (PALA) **1**, which was developed as a result of the bio-rational approach (Fig. 1). In fact, the anticancer activity of PALA is based on its structural similarity with the transition state of carbamoyl aspartate, which is involved in the biosynthesis of pyrimidine bases catalyzed by aspartate transcarbamoylase (ATCase) [1–4].

PALA showed high activity against solid tumors and passed two phases of clinical trials [5, 6]. Unfortunately, as is true for many other organophosphorus compounds, the high *in vitro* activity of PALA was not reproduced *in vivo* due to the low bioavailability of this compound and the large number of side-effects associated with its administration [7, 8]. Therefore, the synthesis of new derivatives of phosphonacetic acid with potential anticancer activity and improved pharmacological properties is of high research interest.

Known derivatives of phosphonacetic acid, which are structural analogs of PALA, include compounds **2–4**, whose structures are reported in Fig. 2. These compounds have a lower total charge and improved pharmacological properties than PALA, but they also display significantly lower activity than the mentioned species [9].

Considering the structural similarity of the PALA to the intermediate of carbamoylaspartate biosynthesis, we assumed that the key significance to increase the biological activity of phosphonacetic acid derivatives was the value of the optimal P–C bond angle, which will ensure the stability of the conformation most favorable for the formation of a complex with the active center of the enzyme. Additionally, we

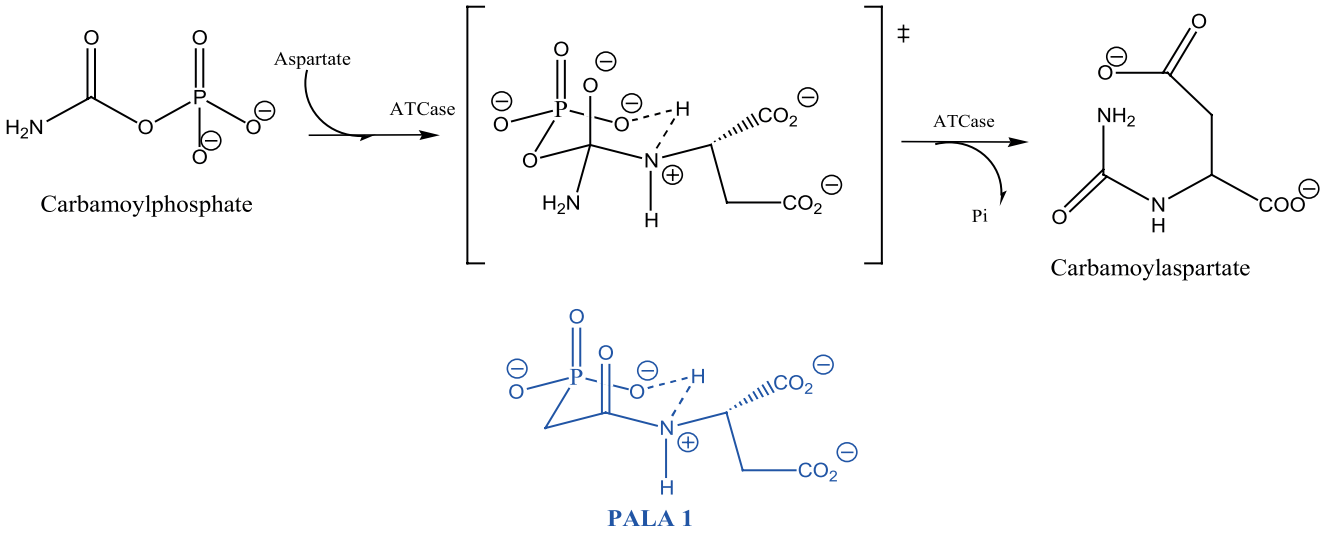

Fig. 1. Structural similarity between *N*-phosphonacetyl-L-aspartate and the intermediate of carbamoylaspartate biosynthesis.

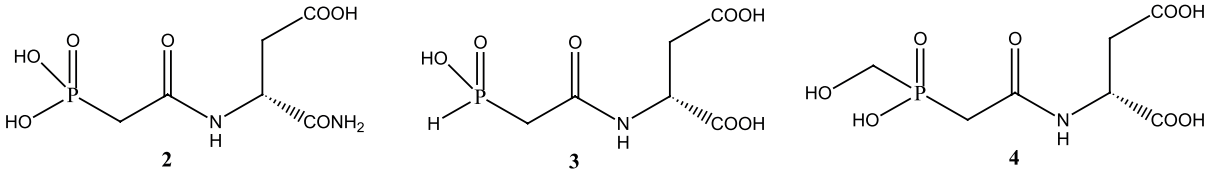

Fig. 2. Structural formulas of *N*-phosphonacetyl-L-aspartate analogs.

considered a pronounced hydrophobic fragment in the structure of a molecule due to the presence of a "hydrophobic pocket" in the ATCase structure, which will increase the strength of the binding between enzyme and the substrate. These objectives may be achieved introducing bulky substituents on the carbon atom of the phosphonoacetate skeleton. Cyclopropanyl-substituted phosphonacetic acids are interesting from the standpoint of synthetic accessibility, variation of the P–C bond angle, and the content of the hydrophobic fragments. In fact, the synthesis and investigation of the anticancer activity of this family of compounds were carried out within the framework of the present study.

MATERIALS AND METHODS

Chromato-mass spectrometric analyses were conducted on a Thermo Fisher Scientific Surveyor MSQ (*Thermo Fisher Scientific*, USA) with a Phenomenex Onyx Monoliythic C18 25 × 4.6 mm high performance liquid chromatography column (*Phenomenex*, USA). A two-component mixture of a 0.1% solution of formic acid and acetonitrile (solvent–100% dimethyl sulfoxide (DMSO), gradient elution, flow rate = 1.5 mL/min, temperature = 25°C, type of ionization used at atmospheric pressure: electrospray) was used as mobile phase. Nuclear magnetic resonance (NMR) ^{1}H spectra were recorded on a Varian MercuryPlus 400 instrument (*Varian*, USA) ($CDCl_3$, DMSO-d_6, tetramethylsilane as internal standard). Melting points were determined on a Stuart SMP20 apparatus (*Stuart*, UK). For thin layer chromatography, we used Merck Thin Layer Chromatography Silica gel 60 F_{254} aluminum plates (size 10 × 20 cm) (*Merck*, Germany). For column chromatography, we used Merck silica gel 60 with a particle size of 0.015 mm to 0.040 mm. A CEM DU 9369 microwave reactor (*CEM Corporation*, USA) was used to carry out reactions under microwave irradiation.

DMSO was distilled over calcium hydride before use; dibromoethane was distilled under reduced pressure; the amino acids used were not pre-purified; triethylamine was distilled over KOH; triethyl phosphite was not pre-purified; extraction solvents were used without any prior treatment.

EXPERIMENTAL

Preparation of triethyl ester of phosphonoacetic acid (5).

In a septum-equipped 10-mL test tube suitable for use in a microwave reactor were placed 3.32 g (0.02 mol) of triethyl phosphite and 2.45 g (0.02 mol) of the ethyl ester of α-chloroacetic acid. The reaction was carried out under 250-W-power microwave irradiation and a temperature of 170°C for 1 h. The isolation of the final product was conducted by vacuum distillation on an oil pump with a yield of 3.85 g (86%). T_{boil} = 110°C (0.1 mm Hg). ^{1}H NMR spectrum (400 MHz, DMSO-d_6): δ (ppm) 4.07 (dq, J = 15.1, 7.1 Hz, 6H), 3.10 (d, J = 21.4 Hz, 2H), 1.22 (dt, J = 18.4, 7.1 Hz, 9H).

Preparation of α-diethoxyphosphorylcyclopropane carboxylic acid ethyl ester (6).

In a 500-mL flat-bottom flask were mixed together 15 g (0.067 mol) of crushed KOH and 100 mL of freshly distilled DMSO. Under stirring, to the resulting suspension were added dropwise in succession 7.48 g (0.03 mol) of diethoxyphosphonoacetic acid ethyl ester and 25.19 g (0.268 mol) of dibromoethane. Another 170 mL of DMSO were then added to the reaction mixture. The resulting suspension was stirred at room temperature for 72 h. In order to separate the reaction products from DMSO, 200 mL of water were added to the reaction mixture, and an extraction was performed using diethyl ether (three consecutive extractions, with 100 mL of solvent at a time) and then chloroform (two consecutive extractions, with 100 mL of solvent at a time). The resulting organic phases were dried over Na_2SO_4, filtered off, combined, and concentrated on a rotary evaporator. The final product was isolated by vacuum distillation on an oil pump with a yield of 5.60 g (67%) . T_{boil} = 110–115°C (0.1 mm Hg). ^{1}H NMR spectrum (400 MHz, DMSO-d_6): δ (ppm) 4.16–3.96 (m, 6H), 1.38–1.27 (m, 1H), 1.21 (dt, J = 16.0, 7.1 Hz, 1H).

Preparation of α-diethoxyphosphorylcyclopropane carboxylic acid (7).

In a 500-mL flat-bottom flask, 20.573 g (0.08 mol) of diethoxyphosphorylcyclopropanecarboxylic acid ethyl ester and 140 mL of 1N (0.14 mol) aqueous KOH solution were added. The mixture thus obtained was stirred for 30 min at room temperature, and it was then acidified with a 20% H_2SO_4 to reach a pH of about 2

(controlled by litmus paper). The mixture was then stirred at room temperature for an additional 30 min. In order to isolate the target compound, an extraction with chloroform (four consecutive extractions, with 50 mL of solvent at a time) was performed. The resulting organic phases were dried over Na_2SO_4, filtered off, combined, and concentrated on a rotary evaporator. The product was purified by recrystallization from diethyl ether with the addition of hexane. White hygroscopic crystals with a yellowish tint weighing 10.7 g were thus obtained, for a reaction yield of 60%. The product's melting point was 85–87°C. ^{1}H NMR spectrum (300 MHz, DMSO): δ (ppm) 4.16 (dq, *J* = 14.2, 7.1 Hz, 4H), 1.45–1.38 (m, 4H), 1.35 (t, *J* = 7.0 Hz, 6H).

Preparation of α-diethoxyphosphorylcyclopropanecarboxylic acid chloride.

In a 25-mL flask were placed 5 g (0.023 mol) of α-diethoxyphosphorylcyclopropanecarboxylic acid and 7 mL (0.23 mol) of $SOCl_2$. The mixture thus obtained was heated under stirring at 50°C for 1 h until gas evolution from the reaction mixture ceased; subsequently, excess $SOCl_2$ was distilled off in a water-jet pump vacuum. The resulting acid chloride was immediately added to the acylation reaction without preliminary purification.

Procedure for the synthesis of α-diethoxyphosphoryl-cyclopropanecarboxylic acid amides 8–11.

In a 100-mL three-neck flask equipped with a thermometer, a dropping funnel, and a reflux condenser comprising a calcium chloride tube, were placed 0.014 mol of dry amino acid ethyl or methyl ester hydrochloride, after it had been ground it in a porcelain dish. About 30 mL of chloroform was then added to the reaction flask, and 0.04 mol of triethylamine were added under stirring using a pipette. The reaction mixture was cooled to 0°C in a bath with ice and salt and stirred for 0.5 h. Afterwards, 0.014 mol of α-diethoxyphosphorylcyclopropanecarboxylic acid chloride were added using a dropping funnel, while not allowing the temperature of the mixture to rise above 5°C. After adding the entire amount of acid chloride, the mixture was stirred for another 0.5 h at room temperature. The solvent of the reaction mixture was then evaporated on a rotary evaporator, and to the residue were added 100 mL of ethyl acetate; the mixture thus obtained was stirred for 10 min at room temperature, and the triethylamine hydrochloride was filtered off. The solvent of the resulting filtrate was again evaporated on a rotary evaporator. A viscous yellow-orange liquid was obtained. The product was purified by column chromatography on silica gel using ethyl acetate as eluent. A viscous liquid characterized by a bright yellow color was obtained.

***N*-(α-diethoxyphosphorylcyclopropylcarbonyl)-glycine ethyl ester (8)**, 3.18 g (74%) yield.

^{1}H NMR spectrum (400 MHz, DMSO-d_6): δ (ppm) 8.04 (t, *J* = 5.5 Hz, 1H), 4.20–4.04 (m, 6H), 3.94 (d, *J* = 5.7 Hz, 2H), 1.29 (t, *J* = 7.1 Hz, 9H), 1.26–1.13 (m, 4H).

Liquid chromatography–mass spectrometry (LC–MS) data, m/z (*I*, %): exp. 308.062 $[MH]^+$, 100%; calc. 308.29 $[MH]^+$.

***N*-(α-diethoxyphosphorylcyclopropylcarbonyl)-aspartic acid dimethyl ester (11),** 3.88 g (76%) yield. ^{1}H NMR spectrum (400 MHz, DMSO-d_6): δ (ppm) 8.19 (d, *J* = 7.9 Hz, 1H), 4.74 (dt, *J* = 7.9, 5.5 Hz, 1H), 4.08 (dq, *J* = 11.3, 7.1 Hz, 4H), 3.64 (d, *J* = 14.3 Hz, 6H), 2.93–2.74 (m, 2H), 1.30–1.22 (m, 6H), 1.22–1.06 (m, 4H).

LC–MS data, m/z (*I*, %): exp. 366.108 $[MH]^+$, 100%; calc. 366.13 $[MH]^+$.

***N*-(α-diethoxyphosphorylcyclopropylcarbonyl)-methionine ethyl ester (9)**, 3.38 g (77%) yield. ^{1}H NMR spectrum (400 MHz, $CDCl_3$): δ (ppm) 8.05 (d, *J* = 7.5 Hz, 1H), 4.67 (td, *J* = 7.4, 4.9 Hz, 1H), 4.17 (m, 4H), 3.74 (s, 3H), 2.58–2.46 (m, 2H), 2.17 (tt, *J* = 14.2, 6.3 Hz, 1H), 2.08 (s, 3H), 2.06–1.95 (m, 1H), 1.51–1.42 (m, 2H), 1.35 (q, *J* = 7.3 Hz, 6H), 1.31–1.22 (m, 2H).

LC–MS data, m/z (*I*, %): exp. 354.336 $[MH]^+$, 100%; calc. 354.38 $[MH]^+$.

***N*-(α-diethoxyphosphorylcyclopropylcarbonyl)-γ-aminobutyric acid methyl ester (10),** 3.77 g (84%) yield. ^{1}H NMR spectrum (400 MHz, DMSO-d_6): δ (ppm) 7.71 (t, *J* = 5.5 Hz, 1H), 4.21–3.98 (m, 4H), 3.62 (s, 3H), 3.16 (q, *J* = 6.5 Hz, 2H), 2.42–2.29 (m, 2H), 1.70 (p, *J* = 7.1 Hz, 2H), 1.28 (t, *J* = 7.0 Hz, 6H), 1.24–1.01 (m, 4H).

Hydrolysis of the esters of N-(α-diethoxyphosphorylcyclo-propylcarbonyl)amino acids 12–15.

6.51 mmol of the ester of the *N*-(α-diethoxyphosphoryl-cyclopropylcarbonyl) amino acid was placed in a 50-mL flat-bottom flask; 7.9 mmol of KOH in the form of a 1 M solution were then added to the mixture under stirring. Stirring was carried out for another 24 h at room temperature. The potassium salt solution was then acidified with 20% HCl to reach a pH of about 3, and it was then stirred for 30 min at room temperature. At the end of the reaction, the solvent was removed by evaporation on a rotary evaporator. 50 mL of isopropyl alcohol were added to the resulting mixture, and the thus-formed precipitate was separated. The filtrate was concentrated on a rotary evaporator and cooled in a freezer until the desired product was observed to precipitate in crystalline form.

***N*-(α-diethoxyphosphorylcyclopropylcarbonyl)-glycine (12),** 1.27 g (70%) yield. Melting point: 75–77°C. ^{1}H NMR spectrum (400 MHz, DMSO-d_6): δ (ppm) 7.94 (t, *J* = 5.5 Hz, 1H), 4.19–4.01 (m, 4H), 3.83 (d, *J* = 5.5 Hz, 2H), 1.24 (t, *J* = 7.0 Hz, 6H), 1.22–1.00 (m, 4H).

LC–MS data, m/z (*I*, %): exp. 279.97 $[MH]^+$, 100%; calc. 280.24 $[MH]^+$.

***N*-(α-diethoxyphosphorylcyclopropylcarbonyl)-aspartic acid (15),** 1.18 g (54%) yield. ^{1}H NMR spectrum (400 MHz, DMSO-d_6): δ (ppm) 8.32 (s, 1H), 8.13 (d, *J* = 7.8 Hz, 1H), 4.58 (dt, *J* = 7.9, 5.0 Hz, 1H), 4.12–4.02 (m, 4H), 2.82–2.63 (m, 2H), 1.29–1.21 (m, 6H), 1.21–1.13 (m, 4H).

LC–MS data, m/z (*I*, %): exp. 338.111 $[MH]^+$, 100%; calc. 338.27 $[MH]^+$.

***N*-(α-diethoxyphosphorylcyclopropylcarbonyl)-methionine (13),** 1.56 g (68%) yield. ^{1}H NMR spectrum (400 MHz, $CDCl_3$): δ (ppm) 8.00 (d, *J* = 7.3 Hz, 1H), 4.65 (td, *J* = 7.2, 5.1 Hz, 1H), 4.17 (p, *J* = 5.7 Hz, 4H), 2.72–2.48 (m, 2H), 2.30–2.15 (m, 1H), 2.08 (s, 3H), 2.07–1.95 (m, 1H), 1.56–1.40 (m, 2H), 1.38–1.31 (m, 6H) 1.31–1.22 (m, 2H).

LC–MS data, m/z (*I*, %): exp. 354.336 $[MH]^+$, 100%; calc. 354.38 $[MH]^+$.

***N*-(α-diethoxyphosphorylcyclopropylcarbonyl)-γ-aminobutyric acid (14),** 1.28 g (64%) yield. ^{1}H NMR spectrum (400 MHz, $CDCl_3$): δ (ppm) 9.14 (s, 1H), 7.70 (t, *J* = 5.7 Hz, 1H), 4.14 (dt, *J* = 8.2, 7.0 Hz, 4H), 3.32 (q, *J* = 6.6 Hz, 2H), 2.36 (t, *J* = 7.3 Hz, 2H), 1.85 (h, *J* = 7.5 Hz, 2H), 1.54–1.39 (m, 2H), 1.32 (t, *J* = 7.1 Hz, 6H), 1.28–1.15 (m, 2H).

LC–MS data, m/z (*I*, %): exp. 308.059 $[MH]^+$, 100%; calc. 308.29 $[MH]^+$.

RESULTS AND DISCUSSION

In order to design a structure acceptable for binding to ATCase (Protein Data Bank code 5G1N[1]), we applied a molecular modeling method using the AutoDock Vina 1.1.2 program [10]. The optimization of geometric parameters was carried out using the molecular mechanics functionality in the Chimera 1.13.1 program[2]. Docking calculations made it possible to show that ATCase has a hydrophobic "pocket" where derivatives of phosphonacetic acid with cyclic substituents at the carbon atom can be incorporated with high probability (Fig. 3). Based on this method, it was also shown that the substitution of an amino acid residue in ATCase affects the value of the substrate–enzyme binding constant. Therefore, we conducted a series of experiments to obtain target *N*-(α-diethoxyphosphorylcyclopropylcarbonyl)-substituted amino acids with various amino acid residues.

The preparation of *N*-(α-diethoxyphosphorylcyclopropylcarbonyl)amino acid esters was carried out according to the scheme reported in Fig. 4. α-Diethoxyphosphorylcyclopropanecarboxylic acid **7** was obtained implementing a multi-stage synthesis whereby triethyl phosphite and ethyl chloroacetate were used as initial substrates; in fact, as a result of the Arbuzov reaction conducted under microwave irradiation conditions, the triethyl phosphonoacetic acid **5** was obtained [11, 12].

Taking into account the presence of an active methylene group in the structure of phosphonacetic acid and its derivatives, we obtained the complete ethyl ester of α-diethoxyphosphorylcyclopropanecarboxylic acid **6** as a result of an interphase alkylation reaction with 1,2-dibromoethane of phosphonoacetic acid triester, in the presence of dimethyl sulfoxide and potassium hydroxide. The complete ester of α-diethoxyphosphorylcyclopropanecarboxylic acid was then subjected to hydrolysis in an alkaline medium over the carboxyl component, which proceeded with the formation of α-diethoxyphosphorylcyclopropanecarboxylic acid **7** [13, 14].

The final stage of the synthetic procedure was the reaction of α-diethoxyphosphorylcyclopropanecarboxylic acid **7** with a number of amino acid esters: the esters of glycine and methionine, as well as the methyl esters of aspartic acid and γ-aminobutyric acid. The reaction was carried out through the preparation of the corresponding α-diethoxyphosphorylcyclopropanecarboxylic acid chloride, which was used further without preliminary isolation

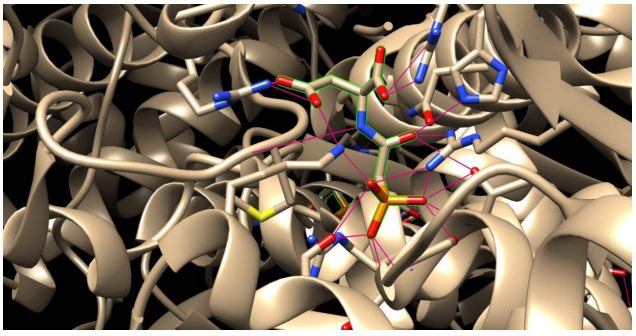

a

Fig. 3a. An *N*-phosphonacetyl-L-aspartate molecule in the active site of aspartate transcarbomoylase (X-ray diffraction data; image obtained using the Chimera software).

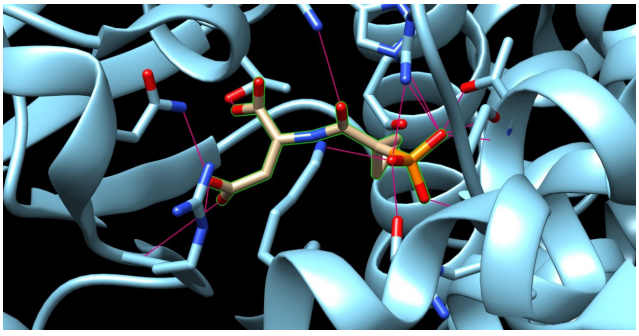

b

Fig. 3b. An *N*-(α-dihydroxyphosphorylcyclopropylcarbonyl) aspartic acid molecule in the active site of aspartate transcarbomoylase (conformation modeled with Autodock; image obtained with the Chimera software).

[1] https://www.rcsb.org/structure/5G1N (Accessed July 01, 2020).
[2] UCSF Chimera 1.13.1. 2018. Available from https://www.cgl.ucsf.edu/chimera/ (Accessed July 20, 2020).

and purification. Carrying out the reaction under cooling to 0ºC in dry chloroform in the presence of triethylamine, which is used as a base and an acceptor of hydrogen chloride, enabled us to obtain esters of *N*-(α-diethoxyphosphorylcyclopropylcarbonyl)-substituted amino acids **8–11** in good yield.

The esters thus synthesized were converted into acids by alkaline hydrolysis of the carboxyl end of the compound (compounds **12–15**).

Note that in Fig. 5 are reported the compounds synthesized implementing the developed scheme, along with the corresponding yields for the last stage of the procedure.

Compounds **12–15** synthesized by us were tested for cytotoxicity toward cell lines of human breast cancer (MDA-MB-231, Fig. 6), skin cancer (A-375, Fig. 7), and glioblastoma (U-87 MG, Fig. 8), according to the method described in reference [15].

Cell viability was assessed via a test that is used to assess the metabolic activity of cells (the MTT test), based on colorimetric measurements of control and test solutions, which were preincubated in CO_2 environment with the addition of the MTT solution (3-(4,5-dimethylthiazole bromide)-2-yl)-2,5-diphenyltetrazolium). Nicotinamide adenine dinucleotide phosphate-H-dependent cellular oxidoreductase enzymes of living cells are able to reduce MTT to the corresponding formazan, which is characterized by a purple coloration. Subsequently, the optical density of the resulting solutions was estimated at 594 nm and 620 nm wavelengths. The results of these tests are reported in Figs. 6–8.

The absence of the expected biological activity of the test compounds may be due to the presence of ether groups at the phosphorus atom of phosphonate group [16]. Thus, one of the main directions of further research is the synthesis of *N*-(α-dihydroxyphosphorylcyclopropylcarbonyl)amino acids and verification of their biological activity.

CONCLUSIONS

The results of PALA studies and molecular docking of cyclopropanated analogs of phosphonacetic acid indicate that *N*-(α-dihydroxyphosphorylcyclopropylcarbonyl)-substituted amino acids have a high potential as anticancer agents. However, the absence of cytotoxicity of the synthesized compounds toward the cancer cell lines used in the present study did not match the expected results; the observed low

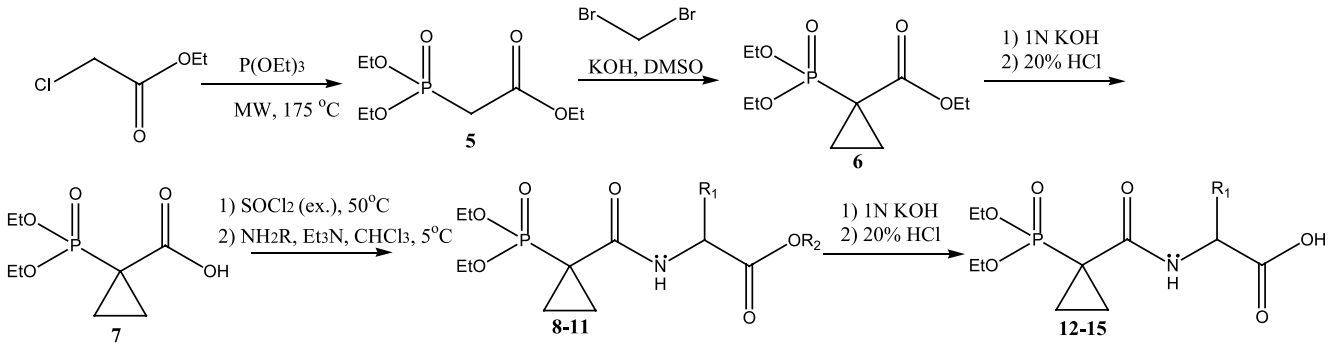

Fig. 4. General scheme for the synthesis of *N*-(α-diethoxyphosphorylcyclopropylcarbonyl)amino acids.

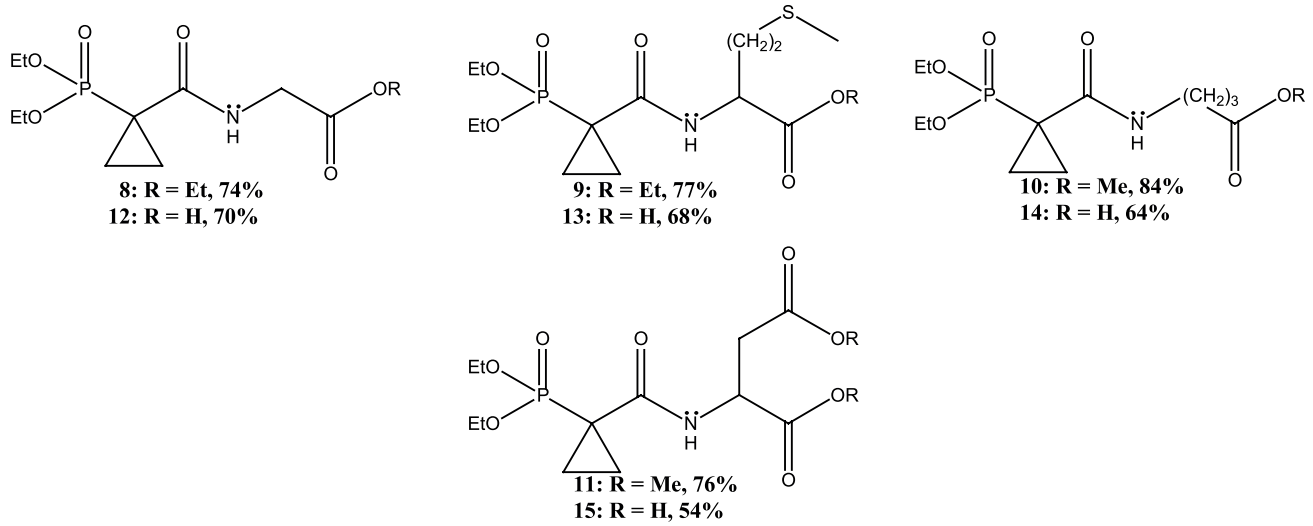

Fig. 5. A series of obtained *N*-(α-diethoxyphosphorylcyclopropylcarbonyl)amino acids, with their respective yields.

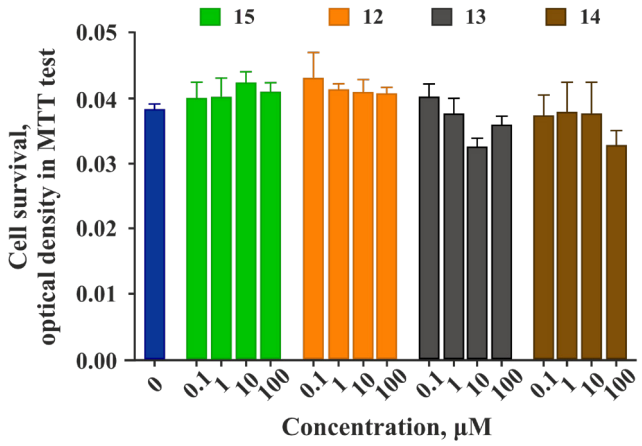

Fig. 6. Cell survival at various concentrations of the compounds under study as measured in cytotoxicity tests run against human breast cancer cell lines.

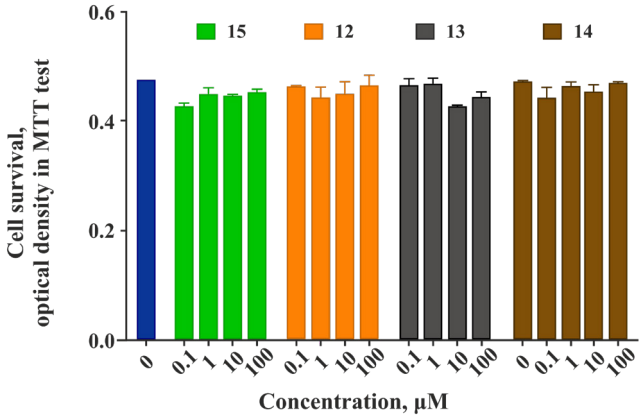

Fig. 7. Cell survival at various concentrations of the compounds under study as measured in cytotoxicity tests run against human skin cancer cell lines.

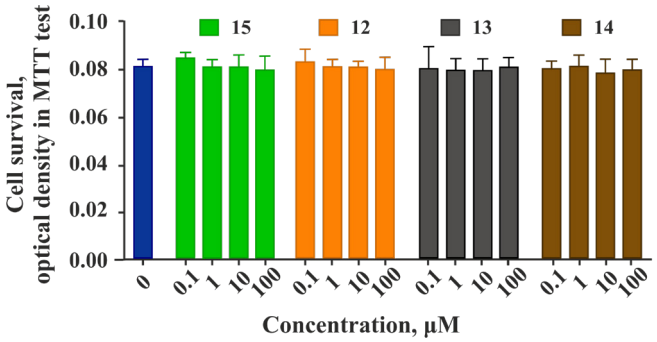

Fig. 8. Cell survival at various concentrations of the compounds under study measured in cytotoxicity tests run against human glioblastoma cell lines.

bioactivity may be due to the presence of ester groups in the phosphonate component of *N*-(α-diethoxyphosphoryl-cyclopropylcarbonyl)amino acids.

Financial support

This study did not have any financial support from outside organizations.

Authors' contribution

I.S. Kuzmin – development of the research design, conducting the study, collecting and providing the material, writing the text of the article, editing the article;

D.Yu. Yuriev – conducting the study, collecting and providing the material, writing the text of the article, editing the article, formalization of the list of references;

G.A. Toporkov – conducting the study, collecting and providing the material;

A.V. Kalistratova – analysis and systematization of the material, writing the text of the article, design of the study;

L.V. Kovalenko – idea, development of the research design, analysis of the scientific work, critical revision with the introduction of valuable intellectual content.

The authors declare that they do not have any conflicts of interest related to financial or personal issues that could affect the work described in this article.

REFERENCES

1. Collins K.I., Stark G.R. Aspartate transcarbamylase. Interaction with the transition state analogue *N*-(phosphonacetyl)-L-aspartate. *J. Biol. Chem.* 1971;246(21):6599-6605. URL: http://www.jbc.org/content/246/21/6599

2. Ruiz-Ramos A., Velázquez-Campoy A., Grande-García A., Moreno-Morcillo M., Ramon-Maiques S. Structure and Functional Characterization of Human Aspartate Transcarbamoylase, the Target of the Anti-tumoral Drug PALA. *J. Structure.* 2016;24(7):1081-1094. https://doi.org/10.1016/j.str.2016.05.001

3. Horsman G.P., Zechel D.L. Phosphonate Biochemistry. *Chem. Rev.* 2016;117(8):5704-5783. https://doi.org/10.1021/acs.chemrev.6b00536

4. Demkowicz S., Rachon J., Dasko M., Kozak W. Selected Organophosphorus Compounds with Biological Activity. Applications in Medicine. *RSC Advances*. 2016;6(12):7101-7112. https://doi.org/10.1039/C5RA25446A

5. Grem J.L., King S.A., O'Dwyer P.J., Leyland-Jones B. Biochemistry and clinical activity of *N*-(phosphonacetyl)-L-aspartate: a review. *Canser Research.* 1988;48(16):4441-4454.

6. Peters G.J. Antipyrimidine effects of five different pyrimidine de novo synthesis inhibitors in three head and neck cancer cell lines. Nucleos. *Nucleot. Nucleic Acids.* 2018;37(6):329-339.
https://doi.org/10.1080/15257770.2018.1460479

7. Lei Z., Wang B., Lu Zh., Wang N., Tan H., Zheng J., Jia Z. New regulatory mechanism-based inhibitors of aspartate transcarbamoylase for potential anticancer drug development. *FEBS J.* 2020;287(16):3579-3599.
https://doi.org/10.1111/febs.15220

8. Cemre Manav M., Sofos N., Hove-Jensen B., Brodersen B.E. The Abc of Phosphonate Breakdown: A Mechanism for Bacterial Survival. *BioEssays.* 2018;40(11):1800091-1800102.
https://doi.org/10.1002/bies.201800091

9. Coudray L., Kantrowitz E.R., Montchamp J.L. Submicromolar phosphinic inhibitors of Escherichia coli aspartate transcarbamoylase. *Bioorganic Med. Chem. Lett.* 2009;19(3):900-902.
https://doi.org/10.1016/j.bmcl.2008.11.115

10. Trott O., Olson A. J. AutoDock Vina: improving the speed and accuracy of docking with a new scoring function, efficient optimization, and multithreading. *J. Comput. Chem.* 2010;31(2):455-461.
https://doi.org/10.1002/jcc.21334

11. Seweryn P., Van L.B., Kjeldgaard M., Russo C.J., Passmore L.A., Hove-Jensen B., Jochimsen B., Brodersen D.E. Structural insights into the bacterial carbon-phosphorus lyase machinery. *Nature.* 2015;525(7567):68-72.
https://doi.org/10.1038/nature14683

12. Balint E., Tajti A., Keglevich G. Application of the Microwave Technique in Continuous Flow Processing of Organophosphorus Chemical Reactions. *Materials.* 2019;12(5):788-803.
https://doi.org/10.3390/ma12050788

13. Grün A., Balint E., Keglevich G. Solid-Liquid Phase *C*-Alkylation of Active Methylene Containing Compounds under Microwave Conditions. *Catalysts.* 2015;5(2):634-652.
https://doi.org/10.3390/catal5020634

14. Boppudi H.B., Gandavaram S.P., Chamarthi N.R., Mandava V.B. Synthesis of Phosphonates via Michaelis-Arbuzov Reaction. *Curr. Org. Synth.* 2017;14(6):883-903.
https://doi.org/10.2174/1570179414666161230144455

15. Kalistratova A.V., Kovalenko L.V., Oshchepkov M.S., Gamisoniya A.M., Gerasimova T.S., Demidov Yu.A., Akimov M.G. Synthesis of new compounds in the series of aryl-substituted ureas with cytotoxic and antioxidant activity. *Mendeleev Commun.* 2020;30;2:153-156.
https://doi.org/10.1016/j.mencom.2020.03.007

16. Mao J.C., Otis E.R., von Esch A.M., Herrin T.R., Fairgrieve J.S., Shipkowitz N.L., Duff R.G. Structure-activity studies on phosphonoacetate. *Antimicrob. Agents Chemother.* 1985;27(2):197-202.
https://doi.org/10.1128/AAC.27.2.197

About the authors:

Ivan S. Kuzmin, Leading Engineer, Department of Chemistry and Technology of Biomedical Drugs, D.I. Mendeleev University of Chemical Technology of Russia (9, Miusskaya pl., Moscow, 125047, Russia). E-mail: kyzka06@mail.ru. https://orcid.org/0000-0002-1542-6931

Danil Yu. Yuriev, Master Student, Department of Chemistry and Technology of Biomedical Drugs, D.I. Mendeleev University of Chemical Technology of Russia (9, Miusskaya pl., Moscow, 125047, Russia). E-mail: DanilYuriev35@yandex.ru. https://orcid.org/0000-0002-5906-4020

Grigorii A. Toporkov, Master Student Department of Chemistry and Technology of Biomedical Drugs, D.I. Mendeleev University of Chemical Technology of Russia (9, Miusskaya pl., Moscow, 125047, Russia). E-mail: gtoporkovmail@gmail.com. https://orcid.org/0000-0002-3826-3100

Antonida V. Kalistratova, Cand. of Sci. (Chemistry), Assistant Professor, Department of Chemistry and Technology of Biomedical Drugs, D.I. Mendeleev University of Chemical Technology of Russia (9, Miusskaya pl., Moscow, 125047, Russia). E-mail: avkalistratova@muctr.ru. ResearcherID B-4401-2018. http://orcid.org/0000-0001-6023-7526

Leonid V. Kovalenko, Dr. of Sci. (Chemistry), Professor, Head of the Department of Chemistry and Technology of Biomedical Drugs, D.I. Mendeleev University of Chemical Technology of Russia (9, Miusskaya pl., Moscow, 125047, Russia). E-mail: lvkbmp23@yandex.ru. https://orcid.org/0000-0002-0027-4664

Об авторах:

Кузьмин Иван Станиславович, ведущий инженер кафедры химии и технологии биомедицинских препаратов Российского химико-технологического университета имени Д.И. Менделеева (125047, Россия, г. Москва, Миусская площадь, д. 9). E-mail: kyzka06@mail.ru. https://orcid.org/0000-0002-1542-6931

Юрьев Данил Юрьевич, магистрант кафедры химии и технологии биомедицинских препаратов Российского химико-технологического университета имени Д.И. Менделеева (125047, Россия, г. Москва, Миусская площадь, д. 9). E-mail: DanilYuriev35@yandex.ru. https://orcid.org/0000-0002-5906-4020

Топорков Григорий Андреевич, магистрант кафедры химии и технологии биомедицинских препаратов Российского химико-технологического университета имени Д.И. Менделеева (125047, Россия, г. Москва, Миусская площадь, д. 9). E-mail: gtoporkovmail@gmail.com. https://orcid.org/0000-0002-3826-3100

Калистратова Антонида Владимировна, к.х.н., доцент кафедры химии и технологии биомедицинских препаратов Российского химико-технологического университета имени Д.И. Менделеева (125047, Россия, г. Москва, Миусская площадь, д. 9). E-mail: avkalistratova@muctr.ru. ResearcherID B-4401-2018. http://orcid.org/0000-0001-6023-7526

Коваленко Леонид Владимирович, д.х.н., профессор, заведующий кафедрой химии и технологии биомедицинских препаратов Российского химико-технологического университета имени Д.И. Менделеева (125047, Россия, г. Москва, Миусская площадь, д. 9). E-mail: lvkbmp23@yandex.ru. https://orcid.org/0000-0002-0027-4664

The article was submitted: September 23, 2020; approved after reviewing: October 10, 2020; accepted for publication: October 17, 2020.

Translated from Russian into English by H. Moshkov
Edited for English language and spelling by Enago, an editing brand of Crimson Interactive Inc.

CHEMISTRY AND TECHNOLOGY OF MEDICINAL COMPOUNDS AND BIOLOGICALLY ACTIVE SUBSTANCES

ХИМИЯ И ТЕХНОЛОГИЯ ЛЕКАРСТВЕННЫХ ПРЕПАРАТОВ И БИОЛОГИЧЕСКИ АКТИВНЫХ СОЕДИНЕНИЙ

ISSN 2686-7575 (Online)

https://doi.org/10.32362/2410-6593-2020-15-5-36-45

UDC 547.461.3: 577.112.343

RESEARCH ARTICLE

Cationic amphiphiles based on malonic acid amides as transfection mediators

Nadezhda A. Romanova, Ulyana A. Budanova[@], Yury L. Sebyakin

MIREA – Russian Technological University (M.V. Lomonosov Institute of Fine Chemical Technologies), Moscow, 119571 Russia

[@]Corresponding author, e-mail: c-221@yandex.ru

Objectives. *The aim of this work is to synthesize cationic amphiphiles based on malonic acid amides. The target compounds should contain saturated and unsaturated alkyl chains in the hydrophobic portion, and one or two positive charges in the polar head as created by ethylenediamine and amino acid L-ornithine. For such cationic amphiphiles, we determined physicochemical properties and transfection efficiency of liposomes based on them.*

Methods. *The initial compound in the synthesis is diethylmalonate. We used C-alkylation to add the first hydrophobic chain (with octylbromide, dodecylbromide, or octadecylbromide). N-oleylamine was used as the second hydrophobic chain, which was attached at the carboxyl group of the malonic acid via amide bond formation. The polar head was represented by ethylenediamine, which was then attached at the second carboxyl group of the malonic acid. Further, L-ornithine was attached to ethylenediamine to produce cationic lipids with two positive charges in the head group. The structures of the compounds were characterized by infrared spectroscopy, nuclear magnetic resonance spectroscopy, and elemental analysis. Particle size distribution was evaluated by photon correlation spectroscopy. The luciferase test was used to determine transfection efficiency using HeLa cells.*

Results. *We have developed a synthesis scheme to produce new cationic amphiphiles with an asymmetric hydrophobic part. The obtained liposomal particles are approximately 120 nm in size and have a relatively high zeta potential of 29–30 mV.*

Conclusions. *The size of these liposomes allows them to penetrate into cells, which makes it possible to use these compositions for transfection. The high zeta potential shows that the particles are stable. Our results demonstrate that the transfection efficiency of our liposomes (mixed with cholesterol) is comparable to a commercial formulation. Cationic amphiphiles based on malonic acid amides have great potential for liposome development for transfection.*

Keywords: *cationic lipids, malonic acid amides, cationic liposomes, transfection efficiency, targeted delivery, cationic amphiphiles.*

For citation: Romanova N.A., Budanova U.A., Sebyakin Yu.L. Cationic amphiphiles based on malonic acid amides as transfection mediators. *Tonk. Khim. Tekhnol. = Fine Chem. Technol.* 2020;15(5):36-45 (Russ., Eng.). https://doi.org/10.32362/2410-6593-2020-15-5-36-45

НАУЧНАЯ СТАТЬЯ

Катионные амфифилы на основе амидов малоновой кислоты в качестве медиаторов трансфекции

Н.А. Романова, У.А. Буданова[@], Ю.Л. Себякин

МИРЭА – Российский технологический университет (Институт тонких химических технологий имени М.В. Ломоносова), Москва, 119571 Россия
[@]Автор для переписки, e-mail: c-221@yandex.ru

Цели. *Задача данной работы заключалась в получении катионных амфифилов, являющихся амидами малоновой кислоты. Целевые амфифилы должны содержать насыщенную и ненасыщенную алкильные цепи в гидрофобном блоке, а также один или два положительных заряда в полярной головной части за счет этилендиамина и аминокислоты L-орнитина. Для таких катионных амфифилов должны быть определены физико-химические свойства и трансфекционная активность липосомальных композиций на их основе.*
Методы. *Исходным соединением в синтезе был диэтиловый эфир малоновой кислоты. С ним проводили реакцию С-алкилирования для присоединения первой гидрофобной цепи (с использованием октилбромида, додецилбромида и октадецилбромида). В качестве второй гидрофобной цепи использовали N-олеиламин, который присоединяли по карбоксильной группе малоновой кислоты путем образования амидной связи. Полярная головная группа была представлена этилендиамином, который присоединяли по оставшейся карбоксильной группе малоновой кислоты. Далее к этилендиамину присоединяли L-орнитин для получения катионных липидов с двумя положительными зарядами в головной группе. Структуры соединений характеризовали с помощью инфракрасной спектроскопии, спектроскопии ядерного магнитного резонанса и элементного анализа. Методом фотонно-корреляционной спектроскопии оценивали распределение частиц по размерам. С помощью люциферазного теста определяли эффективность трансфекции на клеточной линии HeLa.*
Результаты. *Разработана схема синтеза новых катионных амифифилов с несимметричным гидрофобным блоком. Полученные на их основе липосомальные частицы имеют размер около 120 нм и обладают достаточно высоким дзета-потенциалом (29–30 мВ).*
Выводы. *Размер полученных липосом позволяет им проникать в клетки, что делает возможным использование таких композиций для трансфекции. Высокий дзета-потенциал свидетельствует об их стабильности. Наши результаты показали, что эффективность трансфекции полученными липосомами в смеси с холестерином сопоставима с коммерческим препаратом. Катионные амфифилы на основе амидов малоновой кислоты являются перспективными для разработки трансфекционных липосомальных композиций на их основе.*

Ключевые слова: *катионные липиды, амиды малоновой кислоты, катионные липосомы, трансфекционная активность, направленная доставка, катионные амфифилы*

Для цитирования: Романова Н.А., Буданова У.А., Себякин Ю.Л. Катионные амфифилы на основе амидов малоновой кислоты в качестве медиаторов трансфекции. *Тонкие химические технологии.* 2020;15(5):36-45. https://doi.org/10.32362/2410-6593-2020-15-5-36-45

INTRODUCTION

Gene therapy is a promising approach for many genetic disease treatments, which introduces missing genes or replaces defective genes with healthy ones [1]. Since the early stages of the development of the concept of gene therapy in medicine, effective methods of transferring nucleic acids to cells have been proposed [2]. These methods provide the delivery of polynucleotides to biological tissue or cells—the so-called gene transfection. Due to nuclease degradation, "pure" DNA or RNA cannot penetrate the cell membrane without using physical methods such as injections or "gene guns," so carriers able to transport DNA through the bloodstream and effectively release genetic material near the cell nucleus are needed [3].

Polynucleotide delivery systems are divided into two main classes: viral and non-viral vectors [4–5]. Despite high transfection efficiencies, viral systems have disadvantages as they can cause immune responses to a greater or lesser extent [6].

Nucleic acid carrier systems based on cationic lipids are a promising pharmaceutical tool for gene therapy strategy implementation [7]. Unlike viral systems, these complexes do not have immunogenic potential or size restrictions of delivered genetic fragments [8]. However, cationic lipids, as well as other non-viral vectors such as polymers and peptides, exhibit low transfection efficiency and pronounced toxicity [9].

During the development of optimal transfection systems, new lipids are constantly being synthesized and studied. To increase the rate of transfection, the structures of cationic lipids are changed, the ratios with uncharged auxiliary lipids are changed, and varying amounts of DNA are added [10–12]. In this regard, it is important to study the physical and chemical properties of lipids to better understand the structure-efficiency relationship for gene transfer [7]. Therefore, numerous studies with multidisciplinary approaches are needed [13].

The advantage of cationic lipids is that they can be constructed in accordance with the "modular principle"—it is possible to perform structural changes separately in the head group, the linker, and the lipophilic region [11, 14, 15]. The structure of the hydrophobic domain determines the phase transition temperature and bilayer fluidity, which further affects the liposome stability, protection of DNA from nucleases, endosomal output, release of DNA from the lipoplex, and penetration into the nucleus [3, 16]. Oleic unsaturated chains promote endosomal release by increasing the membrane fluidity of transfection complexes [17]. The effectiveness of transfection of cationic lipids is also affected by asymmetry [3]. In addition, multivalent lipids are more active than monovalent lipids [11].

A promising class of cationic lipids is malonic acid diamides [13]. Malonic acid-based cationic lipids were first described in the literature (as nucleic acid carriers) about 10 years ago. Malonic acid diethyl ether is the central building block of synthesis. The chemical properties of malonic acid make it possible to attach alkyl chains via acyl functions in the form of amides or esters [11]. Malonic acid diamides with two long hydrophobic alkyl chains and a polar head group, used as a new class of non-viral gene-transferring agent, have shown high transfection efficiency and moderate toxicity. In addition, amide bonds showed better hydrolytic stability than ester bonds. It was shown that an increase in the cationic head group by combining with two lysine molecules, rather than just one, leads to an increased transfection efficiency [10, 15]. Thus, the characterization of the biocompatibility of effective lipid compositions and the study of therapeutic concepts for the medical use of highly effective cationic lipids derived from malonic acid are an urgent task [11].

The aim of this work is to obtain cationic amphiphiles based on malonic acid amides containing saturated and unsaturated alkyl chains in a hydrophobic block (scheme 1), as well as one or two positive charges in the polar head region created by ethylenediamine and L-ornithine, and study the properties and transfection activities of the liposomal compositions based on them.

MATERIALS AND METHODS

General method

All chemicals and reagents were used without pretreatment: diethylmalonate, ethylenediamine, octylbromide, dodecylbromide, octadecylbromide (all—*Acros Organics*, Belgium), *N*-oleylamine (*Sigma-Aldrich*, USA), di-*tert*-butyl dicarbonate (Boc_2O) (*Sigma-Aldrich*, USA), L-ornithine monohydrochloride (L-Orn*HCl) (*Acros Organics*, Belgium), *N,N'*-dicyclohexylcarbodiimide (DCC) (*Sigma-Aldrich*, USA), 1-hydroxybenzotriazole (HOBT) (*Sigma-Aldrich,* USA), potassium hydroxide (*CHIMMED*, Russia), sodium sulfate anhydrous (*CHIMMED*, Russia), and trifluoroacetic acid (TFA) (*Biochem*, Russia).

^{1}H NMR nuclear magnetic resonance spectra were recorded in deuterated chloroform using a Bruker WM-400 pulsed NMR spectrometer (*Bruker,* Germany) with an operating frequency of 400 MHz. The internal standard is hexamethyldisiloxane. Infrared spectra were recorded on an EQUINOX 55 (*Bruker,* Germany) Fourier transform-infrared spectrometer. Elemental analysis was performed using

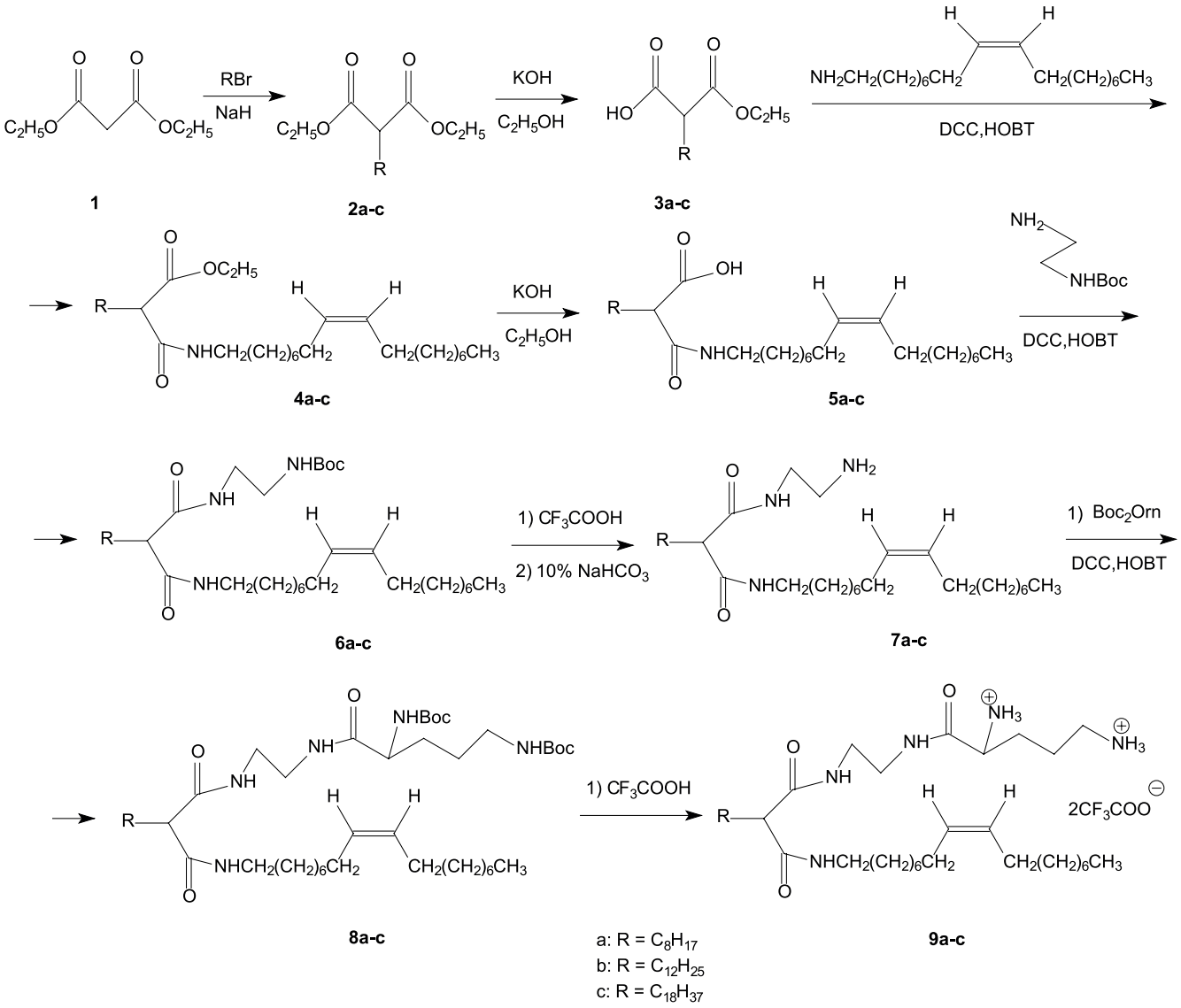

Scheme 1. Malonic acid amides.

a CHNS analyzer FLASH EA 1112 (*Thermo Finnigan Italia S.p.A,* Italia). Thin-layer chromatography (TLC) was performed on Sorbfil plates (*IMID*, Russia), and column chromatography was performed on silica gel with a size of 0.040–0.063 mm (*Merck*, Germany). To detect spots in TLC, heating over the flame of an alcohol lamp was used. To detect substances containing amino groups, a 5% solution of ninhydrin was used, followed by heating to 50°C.

EXPERIMENTAL

Mono-*N*-*tert*-butoxicarbonylethylenediamine (1). 8.01 g (133.5 mmol) of 1,2-ethylenediamine was dissolved in dioxane in an inert argon atmosphere, and a solution of 3.78 g (17.34 mmol) Boc_2O in dioxane was added dropwise for 3 h. The mixture was stirred at room temperature for 24 h. The solvent was distilled in a vacuum, and the remaining solid was dissolved in water. The product was isolated by dichloromethane extraction (3 × 50 mL). The product yield was 2.18 g (78.5%).

IR spectrum (ν_{max}, cm^{-1}): 3355 (NH), 2978, 2934 (CH_2), 1693 (C=O, "I amide band"), 1526 (NH, "II amide band"), 1392, 1367, 1278, 1253 (C–O), 1173 (C–N), 1045 (CH_2), 966 (CH_3).

Diethyl ether of octylmalonic acid (2a). 0.49 g (20.42 mmol) sodium hydride was gradually added to a solution of diethylmalonate 3 g (18.75 mmol) in anhydrous tetrahydrofuran and mixed for 1 h at room temperature. After that, a solution of 3.29 g (17.05 mmol) of octylbromide in anhydrous tetrahydrofuran was added to the protonated diethylmalonate drop by drop and mixed for 24 h. The solvent was distilled on a rotary evaporator. Ice water was added to the reaction mass, the products were extracted with ethyl acetate, dried

with sodium sulfate, and the solvent was distilled on a rotary evaporator. We obtained 4.23 g (82.9%) of the product.

^{1}H NMR spectrum of compound **2a** ($CDCl_3$, δ, ppm): 0.86 (t, 3H, $-CH_3$), 1.27 (m, 18H, $-\underline{CH_2}CH_3$, $-OCH_2\underline{CH_3}$), 1.89 (m, 2H, $-CH\underline{CH_2}-$), 3.35 (t, 1H, –CH–), 4.18 (m, 4H, $-O\underline{CH_2}CH_3$).

Diethyl ether of dodecylmalonic acid (2b). Similarly, from 3 g (18.75 mmol) of diethylmalonate, 0.49 g (20.42 mmol) of sodium hydride, and 4.24 g (17.03 mmol) of dodecylbromide. The product yield was 5.16 g (83.9%).

^{1}H NMR spectrum of compound **2b** ($CDCl_3$, δ, ppm): 0.87 (t, 3H, $-CH_3$), 1.28 (m, 26H, $-\underline{CH_2}CH_3$, $-OCH_2\underline{CH_3}$), 1.78 (m, 2H, $-CH\underline{CH_2}-$), 3.30 (t, 1H, –CH–), 4.20 (m, 4H, $-O\underline{CH_2}CH_3$).

Diethyl ether of octadecylmalonic acid (2c). Similarly: from 2 g (12.50 mmol) of diethylmalonate, 0.33 g (13.75 mmol) of sodium hydride and 3.79 g (11.37 mmol) of octadecylbromide. The product yield was 3.91 g (83.5%).

^{1}H NMR spectrum of compound **2c** ($CDCl_3$, δ, ppm): 0.90 (t, 3H, $-CH_3$), 1.27 (m, 38H, $-\underline{CH_2}CH_3$, $-OCH_2\underline{CH_3}$), 1.84 (m, 2H, $-CH\underline{CH_2}-$), 3.37 (t, 1H, –CH–), 4.21 (m, 4H, $-O\underline{CH_2}CH_3$).

Monoethyl ether of octylmalonic acid (3a). To a solution of 8.37 g (30.77 mmol) of compound **2a** in ethanol, a solution of 2.07 g (36.96 mmol) KOH in ethanol was added dropwise for 1 h. Then the mixture was mixed for 3 h and left overnight without stirring. After that, ethanol was distilled to half the volume and the solution was acidified with an equimolar amount of 0.1 M hydrochloric acid. The target compound was extracted with ethyl acetate, dried with sodium sulfate, and the solvent was distilled on a rotary evaporator. The product was extracted by flash chromatography with hexane elution, then by a 15 : 1 chloroform : methanol system. We obtained 3.69 g (49.2%) of the product.

^{1}H NMR spectrum of compound **3a** ($CDCl_3$, δ, ppm): 0.86 (t, 3H, $-CH_3$), 1.28 (m, 15H, $-\underline{CH_2}CH_3$, $-OCH_2\underline{CH_3}$), 1.89 (m, 2H, $-CH\underline{CH_2}-$), 3.37 (t, 1H, –CH–), 4.19 (m, 2H, $-O\underline{CH_2}CH_3$).

Monoethyl ether of dodecylmalonic acid (3b). Similarly: of the 7.83 g (23.87 mmol) compound **2b** and 1.6 g (28.57 mmol) KON. The product yield was 2.9 g (33.6%).

^{1}H NMR spectrum of compound **3b** ($CDCl_3$, δ, ppm): 0.87 (t, 3H, $-CH_3$), 1.24 (m, 23H, $-\underline{CH_2}CH_3$, $-OCH_2\underline{CH_3}$), 1.70 (m, 2H, $-CH\underline{CH_2}-$), 3.20 (t, 1H, –CH–), 4.16 (m, 2H, $-O\underline{CH_2}CH_3$).

Monoethyl ether of octadecylmalonic acid (3c). Similarly: from 7.02 g (17.04 mmol) of compound **2c** and 1.15 g (20.54 mmol) KOH. The product yield was 2.6 g (39.8%).

^{1}H NMR spectrum of compound **3c** ($CDCl_3$, δ, ppm): 0.88 (t, 3H, $-CH_3$), 1.28 (m, 33H, $-\underline{CH_2}CH_3$, $-OCH_2\underline{CH_3}$), 1.91 (m, 2H, $-CHCH_2\underline{CH_2}-$), 3.38 (t, 1H, –CH–), 3.72 (m, 2H, $-CH\underline{CH_2}-$), 4.18 (m, 2H, $-O\underline{CH_2}CH_3$).

Ethyl ester of 2-{[(9*Z*)-octadec-9-enoylamino]-carbonyl}decanoic acid (4a). To a solution of 217.9 mg (0.89 mmol) of compound **3a** in anhydrous methylene chloride at 0°C, 241 mg (1.79 mmol) HOBT and a solution of 368 mg (1.79 mmol) DCC were added with stirring. After that, 287 mg (1.07 mmol) of oleylamine in anhydrous dichloromethane was added to the solution. The mixture was kept for 2 h when cooled and left for a day while stirring at room temperature, and then the precipitate was filtered out. The solvent was distilled on a rotary evaporator. The product was isolated by column chromatography in a 40 : 1 tetrachloromethane : methanol system. We obtained 299 mg (68.0%) of the product.

^{1}H NMR spectrum of compound **4a** ($CDCl_3$, δ, ppm): 0.86 (t, 6H, $2CH_3$), 1.26 (m, 37H, $-\underline{CH_2}CH_3$, $-OCH_2\underline{CH_3}$), 1.47 (m, 2H, $-NHCH_2\underline{CH_2}-$), 1.84 (m, 2H, $-CH\underline{CH_2}-$), 1.97 (m, 4H, $-\underline{CH_2}CH{=}CH\underline{CH_2}-$), 3.23 (m, 3H, –CH–, $-\underline{CH_2}NHCO-$), 4.18 (m, 2H, $-O\underline{CH_2}CH_3$), 5.35 (m, 2H, –CH=CH–), 6.55 (m, 1H, –NH–).

Ethyl ether of 2-{[(9*Z*)-octadec-9-enoylamino]-carbonyl}tetradecanoic acid (4b). Similarly: from 182 mg (0.61 mmol) of compound **3b**, 164 mg (1.21 mmol) of 1-hydroxybenzotriazole, 251 mg (1.22 mmol) of *N,N'*-dicyclohexylcarbodiimide, and 195 mg (0.73 mmol) of oleylamine. The product yield was 226 mg (67.5%).

^{1}H NMR spectrum of compound **4b** ($CDCl_3$, δ, ppm): 0.87 (t, 6H, $2CH_3$), 1.26 (m, 45H, $-\underline{CH_2}CH_3$, $-OCH_2\underline{CH_3}$), 1.48 (m, 2H, $-NHCH_2\underline{CH_2}-$), 1.86 (m, 2H, $-CH\underline{CH_2}-$), 1.99 (m, 4H, $-\underline{CH_2}CH{=}CH\underline{CH_2}-$), 3.23 (m, 3H, –CH–, $-\underline{CH_2}NHCO-$), 4.18 (m, 2H, $-O\underline{CH_2}CH_3$), 5.34 (m, 2H, –CH=CH–), 6.58 (m, 1H, –NH–).

Ethyl ether of 2-{[(9*Z*)-octadec-9-enoylamino]-carbonyl}eicosanic acid (4c). Similarly: of the 190 mg (0.49 mmol) compound **3c**, 134 mg (0.99 mmol) HOBT, 204 mg (0.99 mmol) DCC, and 159 mg (0.59 mmol) oleylamine. The product yield was 205 mg (65.5%).

^{1}H NMR spectrum of compound **4c** ($CDCl_3$, δ, ppm): 0.87 (t, 6H, $2CH_3$), 1.27 (m, 57H, $-\underline{CH_2}CH_3$, $-OCH_2\underline{CH_3}$), 1.49 (m, 2H, $-NHCH_2\underline{CH_2}-$), 1.83 (m, 2H, $-CH\underline{CH_2}-$), 2.00 (m, 4H, $-\underline{CH_2}CH{=}CH\underline{CH_2}-$), 3.23 (m, 3H, –CH–, $-\underline{CH_2}NHCO-$), 4.18 (m, 2H, $-O\underline{CH_2}CH_3$), 5.34 (m, 2H, –CH=CH–), 6.57 (m, 1H, –NH–).

2-{[(9*Z*)-octadec-9-enoylamino]carbonyl}-decanoic acid (5a). To a solution of 277 mg (0.56 mmol) of compound **4a** in ethanol, a solution of 63 mg (1.13 mmol) KOH in ethanol was added dropwise

for one hour. Then the solution was mixed at boiling conditions for eight hours. After that, ethanol was distilled to half the volume and the reaction mass was acidified with an equimolar amount of 0.1 M hydrochloric acid. The compound was extracted with ethyl acetate, dried with sodium sulfate, and the solvent was distilled on a rotary evaporator. We obtained 245 mg (94.0%) of the product.

^{1}H NMR spectrum of compound **5a** ($CDCl_3$, δ, ppm): 0.87 (t, 6H, $2CH_3$), 1.27 (m, 34H, –$\underline{CH_2}CH_3$), 1.47 (m, 2H, –NHCH$_2\underline{CH_2}$–), 1.94 (m, 6H, –CH$\underline{CH_2}$–, –$\underline{CH_2}$CH=CH$\underline{CH_2}$–), 3.19 (t, 1H, –CH–), 3.30 (m, 2H, –$\underline{CH_2}$NHCO–), 5.34 (m, 2H, –CH=CH–), 6.43 (m, 1H, –NH–).

2-{[(9*Z*)-octadec-9-enoylamino]carbonyl}-tetradecanoic acid (5b). Similarly: of 200 mg (0.36 mmol) compound **4b** and 40 mg (0.71 mmol) KON. The product yield was 153 mg (81.8%).

^{1}H NMR spectrum of compound **5b** ($CDCl_3$, δ, ppm): 0.90 (t, 6H, $2CH_3$), 1.27 (m, 42H, –$\underline{CH_2}CH_3$), 1.53 (m 2H, –NHCH$_2\underline{CH_2}$–), 1.95 (m, 6H, –CH$\underline{CH_2}$–, –$\underline{CH_2}$CH=CH$\underline{CH_2}$–), 3.15 (t, 1H, –H–), 3.31 (m, 2H, –$\underline{CH_2}$NHCO–), 5.35 (m, 2H, –CH=CH–), 6.26 (m, 1H, –NH–).

2-{[(9*Z*)-octadec-9-enoylamino]carbonyl}-eicosanic acid (5c). Similarly: of the 190 mg (0.30 mmol) compound **4c** and 34 mg (0.61 mmol) KON. The product yield was 170 mg (93.6%).

^{1}H NMR spectrum of compound **5c** ($CDCl_3$, δ, ppm): 0.88 (t, 6H, $2CH_3$), 1.27 (m, 54H, –$\underline{CH_2}CH_3$), 1.53 (m, 2H, –NHCH$_2\underline{CH_2}$–), 2.01 (m, 6H, –CH$\underline{CH_2}$–, –$\underline{CH_2}$CH=CH$\underline{CH_2}$–), 3.16 (t, 1H, –CH–), 3.30 (m, 2H, –$\underline{CH_2}$NHCO–), 5.35 (m, 2H, –CH=CH–), 6.33 (m, 1H, –NH–).

The diamide *N*-2-[(*N-tert*-butoxycarbonyl)-amino]ethyl-2-octyl-N'-[(9*Z*)-octadec-9-enoyl]-propane (6a). To a solution of 255 mg (0.55 mmol) of compound **5a** in anhydrous methylene chloride at 0°C, 149 mg (1.1 mmol) HOBT and a solution of 226 mg (1.1 mmol) DCC were added with stirring. Then 105 mg (0.66 mmol) of Boc-protected ethylenediamine in anhydrous dichloromethane was added to the solution. The mixture was kept for 2 h at 0ºC and then stirred for 24 h at room temperature. The precipitate was then filtered out. The solvent was distilled on a rotary evaporator. The product was isolated by column chromatography in the 40 : 1 tetrachloromethane : methanol system. We obtained 259 mg (77.8%) of the product.

^{1}H NMR spectrum of compound **6a** ($CDCl_3$, δ, ppm): 0.88 (t, 6H, $2CH_3$), 1.23 (m, 34H, –$\underline{CH_2}CH_3$), 1.45 (m, 11H, $3CH_3$, –NHCH$_2\underline{CH_2}$–), 1.65 (m, 2H, –CH$\underline{CH_2}$–), 1.95 (m, 4H, –$\underline{CH_2}$CH=CH$\underline{CH_2}$–), 2.95 (t, 1H, –CH–), 3.25 (m, 4H, –OCNH$\underline{CH_2}$–$\underline{CH_2}$NHCO–), 3.43 (m, 2H, –$\underline{CH_2}$NHCO–), 5.01 (m, 1H, –NH–), 5.37 (m, 2H, –CH=CH–), 6.82 (m, 1H, –NH–), 7.28 (m, 1H, –NH–).

The diamide *N*-2-[(*N-tert*-butoxycarbonyl)-amino]ethyl-2-dodecyl-*N'*-[(9*Z*)-octadec-9-enoyl]-propane (6b). Similarly: of 66 mg (0.13 mmol) compound **5b**, 35 mg (0.26 mmol) HOBT, 53 mg (0.26 mmol) DCC, and 26 mg (0.16 mmol) Boc-protected ethylenediamine. The product yield was 55.1 mg (65.6%).

^{1}H NMR spectrum of compound **6b** ($CDCl_3$, δ, ppm): 0.87 (t, 6H, $2CH_3$), 1.16 (m, 42H, –$\underline{CH_2}CH_3$), 1.43 (c, 9H, $3CH_3$),1.63 (m, 2H, –NHCH$_2\underline{CH_2}$–), 1.81 (m, 2H, –CH$\underline{CH_2}$–), 1.99 (m, 4H, –$\underline{CH_2}$CH=CH$\underline{CH_2}$–), 2.94 (t, 1H, –CH–), 3.24 (m, 4H, –OCNH$\underline{CH_2}$–$\underline{CH_2}$NHCO–), 3.43 (m, 2H, –$\underline{CH_2}$NHCO–), 5.00 (m, 1H, –NH–), 5.34 (m, 2H, –CH=CH–), 6.81 (m, 1H, –NH–), 7.26 (m, 1H, –NH–).

The diamide *N*-2-[(*N-tert*-butoxycarbonyl)-amino]ethyl-2-octadecyl-*N'*-[(9*Z*)-octadec-9-enoyl]-propane (6c). Similarly: of 160 mg (0.26 mmol) compound **5c**, 71 mg (0.53 mmol) HOBT, 109 mg (0.53 mmol) DCC, and 51 mg (0.32 mmol) Boc-protected ethylenediamine. The product yield was 179.8 mg (90.8%).

^{1}H NMR spectrum of compound **6c** ($CDCl_3$, δ, ppm): 0.87 (t, 6H, $2CH_3$), 1.20 (m, 54H, –$\underline{CH_2}CH_3$), 1.43 (c, 9H, $3CH_3$),1.60 (m, 2H, –NHCH$_2\underline{CH_2}$–), 1.72 (m, 2H, –CH$\underline{CH_2}$–), 1.95 (m, 4H, –$\underline{CH_2}$CH=CH$\underline{CH_2}$–), 2.93 (t, 1H, –CH–), 3.23 (m, 4H, –OCNH$\underline{CH_2}$–$\underline{CH_2}$NHCO–), 3.42 (m, 2H, –$\underline{CH_2}$NHCO–), 4.98 (m, 1H, –NH–), 5.32 (m, 2H, –CH=CH–), 6.76 (m, 1H, –NH–), 7.21 (m, 1H, –NH–).

Diamide *N*-(2-aminoethyl)-2-octyl-*N'*-[(9*Z*)-octadec-9-enoyl]propane (7a). To 248 mg (0.41 mmol) of compound **6a**, 70 mg (6.14 mmol) of TFA was added in 3 mL of methylene chloride, and stirred for 3 h at 0°C. Then the reaction mass was washed with a 10% solution of sodium bicarbonate and water. The organic residue was dried with sodium sulfate, and the solvent was distilled in a vacuum. We obtained 201.8 mg (97.5%) of the product.

Diamide *N*-(2-aminoethyl)-2-dodecyl-*N'*-[(9*Z*)-octadec-9-enoyl]propane (7b). Similarly: from 135 mg (0.20 mmol) of compound **6b** and 35 mg (3.07 mmol) of TFA. The product yield was 110.4 mg (96.0%).

Diamide *N*-(2-aminoethyl)-2-octadecyl-*N'*-[(9*Z*)-octadec-9-enoyl]propane (7c). Similarly: from 169 mg (0.23 mmol) of compound **6c** and 39 mg (3.42 mmol) of TFA. The product yield was 142.6 mg (97.0%).

Diamide *N'*-2-[(2,5-di(*N-tert*-butoxycarbonyl)-amino-1-oxopentyl)amino]ethyl-2-octyl-N-[(9*Z*)-octadec-9-enoyl]propane (8a). To a 250 mg (0.49 mmol) solution of compound **7a** in anhydrous methylene chloride at 0°C, 133 mg (0.99 mmol) HOBT and a

203 mg (0.99 mmol) DCC solution were added during mixing. Then 196 mg (0.59 mmol) of Boc-protected ornithine in anhydrous dichloromethane was added to the solution. The mixture was kept for 2 h when cooled and stirred for 24 h at room temperature, and the precipitate was filtered out. The solvent was distilled on a rotary evaporator. The product was isolated by column chromatography in the 40 : 1 tetrachloromethane : methanol system. We obtained 219 mg (54.1%) of the product.

^{1}H NMR spectrum of compound **8a** ($CDCl_3$, δ, ppm): 0.85 (t, 6H, $2CH_3$), 1.21 (m, 34H, –$\underline{CH_2}CH_3$), 1.43 (s, 18H, $6CH_3$), 1.54 (m, 2H, –NHC$H_2\underline{CH_2}$–), 1.69 (m, 4H, –CH$\underline{CH_2}\underline{CH_2}CH_2$NHCO–), 1.93 (m, 6H, –CH$\underline{CH_2}$–, –$\underline{CH_2}$CH=CH$\underline{CH_2}$–), 3.08 (m, 2H, –$\underline{CH_2}$NHCO), 3.20 (m, 3H, –CH–, –$\underline{CH_2}$NHCO–), 3.46 (m, 5H, –CH–, –OCNH$\underline{CH_2}$–$\underline{CH_2}$NHCO–), 4.10 (m, 1H, –NH–), 4.89 (m, 1H, –NH–), 5.23 (m, 1H, –NH–), 5.33 (m, 2H, –CH=CH–), 6.96 (m, 1H, –NH–), 7.37 (m, 1H, –NH–).

Diamide *N*'-2-[(2,5-di(*N*-*tert*-butoxycarbonyl)-amino-1-oxopentyl)amino]ethyl-2-dodecyl-*N*-[(9*Z*)-octadec-9-enoyl]propane (8b). Similarly: of 141 mg (0.25 mmol) compound **7b**, 68 mg (0.5 mmol) HOBT, 103 mg (0.5 mmol) DCC, and 100 mg (0.3 mmol) Boc-protected ornithine. The product yield was 166 mg (75.5%).

^{1}H NMR spectrum of compound **8b** ($CDCl_3$, δ, ppm): 0.87 (t, 6H, $2CH_3$), 1.24 (m, 42H, –$\underline{CH_2}CH_3$), 1.43 (s, 18H, $6CH_3$), 1.54 (m, 2H, –NHC$H_2\underline{CH_2}$–), 1.69 (m, 4H, –CH$\underline{CH_2}\underline{CH_2}CH_2$NHCO–), 1.92 (m, 6H, –CH$\underline{CH_2}$–, –$\underline{CH_2}$CH=CH$\underline{CH_2}$–), 3.06 (m, 2H, –$\underline{CH_2}$NHCO), 3.19 (m, 3H, –CH–, –$\underline{CH_2}$NHCO–), 3.44 (m, 5H, –CH–, –OCNH$\underline{CH_2}$–$\underline{CH_2}$NHCO–), 4.10 (m, 1H, –NH–), 4.87 (m, 1H, –NH–), 5.20 (m, 1H, –NH–), 5.33 (m, 2H, –CH=CH–), 6.94 (m, 1H, –NH–), 7.36 (m, 1H, –NH–).

Diamide *N*'-2-[(2,5-di(*N*-*tert*-butoxycarbonyl)-amino-1-oxopentyl)amino]ethyl-2-octadecyl-*N*-[(9*Z*)-octadec-9-enoyl]propane (8c). Similarly: of the 159 mg (0.25 mmol) compound **7c**, 66 mg (0.49 mmol) HOBT, 101 mg (0.49 mmol) DCC, and 97 mg (0.29 mmol) Boc-protected ornithine. The product yield was 158.8 mg (67.3%).

^{1}H NMR spectrum of compound **8c** ($CDCl_3$, δ, ppm): 0.87 (t, 6H, $2CH_3$), 1.20 (m, 54H, –$\underline{CH_2}CH_3$), 1.46 (s, 18H, $6CH_3$), 1.59 (m, 2H, –NHC$H_2\underline{CH_2}$–), 1.70 (m, 4H, –CH$\underline{CH_2}\underline{CH_2}CH_2$NHCO–), 1.92 (m, 6H, –CH$\underline{CH_2}$–, –$\underline{CH_2}$CH=CH$\underline{CH_2}$–), 3.07 (m, 2H, –$\underline{CH_2}$NHCO), 3.26 (m, 3H, –CH–, –$\underline{CH_2}$NHCO–), 3.45 (m, 5H, –CH–, –OCNH$\underline{CH_2}$–$\underline{CH_2}$NHCO–), 4.15 (m, 1H, –NH–), 4.88 (m, 1H, –NH–), 5.25 (m, 1H, –NH–), 5.33 (m, 2H, –CH=CH–), 6.94 (m, 1H, –NH–), 7.38 (m, 1H, –NH–).

Diamide *N*'-2-[(2,5-diamino-1-oxopentyl)amino]-ethyl-2-octyl-*N*-[(9*Z*)-octadec-9-enoyl]propane (9a). To 5 mL of a 208 mg (0.25 mmol) solution of compound **8a** in methylene chloride, 1.59 g (13.95 mmol) of TFA in 1 mL of methylene chloride was added and stirred for three hours at 0°C. The solvent and excess acid were distilled on a vacuum rotary evaporator. We obtained 213 mg (99.1%) of the product. Found, %: C 56.19; H 8.25; N 7.95. $C_{40}H_{73}N_5O_7F_6$. Calculated, %: C 56.54; H 8.60; N 8.25.

Diamide *N*'-2-[(2,5-diamino-1-oxopentyl)amino]-ethyl-2-dodecyl-*N*-[(9*Z*)-octadec-9-enoyl]propane (9b). Similarly: from 64 mg (0.07 mmol) of compound **8b** and 915 mg (8.03 mmol) of TFA. The product yield was 65 mg (98.5%). Found, %: C 57.89; H 8.43; N 7.83. $C_{44}H_{81}N_5O_7F_6$. Calculated, %: C 58.34; H 8.95; N 7.74.

Diamide *N*'-2-[(2,5-diamino-1-oxopentyl)amino]-ethyl-2-octadecyl-*N*-[(9*Z*)-octadec-9-enoyl]-propane (9c). Similarly: from 58 mg (0.06 mmol) of compound **8c** and 1.1 g (9.65 mmol) of TFA. The product yield was 59 mg (98.3%). Found, %: C 60.32; H 9.14; N 6.82. $C_{50}H_{93}N_5O_7F_6$. Calculated, %: C 60.67; H 9.40; N 7.08.

Preparation of liposomal dispersions

Two types of liposomes were obtained: from pure cationic lipid and from a mixture of cationic lipid and cholesterol in a ratio of 7 : 3. Four milligrams of each type of lipid composition were dissolved in chloroform. The solvent was distilled on a vacuum rotary evaporator to form a thin lipid film. The resulting films were dried in vacuum for three hours and then hydrated with 2 mL of distilled water at room temperature. The hydrated films were shaken and processed in an ultrasonic bath (2 × 30 min) at 40°C. The particle size distribution was estimated using photon correlation spectroscopy, which is based on the principles of dynamic light scattering, using a Photocor Compact-Z particle size analyzer (Russia).

Plasmid DNA transfection

Cells were planted in a tablet in the amount of 7×10^5 cells per well in 300 μL of full DMEM culture medium and incubated for 24 h at 37°C in a CO_2 incubator until a monolayer was reached the day before transfection. A dispersion of the transfection agent with a total volume of 80 μL, consisting of 1.177 μL of pGL3 plasmid and 9 μL of liposomal dispersion, was prepared in a serum-free OPTIMEM medium (ratio N : P = 16 : 1). The commercial transfection agent Lipofectamine 2000 (*Thermo Fisher Scientific,* USA) was used as a positive control. A "naked" plasmid was used as a negative control. The prepared mixtures were kept for 20 min at room temperature and applied to a monolayer

of cells in wells. The cells were incubated at 37°C in a CO_2 incubator for 24 h, and then activity was determined using a luciferase test.

Luciferase test

The test was performed using the Luciferase Assay System (*Promega Corporation*, USA) commercial Suite. To do this, growth medium was removed from the wells and then 70 μL of Glo Lysis Buffer, 1X (*Promega Corporation*, USA) was added. The cells were maintained at 37°C for 15 min in a CO_2 incubator to achieve complete lysis. Then they were taken from the bottom of the cells and transferred to Eppendorf plastic tubes (Germany). To precipitate cellular debris, the resulting lysate was centrifuged for three minutes at 10000 rpm. A 50 μL aliquot of the supernatant was selected, and a luciferase substrate was added in a ratio of 1 : 1. The transfection efficiency was assessed by the luminescence level on a GloMax 20/20 Luminometer (USA).

RESULTS AND DISCUSSION

In this work, malonic acid amides were synthesized (Scheme 1), where the initial compound in the synthesis was malonic acid diethyl ether. The mobility of the α-methylene hydrogen link and its increased acidity in the molecule enable the *C*-alkylation reaction, which result in the attachment of the first hydrophobic chain. For this purpose, $C_8H_{17}Br$, $C_{12}H_{25}Br$, and $C_{18}H_{37}Br$ bromides were used, thereby obtaining three corresponding cationic lipids that differ in hydrophobic block length.

The asymmetry effect and presence of unsaturated higher fatty acid residues in the hydrophobic block on the efficiency of transfection is known from literature [3]. Therefore, as the second hydrophobic chain, *N*-oleylamine was used, which was attached to the carboxyl group of malonic acid by forming an amide bond. The polar head group was first represented by ethylenediamine, which was then attached to the remaining carboxyl group of malonic acid by forming an amide bond. Then the natural amino acid L-ornithine was added to ethylenediamine to produce cationic lipids with two positive charges in the head group.

The physicochemical properties of the obtained one- and two-component liposomal dispersions (cationic lipid and a mixture of cationic lipid and cholesterol in a ratio of 7 : 3) were studied, and the particle sizes, zeta potentials, and transfection efficiencies were determined. The particle sizes were practically unchanged when cholesterol was added to the lipid and were within 100 nm, which is necessary for effective transfection (Fig. 1). The zeta potentials of the compositions were 29–30 mV. The values of this parameter at the level of 30 mV refer to the stability of the obtained particles, that is, their stability in relation to aggregation [18].

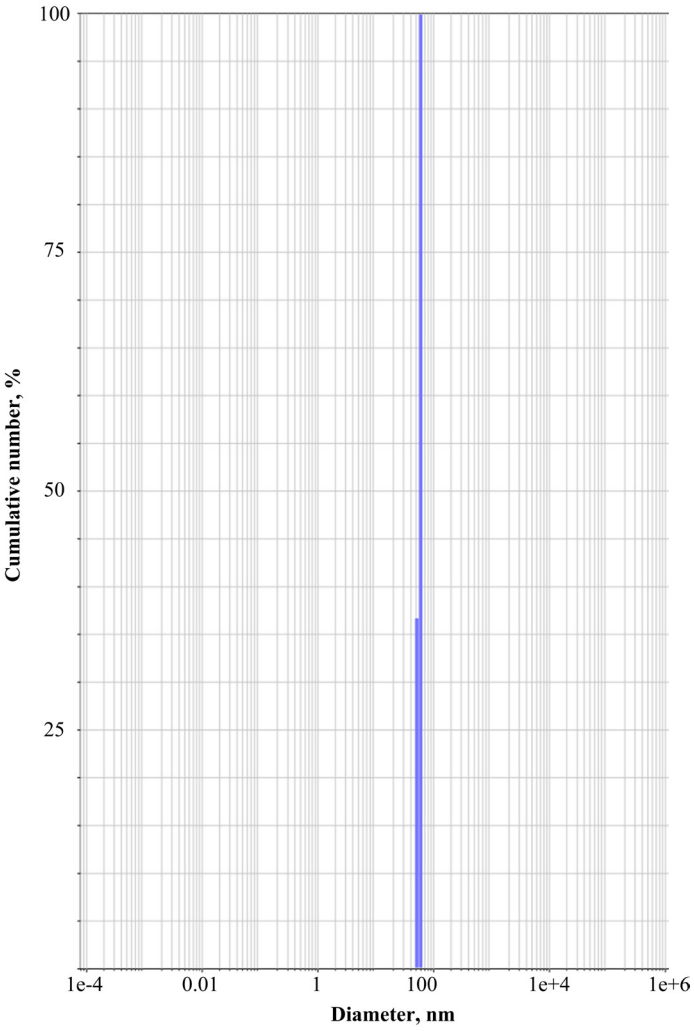

Fig. 1. Size distribution of dispersion particles based on compound **7b**.

Transfection effectiveness of the obtained liposomes was studied on the HeLa cell line (cervical cancer cells) by assessing the level of luminescence in the cell supernatants of the studied samples after delivery of the pGL3 plasmid encoding the luciferase gene. A commercially available transfection agent Lipofectamine 2000 was used as a positive control and a "naked" plasmid was used as a negative control. It was found that sample **7b**, in which cholesterol was added to the cationic lipid, showed a good result, almost reaching the level of transfection activity of Lipofectamine 2000 (Fig. 2).

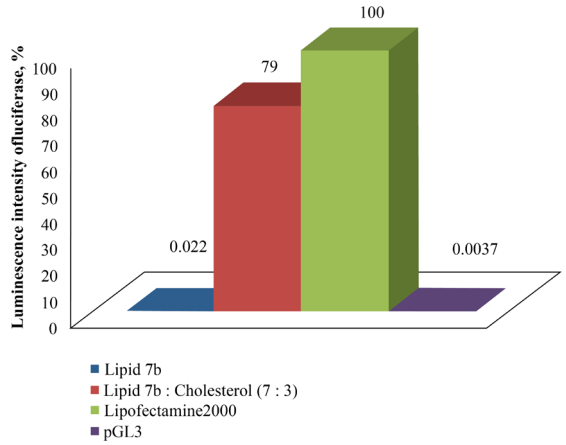

Fig. 2. Transfection efficiency for obtained liposomes.

CONCLUSIONS

A synthesis scheme was developed and new cationic amphiphiles with an asymmetric hydrophobic block were generated. Liposomal dispersions were formed, and their physical and chemical properties and transfection activity were studied. The obtained results indicate good potential of malonic acid amides for creating a new class of cationic amphiphiles used as transfection agents.

Financial support

This work was supported by the Russian Foundation for Basic Research, project No. 19-04-00775.

Authors' contribution

N.A. Romanova – carrying out the study, collection and provision of the material, writing the article;

U.A. Budanova – consultation on conducting individual stages of the study, scientific editing;

Yu.L. Sebyakin – development of the research idea, literature analysis.

The authors declare no conflicts of interest.

REFERENCES

1. O'Connor T.P., Crystal R.G. Genetic medicines: treatment strategies for hereditary disorders. *Nat. Rev. Genet.* 2006;7(4):261-276. https://doi.org/10.1038/nrg1829

2. Maeder M.L., Gersbach C.A. Genome-editing Technologies for Gene and Cell Therapy. *Mol. Ther.* 2016;24(3):430-446. https://doi.org/10.1038/mt.2016.10

3. Tassler S., Pawlowska D., Janich C., Dobner B., Wölk C., Brezesinski G. Lysine-based amino-functionalized lipids for gene transfection: the influence of the chain composition on 2D properties. *Phys. Chem. Chem. Phys.* 2018;20(10):6936-6944. https://doi.org/10.1039/c8cp00047f

4. Sheridan C. Gene therapy finds its niche. *Nat. Biotechnol*. 2011;29(2):121-128. https://doi.org/10.1038/nbt.1769

5. Wagner E. Polymers for siRNA Delivery: Inspired by Viruses to be Targeted, Dynamic, and Precise. *Acc. Chem. Res.* 2012;45(7):1005-1013. https://doi.org/10.1021/ar2002232

6. Crystal R.G. Transfer of Genes to Humans: Early Lessons and Obstacles to Success. *Science.* 1995;270(5235):404-410. https://doi.org/10.1126/science.270.5235.404

7. Dittrich M., Brauer C., Funari S.S., Dobner B., Brezesinski G., Wölk C. Interactions of Cationic Lipids with DNA: A Structural Approach. *Langmuir.* 2018;34(49):14858-14868. https://doi.org/10.1021/acs.langmuir.8b01635

8. Sen J., Chaudhuri A. Design, Syntheses, and Transfection Biology of Novel Non-Cholesterol-Based Guanidinylated Cationic Lipids. *J. Med. Chem.* 2005;48(3):812-820. https://doi.org/10.1021/jm049417w

9. Antipina M.N., Schulze I., Heinze M., Dobner B., Langner A., Brezesinski G. Physical-Chemical Properties and Transfection Activity of Cationic Lipid/DNA Complexes. *ChemPhysChem.* 2009;10(14):2471-2479. https://doi.org/10.1002/cphc.200900069

10. Wölk C., Heinze M., Kreideweiss P., Dittrich M., Brezesinski G., Langner A., Dobner B. Synthesis and DNA transfection properties of new head group modified malonic acid diamides. *Int. J. Pharm.* 2011;409(1-2):46-56. http://doi.org/10.1016/j.ijpharm.2011.02.022

11. Wölk C., Janich C., Bakowsky U., Langner A., Brezesinski G. Malonic acid based cationic lipids – The way to highly efficient DNA-carriers. *Adv. Colloid Interface Sci.* 2017;248:20-34. https://doi.org/10.1016/j.cis.2017.08.003

12. Jones C.H., Chen C.K., Ravikrishnan A., Rane S., Pfeifer B.A. Overcoming Nonviral Gene Delivery Barriers: Perspective and Future. *Mol. Pharm.* 2013;10(11):4082-4098. https://doi.org/10.1021/mp400467x

13. Janich C., Taßler S., Meister A., Hause G., Schäfer J., Bakowsky U., Brezesinski G., Wölk C. Structures of malonic acid diamide/phospholipid composites and their lipoplexes. *Soft Matter.* 2016;12(27):5854-5866. https://doi.org/10.1039/C6SM00807K

14. Ahmad A., Evans H.M., Ewert K., George C.X., Samuel C.E., Safinya C.R. New multivalent cationic lipids reveal bell curve for transfection efficiency versus membrane charge density: lipid-DNA complexes for gene delivery. *J. Gene Med.* 2005;7(6):739-748. https://doi.org/10.1002/jgm.717

15. Serebrennikova G.A., Maslov M.A., Morozova N.G. Modular transport systems based on cationic and neutral amphiphiles for gene therapy. *Tonk. Khim. Tekhnol. = Fine Chem. Technol.* 2011;6(5):72-86 (in Russ.).

16. Denieva Z.G., Budanova U.A., Sebyakin Y.L. Synthesis of Cationic and Ionizable Amphiphiles Based on Heminal Aminodiol as Potential siRNA Delivery Systems. *Tonk. Khim. Tekhnol. = Fine Chem. Technol.* 2019;14(3):42-49 (in Russ.). https://doi.org/10.32362/2410-6593-2019-14-3-42-49

17. Heinze M., Brezesinski G., Dobner B., Langner A. Novel Cationic Lipids Based on Malonic Acid Amides Backbone: Transfection Efficacy and Cell Toxicity Properties. *Bioconjug. Chem.* 2010;21(4):696-708. https://doi.org/10.1021/bc9004624

18. Buck J., Grossen P., Cullis P.R., Huwyler J., Witzigmann D. Lipid-Based DNA Therapeutics: Hallmarks of Non-Viral Gene Delivery. *ACS Nano*. 2019;13(4):3754-3782. https://doi.org/10.1021/acsnano.8b07858

About the authors:

Nadezhda A. Romanova, Master Student, N.A. Preobrazhensky Department of Chemistry and Technology of Biologically Active Compounds, Medicinal and Organic Chemistry, M.V. Lomonosov Institute of Fine Chemical Technologies, MIREA – Russian Technological University (86, Vernadskogo pr., Moscow, 119571, Russia). https://orcid.org/0000-0001-5073-2873

Ulyana A. Budanova, Cand. of Sci. (Chemistry), Assistant, N.A. Preobrazhensky Department of Chemistry and Technology of Biologically Active Compounds, Medicinal and Organic Chemistry, M.V. Lomonosov Institute of Fine Chemical Technologies, MIREA – Russian Technological University (86, Vernadskogo pr., Moscow, 119571, Russia). E-mail: c-221@yandex.ru. Scopus Author ID 14622352500, ResearcherID E-1659-2014, https://orcid.org/0000-0003-1702-9435

Yury L. Sebyakin, Dr. of Sci. (Chemistry), Professor, N.A. Preobrazhensky Department of Chemistry and Technology of Biologically Active Compounds, Medicinal and Organic Chemistry, M.V. Lomonosov Institute of Fine Chemical Technologies, MIREA – Russian Technological University (86, Vernadskogo pr., Moscow, 119571, Russia). Scopus Author ID 6701455145, ResearcherID T-2835-2019, https://orcid.org/0000-0002-7027-378X

Об авторах:

Романова Надежда Александровна, магистрант кафедры химии и технологии биологически активных соединений, медицинской и органической химии им. Н.А. Преображенского Института тонких химических технологий им. М.В. Ломоносова ФГБОУ ВО «МИРЭА – Российский технологический университет» (119571, Россия, Москва, пр-т Вернадского, д. 86). https://orcid.org/0000-0001-5073-2873

Буданова Ульяна Александровна, кандидат химических наук, ассистент кафедры химии и технологии биологически активных соединений, медицинской и органической химии им. Н.А. Преображенского Института тонких химических технологий им. М.В. Ломоносова ФГБОУ ВО «МИРЭА – Российский технологический университет» (119571, Россия, Москва, пр-т Вернадского, д. 86). E-mail: c-221@yandex.ru. Scopus Author ID 14622352500, ResearcherID E-1659-2014, https://orcid.org/0000-0003-1702-9435

Себякин Юрий Львович, доктор химических наук, профессор кафедры химии и технологии биологически активных соединений, медицинской и органической химии им. Н.А. Преображенского Института тонких химических технологий им. М.В. Ломоносова ФГБОУ ВО «МИРЭА – Российский технологический университет» (119571, Россия, Москва, пр-т Вернадского, д. 86). Scopus Author ID 6701455145, ResearcherID T-2835-2019, https://orcid.org/0000-0002-7027-378X

The article was submitted: February 18, 2020; approved after reviewing: June 15, 2020; accepted for publication: August 07, 2020.

Translated from Russian into English by N. Isaeva
Edited for English language and spelling by Enago, an editing brand of Crimson Interactive Inc.

SYNTHESIS AND PROCESSING OF POLYMERS AND POLYMERIC COMPOSITES

СИНТЕЗ И ПЕРЕРАБОТКА ПОЛИМЕРОВ И КОМПОЗИТОВ НА ИХ ОСНОВЕ

ISSN 2686-7575 (Online)

https://doi.org/10.32362/2410-6593-2020-15-5-46-53

UDC 678

RESEARCH ARTICLE

Influence of iron ore concentrate (magnetite) on the kinetics of butadiene–styrene rubber-based blend curing in the presence of different accelerators

Aram A. Khachaturov[@], Evgeniy E. Potapov, Sergei V. Reznichenko, Anna N. Kovaleva

MIREA – Russian Technological University, Moscow, 119454 Russia
[@]Corresponding author, e-mail: xa4aram@mail.ru

Objectives. *To investigate the possibility of using a cheaper ingredient, such as magnetite, in the synthesis of rubber compounds based on butadiene–styrene rubber by examining its effect on the process of sulfuric vulcanization of butadiene–styrene rubber in the presence of various accelerators.*

Methods. *The influence of magnetite on the vulcanization kinetics was studied using an Alpha Technologies PRPA 2000 rotorless rheometer. Thermogravimetric analysis (TGA) and differential scanning calorimetry (DSC) were performed using a Mettler Toledo TGA/DSC 2 device to evaluate the effect of magnetite on the butadiene–styrene rubber-based vulcanizates' oxidation.*

Results. *Magnetite was found to affect the kinetics of SBR-1500 butadiene–styrene rubber sulfuric vulcanization in the presence of thiazole-type accelerators (2-MBT, 2-MBS); in contrast, magnetite was inactive in the case of diphenylguanidine, sulfenamide T, and tetramethylthiuram disulfide. The obtained TGA/DSC data showed that magnetite has no significant effect on the butadiene–styrene rubber-based vulcanizates' oxidation and thermal destruction.*

Conclusions. *The obtained data confirmed magnetite's capability to act as a butadiene–styrene rubber sulfuric vulcanization activator in the presence of various accelerators. The most significant effect was observed in the presence of thiazole-type accelerators.*

Keywords: *iron ore concentrate, magnetite, butadiene–styrene rubber, vulcanization activator, kinetics of curing, thermogravimetric analysis, differential scanning calorimetry*

For citation: Khachaturov A.A., Potapov E.E., Reznichenko S.V., Kovaleva A.N. Influence of iron ore concentrate (magnetite) on the kinetics of butadiene–styrene rubber-based blend curing in the presence of different accelerators. *Tonk. Khim. Tekhnol. = Fine Chem. Technol.* 2020;15(5):46-53 (Russ., Eng.). https://doi.org/10.32362/2410-6593-2020-15-5-46-53

НАУЧНАЯ СТАТЬЯ

Влияние железорудного концентрата (магнетита) на кинетику вулканизации резиновых смесей на основе бутадиен-стирольного каучука в присутствии различных ускорителей

А.А. Хачатуров[@], Е.Э. Потапов, С.В. Резниченко, А.Н. Ковалева

МИРЭА – Российский технологический университет, Москва, 119454 Россия
[@]Автор для переписки, e-mail: xa4aram@mail.ru

Цели. *Изучить возможность применения в рецептурах резиновых смесей на основе бутадиен-стирольного каучука более дешевого ингредиента – магнетита путем оценки его влияния на процесс серной вулканизации бутадиен-стирольного каучука в присутствии различных ускорителей.*

Методы. *Влияние магнетита на кинетику вулканизации исследовали с помощью безроторного реометра AlphaTechnologies PRPA 2000. Методами термогравиметрического анализа (ТГА) и дифференциально-сканирующей калориметрии (ДСК) оценили влияние магнетита на процесс окисления вулканизатов на основе бутадиен-стирольного каучука на приборе Mettler Toledo TGA/DSC 2.*

Результаты. *Показано, что магнетит влияет на кинетику серной вулканизации бутадиен-стирольного каучука SBR-1500 в присутствии ускорителей тиазолового ряда (дибензотиазолдисульфид, 2-меркаптобензотиазол), в то время как в случае с 1,3-дифенилгуанидином, сульфенамидом Т (N-трет-бутил-2-бензтиазолсульфенамид) и тиурамом (тетраметилтиурамдисульфид) магнетит малоактивен. Данные, полученные с ТГА/ДСК, демонстрируют, что магнетит незначительно влияет на окисление, а также на термодеструкцию вулканизатов на основе бутадиен-стирольного каучука.*

Выводы. *Исследовано влияние магнетита на кинетику процесса серной вулканизации бутадиен-стирольного каучука в присутствии различных ускорителей. Наибольший эффект наблюдается в присутствии ускорителей тиазолового ряда.*

Ключевые слова: *железорудный концентрат, магнетит, бутадиен-стирольный каучук, активатор вулканизации, кинетика вулканизации, термогравиметрический анализ, дифференциально-сканирующая калориметрия*

Для цитирования: Хачатуров А.А., Потапов Е.Э., Резниченко С.В., Ковалева А.Н. Влияние железорудного концентрата (магнетита) на кинетику вулканизации резиновых смесей на основе бутадиен-стирольного каучука в присутствии различных ускорителей. *Тонкие химические технологии.* 2020;15(5):46-53.
https://doi.org/10.32362/2410-6593-2020-15-5-46-53

INTRODUCTION

The choice of ingredients for synthesizing various rubber compounds is critical in the production of serial elastomeric products. When developing a new elastomeric compound, three main ingredient characteristics must be considered during compounding—the properties, manufacturability, and price of the elastomeric material [1]. These three characteristics are crucial in the manufacturing sector because certain ingredients can significantly enhance the vulcanization parameters and properties of the final product. However, such products are unaffordable in the market as their costs increase exponentially. Thus, the chemical analysts face the challenge of a) improving product quality, b) attributing it a set of new properties, c) reducing the concentration of expensive system ingredients, d) lowering the synthesis cost without compromising the technological characteristics of the mixtures, and e) reducing the operational properties of the finished product. Therefore, the search for new rubber compound ingredients is an urgent task [2–5].

In previous works [6, 7], the effect of magnetite on the kinetics of butadiene–styrene rubber SKS-30 ARK vulcanization in the absence of zinc oxide was studied. Therein, magnetite acted as an activator of sulfur vulcanization. However, the characteristics of the vulcanizates obtained with its use are slightly inferior to the properties of standard rubbers.

MATERIALS AND METHODS

The primary objective of this work is to study the kinetics of black-extended elastomeric material vulcanization based on SBR-1500 butadiene–styrene rubber in the presence of the classic vulcanizing group and with other sulfur vulcanization accelerators to investigate the potential use of magnetite in the composition of sulfuric vulcanizing systems as an active component that enhances vulcanization parameters of rubber compounds. In addition, the effect of different magnetite contents on the aging process of elastomeric material was examined by studying the nature of the variation in the thermogrvimetric analysis (TGA) curves and differential scanning calorimetry (DSC) of SBR-1500-based vulcanizates.

Herein, we used iron ore concentrate containing more than 69.5% mass fraction of iron, TU 0712-030-001186803-99 (*Lebedinsky Mining and Processing Plant*, Russia).

The dispersion of the iron ore concentrate powder was investigated using an Analysette 22 MicroTec Plus laser diffractometer manufactured by *Fritsch GmbH*, Germany.

RESULTS AND DISCUSSION

The particle size distribution (Fig. 1) is unimodal (from 0.1 to 100 μm). The maximum differential distribution *dQ* of the volume fraction of particles falls on ~20-μm-sized particles. The integral dependence of the volume fraction *Q* of particles on the size shows that 50% and 90% of the iron ore concentrate particles are less than 15 and 40 μm in size, respectively.

Figure 2 shows the X-ray diffractogram of the iron ore concentrate powder obtained on an HZG-4 X-ray diffractometer (*Helmholtz-Zentrum Geesthacht*, Germany) (Ni filter): CuKα = 1.54051 Å on a diffracted beam in the step-by-step mode with a pulse acquisition time of 10 s and a step value of 0.02° in the angular range of 2Θ = 2°–80°.

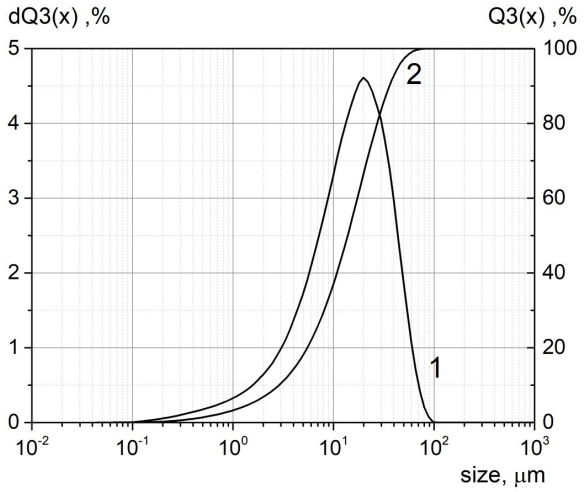

Fig. 1. Differential *dQ* (1) and integral *Q* (2) curves of iron ore concentrate powder particle distribution (obtained using Analysette 22 MicroTec Plus, *Fritsch GmbH*, Germany).

The iron ore concentrate used was magnetite, as evidenced by diffraction reflections at 2Θ values of ~36°, ~57°, and ~63°. The resulting spectrum is consistent with that obtained from the international database of diffraction standards, the Crystallography Open Database[1]. In the angular range of 2Θ = 16°–26°, an amorphous halo and diffraction reflections characteristic of quartz can be observed at 2Θ = ~27° and ~41° [8]. Silicon dioxide content determined from the diffraction patterns via semiquantitative analysis (using the Match! software package, *CRYSTAL IMPACT GbR*, Germany)[2] is about 5–6%.

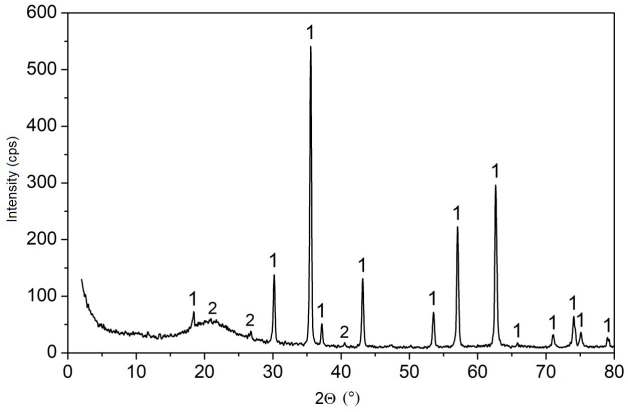

Fig. 2. Diffraction pattern of iron ore concentrate obtained from the *Lebedinsky Mining and Processing Plant*: (1) Fe_3O_4 phase; (2) SiO_2 phase.

The rubber compounds were prepared in a Brabender laboratory rubber mixer (*Brabender GmbH & Co KG*, Germany) at a chamber temperature of T = 60°C and an angular speed of rotor rotation, ω = 60–63 rpm, with the total mixing time being t < 10 min. The mixing was performed in two stages. In the first stage, SBR-1500 butadiene–styrene rubber, zinc oxide (ZnO), stearic acid, and fillers—magnetite, carbon black (CB) N339, or their mixtures having various compositions—were introduced; then, the mixture was cooled. In the second stage, the curing system was introduced, and the resulting mixtures were finalized on rollers.

The amount of magnetite in the mixtures based on SBR-1500 varied in the range of 0, 25, and 50 per hundreds of rubber (phr) at a constant concentration

[1] Crystallography Open Database.
URL: http://www.crystallography.net.
[2] URL: http://www.crystalimpact.com/match/Default.htm

of CB N339: 50 phr (see Table 1). In the case of altax (2-MBS) and sulfenamide T (TBBS), a formulation corresponding to GOST 15627-79[1] and GOST ISO 2322-2013[2] was used. For the remaining accelerators, TBBS accelerators were replaced with an equimolar amount of tetramethylthiuram disulfide (TMTD), diphenylguanidine (DPG), and captax (2-MBT) accelerators in accordance with ISO 2322:2009. In the case of mixtures containing DPG and 2-MBT as accelerators, the accelerator content was increased to 3.0 phr because at lower concentrations (vulcanization temperature T_V = 160°C, process duration τ = 60 min) the torque in the time curve did not reach the vulcanization plateau.

Vulcanization parameters were determined using an RPA 2000 rotorless rheometer (*Alpha Technologies*, USA). Rheometric curves were plotted at a temperature of T_V = 160°C for τ = 60 min.

TGA/DSC studies were performed on samples based on SBR-1500 manufactured according to ISO 2322:2009, with a constant total filler content of 50 phr. The dosage of magnetite was increased from 0 to 50 phr in increments of 10 phr, and the dosage of CB N339 was decreased in the same order. Measurements were conducted on a TGA/DSC 2 device (*Mettler Toledo*, USA) in an atmosphere of nitrogen and oxygen in the temperature range of 25–250°C, at a heating rate of 10 °C/min.

The following parameters were determined based on the kinetic curves—optimal vulcanization time ($t'90$), scorch time(t_S1), minimum (M_L), and maximum (M_H) torque. Table 2 shows the dependence of these parameters on magnetite content in rubber compounds based on SBR-1500.

Different magnetite contents influence the time taken to reach the vulcanization optimum and scorch time as well as the minimum and maximum torque in the presence of different accelerators. The time taken to reach the vulcanization optimum t′90 decreases at T_V = 160°C in the presence of the TBBS, 2-MBS, DPG, and 2-MBT accelerators as magnetite content increases. In addition, the maximum effect manifested in the case of 2-MBT ($t'90$ decreases from 36 to 19 min upon the introduction of 50 phr of magnetite). In the case of TMTD, variation in magnetite content has practically no effect on the time taken to achieve optimum vulcanization. The scorch time in the presence of the TBBS and 2-MBT accelerators decreases with increasing magnetite concentration. In the case of DPG and TMTD, as the magnetite content varies, the dependence of the vulcanization time passes through a maximum, and in the case of 2-MBS, through a minimum. Notably, the change in the absolute value of scorch time is not significant in all cases. The maximum torque in the presence of all accelerators increases linearly

Table 1. Formulations of elastomeric mixtures based on butadiene–styrene rubber SBR-1500 and magnetite with different accelerators

Component	Component content, phr														
	1	2	3	4	5	6	7	8	9	10	11	12	13	14	15
SBR-1500	100	100	100	100	100	100	100	100	100	100	100	100	100	100	100
ZnO	3.00	3.00	3.00	5.00	5.00	5.00	3.00	3.00	3.00	3.00	3.00	3.00	3.00	3.00	3.00
Sulfur	1.75	1.75	1.75	2.00	2.00	2.00	1.75	1.75	1.75	1.75	1.75	1.75	1.75	1.75	1.75
Stearic acid	1.00	1.00	1.00	1.50	1.50	1.50	1.00	1.00	1.00	1.00	1.00	1.00	1.00	1.00	1.00
TBBS	1.00	1.00	1.00	–	–	–	–	–	–	–	–	–	–	–	–
2-MBS	–	–	–	3.00	3.00	3.00	–	–	–	–	–	–	–	–	–
TMTD	–	–	–	–	–	–	1.00	1.00	1.00	–	–	–	–	–	–
DPG	–	–	–	–	–	–	–	–	–	3.00	3.00	3.00	–	–	–
2-MBT	–	–	–	–	–	–	–	–	–	–	–	–	3.00	3.00	3.00
CBN339	50.0	50.0	50.0	40.0	40.0	40.0	50.0	50.0	50.0	50.0	50.0	50.0	50.0	50.0	50.0
Magnetite	0.0	25.0	50.0	0.0	25.0	50.0	0.0	25.0	50.0	0.0	25.0	50.0	0.0	25.0	50.0

[3] GOST 15927-79. State Standard. Synthetic rubbers butadiene-methylstyrene СКМС-30 АРК and butadiene-styrene СКС-30 АРК. Specifications. Moscow: IPK Izd. Stand.; 2003.

[4] GOST ISO 2322-2013. State Standard. Styrene-butadiene rubber (SBR) of emulsion- and solution-polymerized types. Evaluation methods. Moscow: Standartinform; 2014.

Table 2. Dependence of vulcanization characteristics on magnetite concentration in black-extended mixtures based on SBR-1500 in the presence of various accelerators

Accelerator type	Accelerator content, phr	CB N339 content, phr	Magnetite content, phr	Vulcanization characteristics			
				$t'90$, min	t_S1, min	M_L, dyn·m	M_H, dyn·m
TBBS	1.00	50.0	0.0	15.84	5.32	2.8	22.41
	1.00	50.0	25.0	14.88	4.81	2.74	24.63
	1.00	50.0	50.0	12.54	4.55	3.42	26.31
2-MBS	3.00	40.0	0.0	14.62	2.5	1.87	19.65
	3.00	40.0	25.0	12.54	2.06	2.06	21.22
	3.00	40.0	50.0	11.59	2.41	2.4	23.41
TMTD	1.00	50.0	0.0	6.85	1.1	2.95	29.63
	1.00	50.0	25.0	6.26	1.26	3.16	31.67
	1.00	50.0	50.0	6.57	1.28	3.58	34.69
DPG	3.00	50.0	0.0	32.86	2.45	2.58	18.73
	3.00	50.0	25.0	31.93	2.71	2.64	19.48
	3.00	50.0	50.0	31.23	2.49	2.82	20.07
2-MBT	3.00	50.0	0.0	36.29	1.83	2.7	16.99
	3.00	50.0	25.0	23.97	1.33	2.93	20.69
	3.00	50.0	50.0	19.22	1.3	2.98	23.09

(at different speeds) with increasing magnetite content, with a constant content of CB (see Table 2).

According to the above data, magnetite activates the sulfur vulcanization process. The maximum effect of magnetite introduction is observed in the presence of thiazole-type accelerators; this suggests that Fe^{+2} and Fe^{+3} ions on the surface of magnetite particles catalytically accelerate disulfide bond decomposition (scheme) through a mechanism similar to radical polymerization initiation by redox systems based on iron(II) and iron(III) salts [9, 10]. The radicals formed by the decomposition of accelerator disulfide bonds subsequently activate the sulfur vulcanization process.

Thermograms of TGA vulcanizates (Figs. 3 and 4) under nitrogen atmosphere show that when the magnetite is introduced into the rubber mixture based on SBR-1500 in an amount equivalent to the concentration of CB N339 in the standard mixture (50 phr), less weight loss occurred than in the case of samples containing only CB N339, in the entire temperature range. A similar effect occurred in an oxygen atmosphere, wherein the curves are characterized by an increase in mass in the temperature range up to 100°C. This is most likely due to the accumulation of oxidation products.

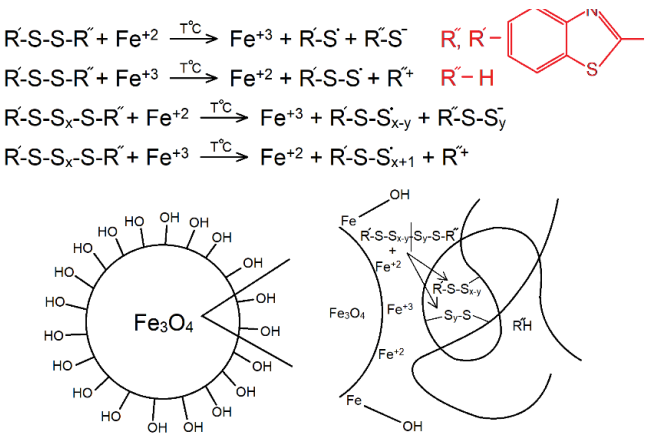

Scheme. Supposed interaction between magnetite particles and butadiene–styrene rubber macromolecules in the presence of accelerators containing disulfide bonds.

The DSC data presented in Fig. 5 (in an inert medium of N_2) indicates that magnetite practically does not accelerate the thermal decomposition (endothermic process) of the vulcanizates. Slight differences were observed only in the temperature range above 150°C.

Similar results were obtained when studying the processes of thermal oxidative degradation in an O_2

medium (Fig. 6). In this case, the thermal oxidation of the vulcanizates begins at 190–220°C. An exothermic peak appears in the temperature range of 210–230°C, and shifts to lower temperatures as the magnetite concentration increases. No significant activating effect of magnetite is observed in these processes.

However, as stated in [11], iron cations of variable valency in the polymer phase accelerate oxidative processes several times. This is true only in cases wherein iron salts are at least partially dissolved in the polymer phase. In the case of magnetite, iron cations of variable valency capable of causing oxidation are available only on the particle surfaces. This considerably complicates the oxidative process' catalysis.

CONCLUSIONS

The above data confirm the capability of magnetite to act as an active agent in the process of sulfuric vulcanization of butadiene–styrene rubber in the presence of various accelerators. Herein, the most significant effect of magnetite, as an active component of the vulcanizing system, manifested in the presence of thiazole-type accelerators (2-MBS and 2-MBT). In addition, the presence of magnetite in SBR-1500-based vulcanizates practically did not affect the oxidation process in the operating temperature range of most elastomeric products.

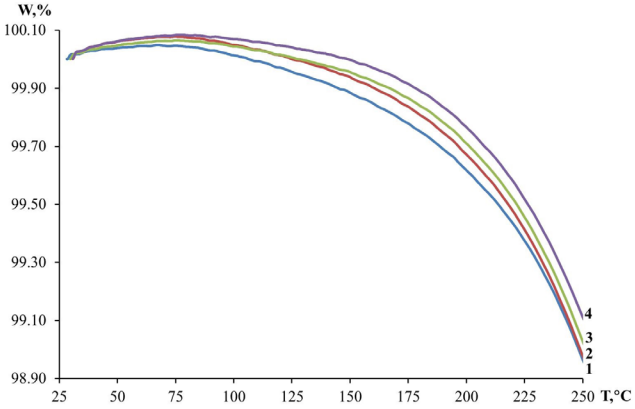

Fig. 3. TGA patterns for vulcanizates based on SBR-1500 with different magnetite and CB N339 (in nitrogen atmosphere) contents: (1) 50 phr of N339 + 0 phr of magnetite; (2) 30 phr of N339 + 20 phr of magnetite; (3) 10 phr of N339 + 40 phr of magnetite; and (4) 0 phr of N339 + 50 phr of magnetite.

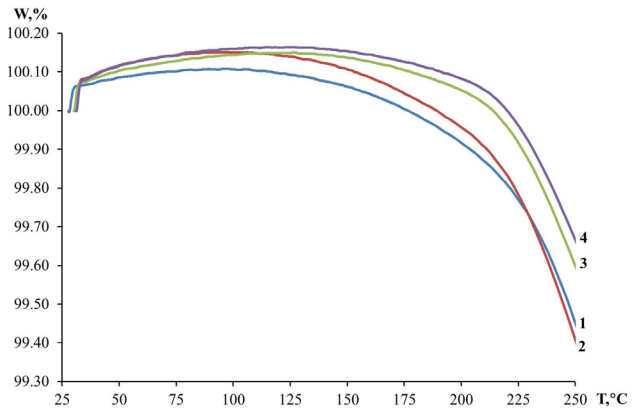

Fig. 4. TGA patterns for vulcanizates based on SBR-1500 with different magnetite and CB N339 (in oxygen atmosphere) contents: (1) 50 phr of N339 + 0 phr of magnetite; (2) 30 phr of N339 + 20 phr of magnetite; (3) 10 phr of N339 + 40 phr of magnetite; and (4) 0 phr of N339 + 50 phr of magnetite.

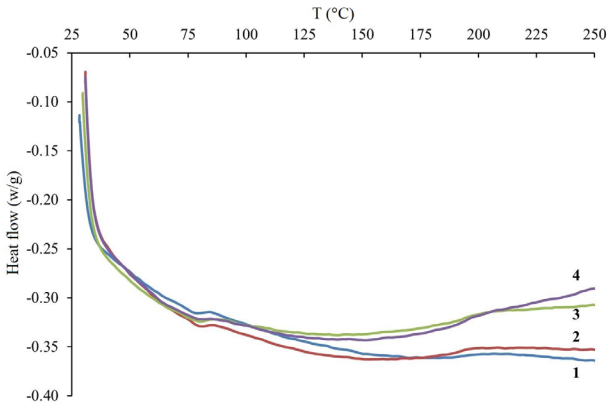

Fig. 5. DSC pattern for vulcanizates based on SBR-1500 with different magnetite and CB N339 (in nitrogen atmosphere) contents: (1) 50 phr of N339 + 0 phr of magnetite; (2) 30 phr of N339 + 20 phr of magnetite; (3) 10 phr of N339 + 40 phr of magnetite; and (4) 0 phr of N339 + 50 phr of magnetite.

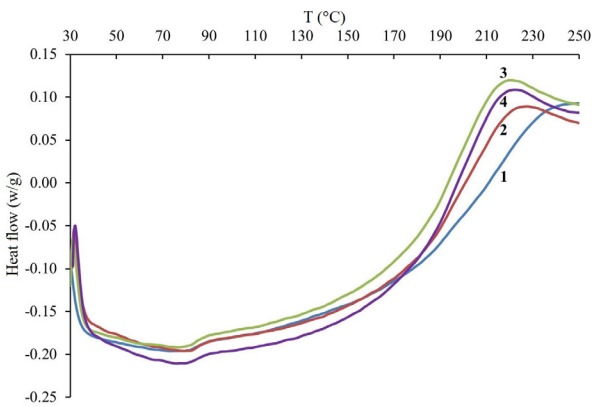

Fig. 6. DSC pattern for vulcanizates based on SBR-1500 with different magnetite and CB N339 (in oxygen atmosphere) contents: (1) 50 phr of N339 + 0 phr of magnetite; (2) 30 phr of N339 + 20 phr of magnetite; (3) 10 phr of N339 + 40 phr of magnetite; and (4) 0 phr of N339 + 50 phr of magnetite.

Financial support

This study did not have any financial support from outside organizations.

Authors' contribution

A.A. Khachaturov – literature analysis, article writing, research planning; carrying out all the stages of the study, formalization of the list of references;

E.E. Potapov – idea, development of the research design, consultation on the problems of carrying out all the stages of the study;

S.V. Reznichenko – consultation on the problems of planning, methodology and implementation of the study;

A.N. Kovaleva – scientific editing, technical editing, formalizing the bibliography.

The authors declare no conflicts of interest.

REFERENSES

1. Dick J.S. *Tekhnologiya reziny: Retsepturostroenie i ispytaniya* (Rubber technology. Compounding and testing for performance). Translated from English by Shershnev V.A. Sankt Peterburg: Nauchnye osnovy i tekhnologii; 2010, 620 p. (in Russ.).

2. Heideman G., Datta R.N., Noordermeer J.W.M. Activators in accelerated sulfur vulcanization. *Rubber Chemistry and Technology.* 2004;77(3):512-541. https://doi.org/10.5254/1.3547834

3. Heideman G., Noordermeer J.W.M., Datta R.N. Zinc loaded clay as activator in sulfur vulcanization: a new route for zinc oxide reduction in rubber compounds. *Rubber Chemistry and Technology.* 2004;77(2):336-355. https://doi.org/10.5254/1.3547827

4. Mostoni S., Milana P., Di Credico B. Zinc-Based Curing Activators: New Trends for Reducing Zinc Content in Rubber Vulcanization Process. *Catalysts*. 2019;9(8):664. https://doi.org/10.3390/catal9080664

5. Zanchet A., Demori R., de Sousa F.D.B. Sugar cane as an alternative green activator to conventional vulcanization additives in natural rubber compounds: Thermal degradation study. *Journal of Cleaner Production.* 2019;207:248-260. https://doi.org/10.1016/j.jclepro.2018.09.203

6. Khachaturov A.A., Potapov E.E., Monahova T.V. Effect of magnetite on the kinetics of oxidation and structuring of elastomeric materials based on styrene-butadiene rubber. *XVII Ezhegodnaya molodezhnaya konferentsiya c mezhdunarodnym uchastiem IBKhF RAN-VUZy "Biokhimicheskaya fizika"-2017: sb. tr. konf.* (The 17th Annual Youth Conference with international participation of the Institute of Biochemical Physics RAS-Universities "Biochemical Physics" -2017: collection of abstracts). Moscow: RUDN; 2017, p. 71-75 (in Russ.).

7. Khachaturov A.A. Functional and elastomeric materials on the basis of butadiene-styrene rubber and magnetite. *XXVIII Mendeleevskaya konferentsiya molodykh uchenykh: sb. tez. i dokl. konf.* (The 28th Mendeleev Conference of Young Scientists: a collection of abstracts and conference reports). Novosibirsk: 2018, p. 111 (in Russ.).

8. Borisov L.A., Grishin Yu.M., Kozlov N.P. *et al.* A method for the direct production of polycrystalline silicon from natural quartz and from its especially pure concentrates: RF Pat. 2516512, 2012. RU2516512C2 (in Russ.).

СПИСОК ЛИТЕРАТУРЫ

1. Дик Дж.С. Технология резины: Рецептуростроение и испытания. Под ред. Дика Дж.С. Пер. с англ. Котовой С.В., Глаголева В.А., Люсовой Л.Р. под ред. Шершнева В.А. СПб.: Научные основы и технологии; 2010. 620 с.

2. Heideman G., Datta R.N., Noordermeer J.W.M. Activators in accelerated sulfur vulcanization. *Rubber Chemistry and Technology.* 2004;77(3):512-541. https://doi.org/10.5254/1.3547834

3. Heideman G., Noordermeer J.W.M., Datta R.N. Zinc loaded clay as activator in sulfur vulcanization: a new route for zinc oxide reduction in rubber compounds. *Rubber Chemistry and Technology.* 2004;77(2):336-355. https://doi.org/10.5254/1.3547827

4. Mostoni S., Milana P., Di Credico B. Zinc-Based Curing Activators: New Trends for Reducing Zinc Content in Rubber Vulcanization Process. *Catalysts.* 2019;9(8):664. https://doi.org/10.3390/catal9080664

5. Zanchet A., Demori R., de Sousa F.D.B. Sugar cane as an alternative green activator to conventional vulcanization additives in natural rubber compounds: Thermal degradation study. *Journal of Cleaner Production.* 2019;207:248-260. https://doi.org/10.1016/j.jclepro.2018.09.203

6. Хачатуров А.А., Потапов Е.Э., Монахова Т.В. Влияние магнетита на кинетику окисления и структурирования эластомерных материалов на основе бутадиен-стирольного каучука. XVII Ежегодная молодежная конференция с международным участием ИБХФ РАН-ВУЗы «Биохимическая физика»-2017: сб. тр. конф. (13–15 ноября 2017 г., г. Москва). Москва: Изд-во РУДН; 2018, с. 71-75.

7. Хачатуров А.А. Функциональные эластомерные композиционные материалы на основе бутадиен-стирольного каучука и магнетита. XXVIII Менделеевская конференция молодых ученых: сб. тез. и докл. конф. (13–18 мая 2018 г., г. Новосибирск). Новосибирск: Изд-во НГУ; 2018, с.111.

8. Борисов Л.А., Гришин Ю.М., Козлов Н.П. и др. Способ прямого получения поликристаллического кремния из природного кварца и из его особо чистых концентратов: РФ Пат. 2516512, МПК7 C 30 B 30/02, C 30 B 29/06. N 2012128656/05; заявл. 09.07.12; опубл. 20.05.14, Бюл. N 14.

9. Dogadkin B.A., Doncov A.A., Shershnev V.A. *Khimiya elastomerov* (Chemistry of Elastomers). 2nd ed. reslave. and add. Moscow: Khimiya; 1981. 376 p. (in Russ.).

10. Al-Ghamdi A.A., Al-Hartomy O.A., Al-Solamy F.R. Preparation and characterisation of natural rubber composites comprising hybrid fillers of activated carbon / *in situ* synthesised magnetite. *Journal of Rubber Research.* 2018;21(2):94-118. https://doi.org/10.1007/bf03449164

11. Grassie N., Skott G. *Destruktsiya i stabilizatsiya polimerov* (Polymer degradation and stabilisation). Translated from English. Moscow: Mir; 1988, 446 p. (in Russ.).

9. Догадкин Б.А., Донцов А.А., Шершнев В.А. Химия эластомеров. 2-е изд. перераб. и доп. М.: Химия; 1981; 376 с.

10. Al-Ghamdi A.A., Al-Hartomy O.A., Al-Solamy F.R. Preparation and characterisation of natural rubber composites comprising hybrid fillers of activated carbon / *in situ* synthesised magnetite. *Journal of Rubber Research.* 2018;21(2):94-118. https://doi.org/10.1007/bf03449164

11. Грасси Н., Скотт Дж. Деструкция и стабилизация полимеров. Пер. с англ. М.: Мир; 1988, 446 с.

About the authors:

Aram A. Khachaturov, Postgraduate Student, B.A. Dogadkin Department of Physics and Chemistry of Materials, Institute of Physics and Technology, MIREA – Russian Technological University (78, Vernadskogo pr., Moscow, 119454, Russia). E-mail: xa4aram@mail.ru, https://orcid.org/0000-0002-3852-581X

Evgeniy E. Potapov, Dr. of Sci. (Chemistry), Professor, B.A. Dogadkin Department of Physics and Chemistry of Materials, Institute of Physics and Technology, MIREA – Russian Technological University (78, Vernadskogo pr., Moscow, 119454, Russia). E-mail: svitar@yandex.ru. Scopus Author ID 7006238695.

Sergei V. Reznichenko, Dr. of Sci. (Technology), Professor, Head of the B.A. Dogadkin Department of Physics and Chemistry of Materials, Institute of Physics and Technology, MIREA – Russian Technological University (78, Vernadskogo pr., Moscow, 119454, Russia). E-mail: svrezn@gmail.com, Scopus Author ID 6603145791.

Anna N. Kovaleva, Cand. of Sci. (Chemistry), Assistant Professor, Department of Chemistry and Technology for Processing Plastics and Polymer Composites, M.V. Lomonosov Institute of Fine Chemical Technologies, MIREA – Russian Technological University (86, Vernadskogo pr., Moscow, 119571, Russia). E-mail: kovaleva_anna79@mail.ru, https://orcid.org/0000-0002-6389-3833

Об авторах:

Хачатуров Арам Арнольдович, аспирант кафедры Физики и химии материалов им. Б.А. Догадкина Физико-технологического института ФГБОУ ВО «МИРЭА – Российский технологический университет» (119454, Россия, Москва, пр-т Вернадского, д. 78). E-mail: xa4aram@mail.ru, https://orcid.org/0000-0002-3852-581X

Потапов Евгений Эдуардович, доктор химических наук, профессор, профессор кафедры Физики и химии материалов им. Б.А. Догадкина Физико-технологического института ФГБОУ ВО «МИРЭА – Российский технологический университет» (119454, Россия, Москва, пр-т Вернадского, д. 78). E-mail: svitar@yandex.ru. Scopus Author ID 7006238695.

Резниченко Сергей Владимирович, доктор технических наук, профессор, зав. кафедрой Физики и химии материалов им. Б.А. Догадкина Физико-технологического института ФГБОУ ВО «МИРЭА – Российский технологический университет» (119454, Россия, Москва, пр-т Вернадского, д. 78). E-mail: svrezn@gmail.com. Scopus Author ID 6603145791.

Ковалева Анна Николаевна, кандидат химических наук, доцент кафедры химии и технологии переработки пластмасс и полимерных композитов Института тонких химических технологий им. М.В. Ломоносова ФГБОУ ВО «МИРЭА – Российский технологический университет» (119571, Россия, Москва, пр-т Вернадского, д. 86). E-mail: kovaleva_anna79@mail.ru, https://orcid.org/0000-0002-6389-3833

The article was submitted: December 30, 2019; approved after reviewed: June 05, 2020; accepted for publication: August 05, 2020.

Translated from Russian into English by M. Povorin
Edited for English language and spelling by Enago, an editing brand of Crimson Interactive Inc.

ХИМИЯ И ТЕХНОЛОГИЯ НЕОРГАНИЧЕСКИХ МАТЕРИАЛОВ

CHEMISTRY AND TECHNOLOGY OF INORGANIC MATERIALS

ISSN 2410-6593 (Print), ISSN 2686-7575 (Online)

https://doi.org/10.32362/2410-6593-2020-15-5-54-62

UDC 546(65+284)

RESEARCH ARTICLE

Determining the phase stability of luminescent materials based on the solid solutions of oxyorthosilicates $(Lu_{1-x}Ln_x)[(SiO_4)_{0.5}O_{0.5}]$, where Ln = La–Yb

Eugeni I. Get'man[1], Yuliia A. Oleksii[1], Serhii V. Radio[1,@], Lyudmyla I. Ardanova[2]

[1]Department of Inorganic, Organic, and Analytical Chemistry, Faculty of Chemistry, Biology, and Biotechnologies, Vasyl' Stus Donetsk National University, Vinnytsia, 21021 Ukraine
[2]Department of Biochemistry, Chemistry, and Geology, Minnesota State University, Mankato, Minnesota, 56001 USA
[@]Corresponding author, e-mail: radio@donnu.edu.ua

Objectives. *This study aimed to predict the limits of substitution and stability of luminescent materials based on low-temperature modifications of solid solutions (spatial group $P2_1/c$) with lutetium oxyorthosilicates $(Lu_{1-x}Ln_x)[(SiO_4)_{0.5}O_{0.5}]$, where Ln represents the rare-earth elements (REEs) of the La–Yb series.*

Methods. *The V.S. Urusov's crystal energy theory of isomorphous substitutions and a crystallochemical approach in the regular solid solution approximation were used to calculate the energies of the mixing (interaction parameters) of the solid solutions.*

Results. *Using the V.S. Urusov's theory, we calculated the energies of mixing (interaction parameters) in the systems under study. The dependences of the decomposition temperatures of solid solutions on the REE number and composition (x) were obtained and used to create a diagram of the thermodynamic stability of the solid solutions, allowing us to predict the substitution limits depending on the temperature or determine the decomposition temperature using the given substitution limits.*

Conclusions. *The results of the study can be useful when choosing the ratio of components in matrices (host materials) and the amount of the activator (dopant) in the new luminescent, laser, and other materials based on low-temperature modifications of solid solutions of "mixed" REE oxyorthosilicates $(Lu_{1-x}Ln_x)[(SiO_4)_{0.5}O_{0.5}]$.*

Keywords: *oxyorthosilicate, rare-earth elements, isomorphous substitution, solid solution, energy of mixing*

For citation: Get'man E.I., Oleksii Yu.A., Radio S.V., Ardanova L.I. Determining the phase stability of luminescent materials based on the solid solutions of oxyorthosilicates $(Lu_{1-x}Ln_x)[(SiO_4)_{0.5}O_{0.5}]$, where Ln = La–Yb. *Tonk. Khim. Tekhnol. = Fine Chem. Technol.* 2020;15(5):54-62. https://doi.org/10.32362/2410-6593-2020-15-5-54-62

НАУЧНАЯ СТАТЬЯ

Определение фазовой стабильности люминесцентных материалов на основе твердых растворов оксиортосиликатов $(Lu_{1-x}Ln_x)[(SiO_4)_{0.5}O_{0.5}]$, где Ln = La–Yb

Е.И. Гетьман[1], Ю.А. Олексий[1], С.В. Радио[1,@], Л.И. Арданова[2]

[1]Донецкий национальный университет им. Васыля Стуса, Винница, 21021 Украина
[2]Государственный университет Миннесоты, Манкейто, Миннесота, 56001, США
[@]Автор для переписки, e-mail: radio@donnu.edu.ua

Цели. *Целью работы явилось прогнозирование пределов замещения и стабильности люминесцентных материалов на основе низкотемпературных модификаций твердых растворов (пространственная группа $P2_1/c$) на основе оксиортосиликата лютеция $(Lu_{1-x}Ln_x)[(SiO_4)_{0.5}O_{0.5}]$, где Ln – редкоземельный элемент серии La–Yb.*

Методы. *Для расчета энергий смешения (параметров взаимодействия) для твердых растворов была использована теория изоморфной смесимости В.С. Урусова и кристаллохимический подход в приближении регулярного твердого раствора.*

Результаты. *Получены зависимости температур распада твердых растворов от порядкового номера редкоземельных элементов и состава, которые использованы для построения диаграмм термодинамической устойчивости твердых растворов, что позволило прогнозировать пределы замещения в зависимости от температуры или определять температуру распада на основе заданных пределов замещения.*

Выводы. *Результаты исследования могут быть полезны при выборе соотношения компонентов в матрице («хозяине») и количества активатора (допанта) в новых люминесцентных, лазерных и других материалах на основе низкотемпературных модификаций твердых растворов «смешанных» оксиортосиликатов редкоземельных элементов $(Lu_{1-x}Ln_x)[(SiO_4)_{0.5}O_{0.5}]$.*

Ключевые слова: *оксиортосиликат; редкоземельные элементы; изоморфное замещение; твердый раствор; энергия смешения*

Для цитирования: Get'man E.I., Oleksii Yu.A., Radio S.V., Ardanova L.I. Determining the phase stability of luminescent materials based on the solid solutions of oxyorthosilicates $(Lu_{1-x}Ln_x)[(SiO_4)_{0.5}O_{0.5}]$, where Ln = La−Yb. *Tonk. Khim. Tekhnol. = Fine Chem. Technol.* 2020;15(5):54-62. https://doi.org/10.32362/2410-6593-2020-15-5-54-62

INTRODUCTION

Oxyorthosilicates of rare-earth elements (REEs), $Ln[(SiO_4)_{0.5}O_{0.5}]$, and solid solutions $(Lu_{1-x}Ln_x)[(SiO_4)_{0.5}O_{0.5}]$ have attracted the attention of researchers, as they can be applied as materials for producing luminophores [1, 2], scintillators [3–7], lasers [8], among other purposes. Initially, they were synthesized at a temperature of 1773 K, and then single crystals were grown by the Czochralski method, as they have significantly high melting points [4]. The oxyorthosilicates obtained under these conditions crystallize in the space groups $P2_1/c$ (for the cerium subgroup) and in C2/c (for the yttrium subgroup) into a monoclinic crystal system [3–5]. Subsequently, the authors of [1] established that the oxyorthosilicates of the yttrium subgroup can also be obtained as a low-temperature modification (1173–1273 K) of nanosized polycrystals (space group $P2_1/c$). In this case, they are isostructural crystals of the cerium subgroup.

The study of luminescent properties showed that the polycrystalline oxyorthosilicate $Lu[(SiO_4)_{0.5}O_{0.5}]$:Ce had better spatial resolution and image sharpness than luminophore Gd_2O_2Si:Tb, which has been used in most medical imaging methods in the last decades [6]. This luminophore can be used in X-ray mammography for visualization in both radiographic cassettes and digital detectors. It has an excellent spectral compatibility with the currently used Si-based films

and photodiodes [7]. The luminescence intensity of a polycrystalline, nanosized lutetium oxyorthosilicate obtained by solution combustion synthesis (SCS) and excited by X-rays is significantly higher (64 ± 4) than those of gadolinium (36 ± 4) and yttrium (44.3 ± 1.5) oxyorthosilicates obtained by the same method, but it is slightly lower than those of Gd and Y single crystals (94 ± 13 and 97 ± 14 s^{-1} mg^{-1}, respectively) synthesized by the Czochralski method [9].

Luminophores derived from lutetium oxyorthosilicate ($Lu[(SiO_4)_{0.5}O_{0.5}]$) suffer from several drawbacks. First, they contain nearly 2.6% of the radioactive isotope ^{176}Lu, which undergoes beta decay and causes noise in scintillation devices. Second, lutetium is more expensive than other REEs [10].

These drawbacks can be minimized by using "mixed" oxyorthosilicates ($(Lu_{1-x}Ln_x)[(SiO_4)_{0.5}O_{0.5}]$), which contain not only lutetium but also other REEs [4, 9–12].

However, the physicochemical bases for the synthesis of "mixed" solid solutions—phase diagrams and, particularly, solubility regions of solutions based on REE oxyorthosilicates—have not been studied yet. The experimental determination of the solubility regions in a solid phase is an independent task, which requires special equipment expensive reagents, and long research periods.

Therefore, most researchers studying the luminescent properties of mixed REE oxyorthosilicates have to choose the composition of the matrices and activators either by analogy with similar systems or by trial and error.

Occasionally, researchers do not consider the fact that solid solutions synthesized at high temperatures are prone to decaying upon cooling and can change their phase compositions and properties. This can lead to the degradation of the materials that are based on these solutions in practical scenarios. Therefore, before synthesizing and studying the properties, one must evaluate the limits of isomorphous substitutions and stability of solid solutions in the corresponding systems both during their synthesis and intended use.

Accordingly, this study aims to predict the limits of substitution and stability of luminescent materials based on low-temperature modifications of solid solutions (spatial group $P2_1/c$) with lutetium oxyorthosilicates ($(Lu_{1-x}Ln_x)[(SiO_4)_{0.5}O_{0.5}]$), where Ln represents REEs.

METHODOLOGY OF CALCULATION AND INITIAL DATA

The calculations were performed within the framework of the V.S. Urusov's crystal energy theory of isomorphous miscibility [13] in regular solid solution approximation for one gram-atom number of the substituting structural units in pseudobinary ($(Lu_{1-x}Ln_x)[(SiO_4)_{0.5}O_{0.5}]$) systems.

To calculate the substitution limit (x) for a given decomposition temperature of a solid solution (T_d) or to define a decomposition temperature for a given substitution limit in the approximation of regular solutions, we used the Becker equation [14] as follows:

$$-(1-2x)/\ln[x/(1-x)] = RT_d/Q_{mix}, \quad (1)$$

where R denotes the universal gas constant and Q_{mix} the mixing energy (or interaction parameter). Equation 1 can be used in our case if the dimensional parameter of interatomic distances (the dimensional parameter is calculated using the values of the substitutable structural units or dimensions of the unit cells of the system components) does not exceed 0.1 [13, 15, 16]. In the systems under consideration, the value of the dimensional parameter, which is calculated using the volumes of unit cells as [$\delta = (V_{Ln}^{1/3} - V_{Lu}^{1/3})/V_{Lu}^{1/3}$], does not exceed 0.066 (see the table); therefore, it is expedient to apply the Becker equation. We used the volumes of unit cells in our calculation because the literature data [1, 10, 17] (pertaining to the synthesis and investigation of the properties of nanoscale low-temperature modification of $Lu[(SiO_4)_{0.5}O_{0.5}]$) did not contain the information on its structural data. The authors in [1], who described the low-temperature modifications of $Ln[(SiO_4)_{0.5}O_{0.5}]$, provided cell parameters only for the compounds of other REEs that belonged to the yttrium subgroup, and not for $Lu[(SiO_4)_{0.5}O_{0.5}]$. Therefore, the volume of the low-temperature modification of the $Lu[(SiO_4)_{0.5}O_{0.5}]$ unit cell (approximately 384 $Å^3$) was determined by extrapolating the relationship between the volumes of low-temperature modifications of $Ln[(SiO_4)_{0.5}O_{0.5}]$ unit cells, provided in [1], and the ionic radii of REEs according to R. Shannon [18] (see Fig. 1).

In the regular solution approximation, the mixing energy can be determined by the enthalpy of mixing (ΔH_{mix}) as $Q_{mix} = \Delta H_{mix}/(x_1 \times x_2)$, where x_1 and x_2 denote the mole fractions of the solvent and dissolved substance, respectively. Thus, the main task while calculating the substitution limit for a given decomposition temperature of a solid solution or while determining the decomposition temperature for a given substitution limit is to estimate the enthalpy of mixing.

Normally, the enthalpy of mixing (ΔH_{mix}) in Equation 2 proposed by V.S. Urusov [13, 15, 16] arises because of three factors: the difference among the sizes of the substituting structural units (ΔH_δ), different degrees of ionicity of the chemical bonds between the system components (ΔH_ε), and the difference in their crystal structures (ΔH_{II-I} denotes the enthalpy during the polymorphic transition from the structure of the substituting component to the structure of the substitutable component). One has the following:

Energies of mixing and critical decomposition temperatures of solid solutions $(Lu_{1-x}Ln_x)[(SiO_4)_{0.5}O_{0.5}]$

Ln	V, Å^3	δ	Q_R, J/mol	χ_{Ln}	ε	Δε	Q_ε, J/mol	Q_{mix}, J/mol	T_{cr}, K
La	465.2	0.06602	57428	1.327	0.724	0.019	585	58013	3460
Ce	455.2	0.05841	44947	1.348	0.720	0.015	365	45312	2700
Pr	445.1	0.05045	33528	1.374	0.716	0.011	196	33724	2010
Nd	439.3	0.04577	27719	1.382	0.714	0.009	131	27850	1660
Pm	431.9	0.03998	21058	1.391	0.712	0.007	79	21137	1260
Sm	424.4	0.03390	15134	1.410	0.708	0.003	15	15149	900
Eu	417.9	0.02860	10776	1.433	0.704	0.001	2	10778	640
Gd	414.0	0.02538	8484	1.386	0.712	0.007	79	8563	510
Tb	409.2	0.02141	5967	1.410	0.708	0.003	15	5982	360
Dy	404.0	0.01706	3834	1.426	0.706	0.001	2	3836	230
Ho	397.5	0.01158	1767	1.433	0.704	0.001	2	1769	100
Er	395.6	0.009961	1305	1.438	0.703	0.002	6	1311	80
Tm	389.7	0.004925	317	1.455	0.700	0.005	40	357	20
Yb	387.0	0.002600	85	1.479	0.695	0.010	162	247	10
Lu	384.0	–	–	1.431	0.705	–	–	–	–

Note: The volumes of the unit cells of cerium and promethium oxyorthosilicates are defined as the arithmetic mean of the volumes of the unit cells of lanthanum and praseodymium oxyorthosilicates, as well as of neodymium and samarium, respectively.

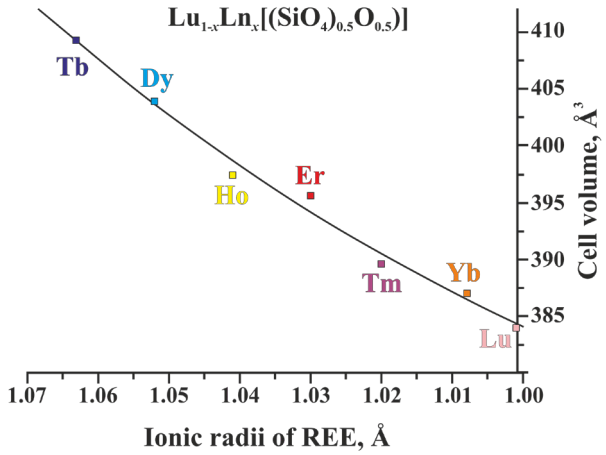

Fig. 1. Dependence of the volumes of the unit cells of low-temperature modifications of $Ln[(SiO_4)_{0.5}O_{0.5}]$ on the ionic radii of REE.

$$\Delta H_{mix} = \Delta H_\delta + \Delta H_\varepsilon + x_2\Delta H_{II-I} = Cx_1x_2mnz_mz_x\delta^2 + \\ + 1390x_1x_2mz_mz_x\alpha(\Delta\varepsilon)^2/(2r) + x_2\Delta H_{II-I} \quad (2)$$

However, to the best of our knowledge, no data in the literature pertains to the enthalpies of polymorphic transitions ΔH_{II-I} for the oxyorthosilicates of REEs. This equation can still be used for performing calculations in cases wherein the system components are isostructural (i.e., at $\Delta H_{II-I} = 0$) or wherein the amount of the dissolved substance is significantly low (at $x_1 \approx 1$ or at $x_2 << 1$) [13, 15].

While performing calculations in systems with isostructural components, the ΔH_{mix} value consists of two factors (see Equation 3): the difference in the sizes of the substituting structural units (ΔH_δ), and different degrees of ionicity of the chemical bonds between the system components (ΔH_ε). One has the following:

$$\Delta H_{mix} = \Delta H_\delta + \Delta H_\varepsilon = Cx_1x_2mnz_mz_x\delta^2 + \\ + 1390x_1x_2mz_mz_x\alpha(\Delta\varepsilon)^2/(2r), \text{ (kJ/mol)} \quad (3)$$

Therefore, the energy of mixing can also be determined as the sum of two factors as follows:

$$Q_{mix} = Q_\delta + Q_\varepsilon = Cmnz_mz_x\delta^2 + 1390mz_mz_x\alpha(\Delta\varepsilon)^2/(2r) \quad (4)$$

In this equation, C denotes a constant equal to 112.6 kJ and is calculated as $C = 20(2\Delta\chi + 1)$ [16] by using the electronegativity difference between cations and anions, $\Delta\chi$ [19–20] in a pseudobinary approximation. The term m denotes the number of formula units in the pseudobinary approximation, calculated per mole of a substitutable structural unit (1 + 0.5 + 0.5 = 2). The term n denotes the coordination number of a substitutable structural unit in the pseudobinary approximation of the structure (at the first cation position (n = 7), there are 6 SiO_4^{4-} tetrahedra and one O^{2-} ions; at the second position (n = 6), there are 3 SiO_4^{4-} tetrahedra and three O^{2-} ions; i.e., on average n = 6.5. The terms z_m and z_x denote the formal charges of the substitutable and common structural units of the components, respectively: $z_m = 3$, as $z_x = 4 \times 0.5 + 2 \times 0.5 = 3$. The term δ denotes a dimensional parameter, which is calculated for each

system using the volumes of the unit cells, as shown in [1, 21]. The term α denotes a reduced Madelung constant equal to 1.9 and is calculated by the Hoppe's formula [22] as follows: $(\alpha/n)^2 + \alpha = 1.81$, where $n = 6.5$ is a coordination number in the pseudobinary approximation of the structure. The degrees of ionicity of the chemical bond ε were determined using the electronegativity difference (Δχ) between the REE anions and cations, as provided in [19]. The χ value of the SiO_4^{4-} anion according to the recommendation provided in [20] was assumed to be equal to that of the oxide anion, i.e., 3.7 [19]. The term r denotes the average interatomic "cation–anion" distance in the pseudobinary approximation, and it was calculated for one of the previously studied structures of this structural type, i.e., $Gd[(SiO_4)_{0.5}O_{0.5}]$. The "cation–tetrahedral anion" distances for two positions of gadolinium were considered as the sum of distances (Gd–O + Si–O) and the "cation–oxygen" distance (Gd–O), not bounded to silicon [21]. In the first position: the cation was surrounded by 6 SiO_4^{4-} tetrahedral ions and 1 oxygen atom, and the average distance was [6 × (2.49 + 1.63) + 2.35]/7 = 3.86 Å. In the second position: the cation was surrounded by 3 SiO_4^{4-} tetrahedral ions and 3 oxygen atoms, and the average distance was [3 × (2.39 + 1.63) + 3 × 2.30)]/6 = 3.15 Å. The average distance between the two positions of the cation was r = 3.5 Å.

RESULTS AND DISCUSSION

Some initial data and calculations results are presented in the table. From the table, it is evident that the values of size parameter (δ) do not exceed 0.1, with the maximum value being 0.066. Consequently, according to [13], the dependence of the decomposition temperatures of solid solutions on the system composition will be almost symmetric, and the T_d values can be calculated using the Becker equation for regular solid solutions.

As the REE number increases, the contributions to the total energy of mixing Q_R consequently decreases, as explained by the decreasing difference in the size of the replacing structural units—REE ions. Their electronegativity values (χ_{Ln}) vary non-monotonically unlike their ion radii: they grow with increase in the REE number in the La–Eu series, sharply decrease during the transition to Gd, and then again increase with increase in the REE number in the Gd–Yb series. The electronegativity of Lu, as in the case of Gd, is also significantly low. Such a change in the χ_{Ln} of REEs leads to a situation wherein the differences in the degrees of ionicity of the chemical bonds vary within the range of 0.001–0.019 and do not significantly affect the total energy of mixing, which decreases with increase in the REE number. As recommended in [13], if $\Delta\varepsilon < 0.05$, the contribution of ΔH_ε to the mixing energy can be neglected.

The critical decomposition temperatures T_{cr} of the solid solutions were calculated as $T_{cr} = Q_{mix}/2kN$ [13], where k denotes the Boltzmann constant and N the Avogadro number. As can be seen from the table and Fig. 2 (curve for x = 0.50), their T_{cr} values, as expected, decrease with increase in the REE number.

Using the values of the decomposition temperatures of solid solutions calculated by the Becker equation, we plotted the dependences of the decomposition temperature on the REE number (see Fig. 2) for the substitution limits x = 0.01, 0.03, 0.05, 0.1, and 0.2. These dependences can be used to define the substitution limit for lutetium, replaced by REE, based on the given temperature or to calculate the decomposition temperature by using the substitution limit [23–24]. In the first case, we must draw an isotherm from the given temperature to the intersection with the vertical line of this REE. From the point of the intersection, one can estimate the range of x values, within which the substitution limit is located. The substitution limit should be refined by interpolating the vertical segment between the decomposition temperature and REE number dependences, which are the closest to the intersection points. In the second case, the position of a point on the vertical line of given REE is determined by its composition, after which a horizontal line is drawn up to the intersection with the temperature axis. These problems can be solved more precisely by plotting the dependence of the decomposition temperature of the solid solution on the composition (x) for each system by using the Becker equation.

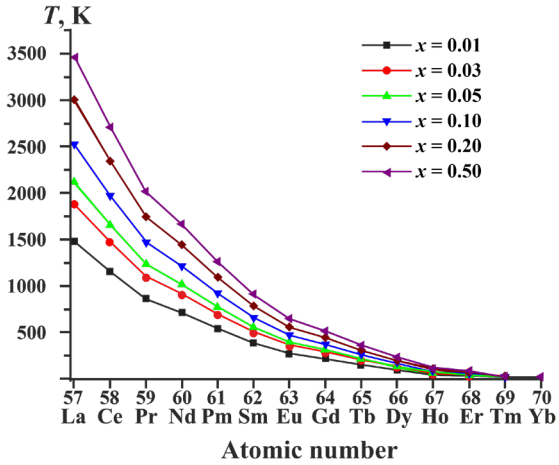

Fig. 2. Thermodynamic stabilities of the solid solutions of $(Lu_{1-x}Ln_x)[(SiO_4)_{0.5}O_{0.5}$ systems.

However, in contrast with the previously described systems [23–24], the component $Lu[(SiO_4)_{0.5}O_{0.5}]$, which serves as a basis for solid solution formation, undergoes a polymorphic transition from the $P2_1/c$ space group to C2/c at 1173 K in the case of synthesis by the sol–gel method [1], or at 1273 K in the case of synthesis by SCS [10, 17]. This affects the phase relationships in the systems. At the synthesis temperature or operation temperature lower

than the temperature of the polymorphic transition of $Lu[(SiO_4)_{0.5}O_{0.5}]$, both the components in the systems are isostructural, and the results can be used both to select the ratio of components in solid solutions and the number of activators.

However, if the synthesis temperature or operating temperature exceeds the temperature of the polymorphic transition of $Lu[(SiO_4)_{0.5}O_{0.5}]$, a complete miscibility does not work, as the oxyorthosilicates of the cerium subgroup, unlike $Lu[(SiO_4)_{0.5}O_{0.5}]$, do not undergo a polymorphic transition to a structure with the C2/c space group, and the calculation results without regard to the enthalpy of polymorphic transition may be incorrect. Simultaneously, when choosing the amount of the activator to be introduced at low substitution rates (usually from a fraction of percent to several percent), the contribution of the enthalpy of polymorphic transition to the enthalpy of mixing will be negligible, and the calculation results in this case can be considered indubitable.

Noteworthily, when choosing the conditions for obtaining solid solutions, one should consider that the temperatures of the polymorphic transitions of REE oxyorthosilicates exceed the temperatures of their synthesis by the sol–gel method by only 50–75 K [1], thereby requiring highly accurate temperature regulation.

From the diagram, one can estimate the regions of thermodynamic stability of solid solutions. Thus, at $T > T_{cr}$ (i.e., in the region above the curve for $x = 0.50$, see Fig. 2) the unbounded solid solutions, synthesized at temperatures below the polymorphic transition temperatures, are thermodynamically stable over the entire concentrations range, i.e., $0 < x < 1$. However, in the region below the curve for $x = 0.50$ ($T < T_{cr}$), the unbounded solid solutions are thermodynamically unstable and can decay into phases with partial miscibility. Similarly, the solid solutions with $x = 0.01$, 0.03, 0.05, 0.10, and 0.20 are thermodynamically stable in the regions above the curves but are unstable in the regions below them.

With decrease in the temperature, the structural units of a solid solution become less mobile owing to the decrease in the diffusion rate while the solubility regions become smaller [13]. This phenomenon proceeds until the diffusion rate becomes so low that the solubility regions practically stop decreasing, meaning that spontaneous hardening occurs and solid solutions become metastable. If we assume that the quenching temperature is close to the minimum temperature at which the components in the solid phase start interacting and thus forming a solid solution, then we can estimate the temperature of spontaneous hardening and the region of metastability in the system. REE oxyorthosilicates and solid solutions based on them are usually synthesized at temperatures ranging from 1773 K (using the conventional solid phase method with oxides of the corresponding elements as initial reagents [5]) to 1173 K (using the sol–gel method [1]). The latter agrees with the Tammann's rule, according to which the structural units during heating begin to interact in a mixture of solids at a temperature approximately 50% of the melting point [25]. Below the Tammann temperature, the mobility of the structural units is so low that the formation or decomposition of the solid solutions does not occur. Considering that the melting points of REE oxyorthosilicates range from 2170 K to 2320 K [26], one can assume that when solid solutions cool down to the temperature below ~1173 K, the mobility of the structural units will be insufficient for the thermodynamically unstable solid solutions to decompose; i.e., the solid solutions will become metastable.

Therefore, in $(Lu_{1-x}Ln_x)[(SiO_4)_{0.5}O_{0.5}]$ systems containing REEs from La to Nd, the solid solutions, which are thermodynamically stable at temperatures above the critical temperature (3460–1660 K, see the table and Fig. 2), become thermodynamically unstable and can decay when the temperature decreases within the range between T_{cr} and ~1173 K. This occurs if the diffusion rate and time are sufficient for the stable nuclei of a new phase to emerge and start growing. At temperatures below 1173 K, the solid solutions will not decay, meaning that spontaneous hardening occurs and the solid solutions become metastable.

In systems containing REEs from Sm to Yb, the critical decomposition temperatures (900–10 K) are significantly lower than the Tammann temperature; therefore, unbounded solid solutions do not decay upon cooling and are stable at temperatures higher than the critical temperatures and metastable at temperatures lower than the critical temperatures.

The difference between the critical temperature in a system with Pm (1260 K) and the spontaneous quenching temperature (~1173 K) is close to the calculation error (±100 K); therefore, it becomes difficult to predict the decomposition temperature of an unbounded solid solution in this system.

To the best of our knowledge, the literature contains no data pertaining to the energies of mixing and the limits of substitution of lutetium by REEs for solid solutions of REE oxyorthosilicates with partial miscibility of components. Therefore, it becomes difficult to assess the validity of the calculations performed. However, there are data on the compositions and temperatures during the synthesis of solid solutions $(Lu_{1-x}Ce_x)[(SiO_4)_{0.5}O_{0.5}]$, where $x = 0.01$ at 1273 K [27] and $x = 0.02$ at 1373 K [28]. The graphical dependence of the calculated decomposition temperatures of the solid solutions $(Lu_{1-x}Ce_x)[(SiO_4)_{0.5}O_{0.5}]$ on the mole fraction of Ce (see

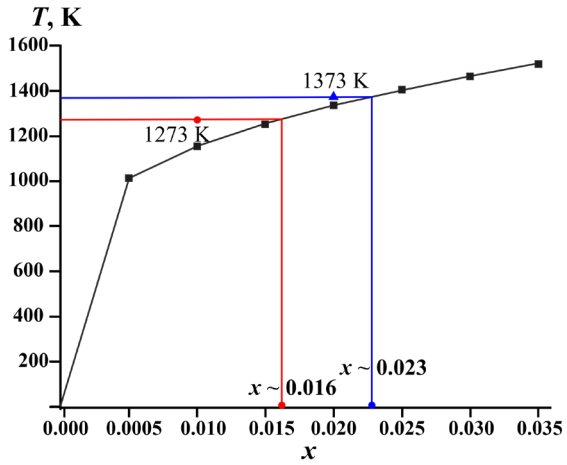

Fig. 3. Fragment of the dependence of the calculated decomposition temperatures of the solid solutions in the $(Lu_{1-x}Ce_x)[(SiO_4)_{0.5}O_{0.5}]$ system on the mole fraction of Ce. Also presented are the experimental data for the compositions wherein $x = 0.01$ at 1273 K [26] and $x = 0.02$ at 1373 K [28].

Fig. 3) shows that when $x = 0.01$ at 1273 K [27] or/and $x = 0.02$ at 1373 K [28], the calculation results do not contradict the experimental data. This means that these solid solutions are in the region of thermodynamic stability as predicted by us. Both the compositions of the $(Lu_{1-x}Ce_x)[(SiO_4)_{0.5}O_{0.5}]$ system, i.e., with $x = 0.01$ and $x = 0.02$, synthesized at 1273 and 1373 K [27–28], are located in the regions of solid solutions, which, according to the calculation results, extend to $x = 0.016$ and $x = 0.023$, respectively, at these temperatures.

CONCLUSIONS

A crystallochemical approach in the regular solution approximation was used to calculate the energies of mixing (interaction parameters) of solid solutions, which were based on the low-temperature modification of lutetium oxyorthosilicate $Lu[(SiO_4)_{0.5}O_{0.5}]$ and modified with REEs for compositions with $x = 0.01$, 0.03, 0.05, 0.10, 0.20, and 0.5. With increase in the REE number, the calculated energies of mixing and the critical decomposition temperatures of the solid solutions decreased, as explained by the decrease in the REE ionic radii in the series from La to Yb. It was shown that the contribution of a system component to the energy of mixing, caused by the difference in the sizes of the substituting structural units, was significantly greater than the one caused by the differences in the degrees of ionicity of the chemical bonds in the components, and hence the latter could be neglected.

The thermodynamic stability diagrams of $(Lu_{1-x}Ln_x)[(SiO_4)_{0.5}O_{0.5}]$ systems were shown, allowing to estimate not only the stability of solid solutions in a wide range of compositions and temperatures, but also to determine the substitutions limits for a bounded series of solid solutions at a given decomposition temperature or calculate the decomposition temperature at a given substitution limit.

In $(Lu_{1-x}Ln_x)[(SiO_4)_{0.5}O_{0.5}]$ systems containing REEs from La to Nd, the solid solutions, which are thermodynamically stable at temperatures above the critical decomposition temperatures 3460–1660 K, become thermodynamically unstable and can decay to form the bounded regions of solid solutions at temperatures between T_{cr} and ~1173 K. Below ~1173 K, they do not decay and are metastable.

In systems containing REEs from Sm to Yb, the critical decomposition temperatures (900–10 K) are significantly lower than ~1173 K; therefore, unbounded solid solutions do not decay upon cooling and remain stable at temperatures higher than the critical ones and metastable at temperatures lower than the critical ones.

The calculation results for the $(Lu_{1-x}Ce_x)[(SiO_4)_{0.5}O_{0.5}]$ system did not contradict with the experimental data obtained earlier by instrumental investigation methods for solid solutions wherein $x = 0.01$ at 1273 K and $x = 0.02$ at 1373 K [26–27]. This means that these solid solutions are located in the region of thermodynamic stability as predicted by us.

Financial support

This study was supported by the Fundamental Research Program funded by the Ministry of Education and Science of Ukraine (Projects Nos. 0119U100025 and 0120U102059).

Authors' contribution

All authors equally contributed to the research work.

The authors declare no conflicts of interest.

REFERENCES

1. Wang J., Tian S., Li G., Liao F., Jing X. Preparation and X-ray characterization of low-temperature phases of R_2SiO_5 (R = rare earth elements). *Mater. Res. Bull.* 2001;36(10):1855-1861. https://doi.org/10.1016/S0025-5408(01)00664-X

2. Liu Y., Xu C.N., Nonaka K., Tateyama H. Strong blue, green and red light emission at elevated temperatures from Y_2SiO_5 doped by the rare-earth ions. *J. Mater. Sci.* 2001;36:4361-4364. https://doi.org/10.1023/A:1017953913334

3. Loutts G., Zagumennyi A., Lavrishchev S., Zavartsev Yu., Studenikin P. Czochralski growth and characterization of $(Lu_{1-x}Gd_x)_2SiO_5$ single crystals for scintillators. *J. Cryst. Growth.* 1997;174(1-4):331-336. https://doi.org/10.1016/S0022-0248(96)01171-2

4. Dominiak-Dzik G., Ryba-Romanowski W., Lisiecki R., Solarz P., Macalik B., Berkowski M., Gzowacki M., Domukhovski V. The Czochralski Growth of $(Lu_{1-x}Gd_x)_2SiO_5$:Dy Single Crystals: Structural, Optical, and Dielectric Characterization. *Cryst. Growth Des.* 2010;10(8):3522-3530. https://doi.org/10.1021/cg100429b

5. Glowacki M., Dominiak-Dzik G., Ryba-Romanowski W., Lisiecki R., Strzep A., Runka T., Drozdowski M., Domukhovski V., Diduszko R., Berkowski M. Growth conditions, structure, Raman characterization and optical properties of Sm-doped $(Lu_xGd_{1-x})_2SiO_5$ single crystals grown by the Czochralski method. *J. Solid State Chem.* 2012;186:268-277.
https://doi.org/10.1016/j.jssc.2011.12.021

6. Michail C., David S., Liaparinos P., Valais I., Nikolopoulos D., Kalivas N., Toutountzis A., Cavouras D., Kandarakis I., Panayiotakis G. Evaluation of the imaging performance of LSO powder scintillator for use in X-ray mammography. *Nucl. Instrum. Methods Phys. Res., Sect. A.* 2007;580(1):558-561.
https://doi.org/10.1016/j.nima.2007.05.234

7. Michail C.M., Fountos G.P., David S.L., Valais I.G., Toutountzis A.E., Kalyvas N.E., Kandarakis I.S., Panayiotakis G.S. A comparative investigation of Lu_2SiO_5:Ce and Gd_2O_2S:Eu powder scintillators for use in X-ray mammography detectors. *Meas. Sci. Technol.* 2009;20(10):104008.

8. Zheng L., Su L., Xu J. Growth and Characterization of Ytterbium Doped Silicate Crystals for Ultra-Fast Laser Applications. *Modern Aspects of Bulk Crystal and Thin Film Preparation.* 2012;25-42.
https://doi.org/10.5772/30457.
Available from: https://www.intechopen.com/books/modern-aspects-of-bulk-crystal-and-thin-film-preparation/growth-and-characterization-of-ytterbium-doped-silicate-crystals-for-ultra-fast-laser-applications

9. Yukihara E.G., Jacobsohn L.G., Blair M.W., Bennett B.L., Tornga S.C., Muenchausen R.E. Luminescence properties of Ce-doped oxyorthosilicate nanophosphors and single crystals. *J. Lumin.* 2010;130(12):2309-2316.
https://doi.org/10.1016/j.jlumin.2010.07.010

10. Głowacki M.M. *Właściwości optyczne i strukturalne krzemianow ziem rzadkich i ich roztworow stałych. Praca doktorska* (Optical and structural properties of rare-earth silicates and their solid solutions. Doctoral thesis). Warszawa: Instytut Fizyki Polskiej Akademii Nauk; 2012. 1-102 (in Polish).

11. Ryba-Romanowski W., Strzęp A., Lisiecki R., Berkowski M., Rodriguez-Rodriguez H., Martin I. R. Effect of substitution of lutetium by gadolinium on emission characteristics of $(Lu_xGd_{1-x})_2SiO_5:Sm^{3+}$ single crystals. *Opt. Mater. Express.* 2014;4(4):739-752.
https://doi.org/10.1364/OME.4.000739

12. Kurtsev D.O. Obtaining of efficient scintillators based on $Lu_{2x}Gd_{2-2x}SiO_5$:Ce (LGSO:Ce) crystals. PhD Manuscript. Kharkiv: Institute for Single Crystals of NAS of Ukraine; 2016. (In Ukrainian).

13. Urusov V.S. *Teoriya izomorfnoi smesimosti* (Theory of isomorphous miscibility). Moscow: Nauka; 1977. 251 p. (in Russ.).

14. Becker R. Über den Aufbau binarer Legierungen. *Z. Metallkunde.* 1937;29:245-249 (in German).

15. Urusov V.S. Energetic theory of miscibility gaps in mineral solid solutions. *Fortschr. Mineral.* 1975;52:141-150.

16. Urusov V.S., Tauson V.L., Akimov V.V. *Geokhimiya tverdogo tela* (Geochemistry of solid state). Moscow: GEOS; 1997. 500 p. (in Russ.). ISBN 5-89118-012-X

17. Muenchausen R.E., McKigney E.A., Jacobsohn L.G., Blair M.W., Bennett B.L., Wayne Cooke D. Science and Application of Oxyorthosilicate Nanophosphors. *IEEE Transactions on Nuclear Science.* 2008;55(3):1532-1535.
https://doi.org/10.1109/TNS.2008.922844

18. Shannon R.D. Revised effective ionic radii and systematic studies of interatomic distances in halides and chalcogenides. *Acta Crystallographica Section A.* 1976;32(5):751-767.
https://doi.org/10.1107/S0567739476001551

19. Li K., Xue D. Estimation of Electronegativity Values of Elements in Different Valence States. *J. Phys. Chem. A.* 2006;110(39):11332-11337.
https://doi.org/10.1021/jp062886k

20. Batsanov S.S. The Concept of Electronegativity. Conclusions and Prospects. *Russ. Chem. Rev.* 1968;37(5):332-351.
http://dx.doi.org/10.1070/RC1968v037n05ABEH001639

21. Felsche J. The crystal chemistry of the rare-earth silicates. In: Rare Earths. Structure and Bonding. 1973;13:99-197. Berlin, Heidelberg: Springer.
https://doi.org/10.1007/3-540-06125-8_3

22. Hoppe R. Madelung Constants as a New Guide to the Structural Chemistry of Solids. *Adv. Fluor. Chem.* 1970;6:387-438.

23. Get'man E.I., Radio S.V. Mixing Energies (Interaction Parameters) and Decomposition Temperatures in Solid Solutions of Monazites of Rare Earth Elements with Structure $La_{1-x}Ln_xPO_4$. *Inorg. Mater.* 2017;(53)7):718-721.
https://doi.org/10.1134/S0020168517070044

24. Get'man E.I., Radio S.V., Ardanova L.I. Predicting the Phase Stability of $Sc_{1-x}Ln_xPO_4$ (Ln = Gd–Lu, Y) Zircon-Structured Solid Solutions. *Inorg. Mater.* 2018;54(6):596-600.
https://doi.org/10.1134/S0020168518060031

25. Garner W.E. Chemistry of the Solid State. London: Butterworths Scientific Publications; 1955. 417 p.

26. Grynyov B., Ryzhikov V., Kim J.K., Jae M. Scintillator Crystals, Radiation Detectors & Instruments on Their Base. Kharkiv, Ukraine: Nat. Acad. of Sciences of Ukraine; 2004. 374 p.

27. Fan L., Jiang M., Lin D., Zhou D., Shi Y., Wu Y., Yao H., Xu F., Xie J., Lei F., Zhang L., Zhang J. Densification of cerium-doped lutetium oxyorthosilicate scintillation ceramics by hot isostatic pressing. *J. Alloys Compd.* 2017;720:161-168.

28. Xie J., Zhang F., Shen S., Lin D., Fan L., Zhang L., Lei F., Shi Y., Liu P. Luminescent properties study of $Lu_2SiO_5:(Ce^{3+}, Tb^{3+})$ optical films prepared by sol-gel method. In: Proc. SPIE 9796, Selected Papers of the Photoelectronic Technology Committee Conferences held November 2015, 97960T (26 January 2016).
https://doi.org/10.1117/12.2228576

About the authors:

Eugeni I. Get'man, Dr. of Sci. (Chemistry), Full Professor at the Department of Inorganic, Organic, and Analytical Chemistry, Faculty of Chemistry, Biology, and Biotechnologies, Vasyl' Stus Donetsk National University, (21, vul. 600–richchia, Vinnytsia, 21021, Ukraine). E-mail: ie.getman@donnu.edu.ua, gtmn@i.ua. Scopus Author ID 6602738183, https://orcid.org/0000-0002-7665-556X

Yuliia A. Oleksii, Master Student, Laboratory Assistant of the Educational-Scientific Laboratory of Special Research Methods in Analytical Chemistry, Faculty of Chemistry, Biology, and Biotechnologies, Vasyl' Stus Donetsk National University (21, vul. 600–richchia, Vinnytsia, 21021, Ukraine). E-mail: oleksii.i@donnu.edu.ua. https://orcid.org/0000-0002-7328-6674

Serhii V. Radio, Cand. of Sci. (Chemistry), Head of the Department for Research, Associate Professor at the Department of Inorganic, Organic, and Analytical Chemistry, Faculty of Chemistry, Biology, and Biotechnologies, Vasyl' Stus Donetsk National University (21, vul. 600–richchia, Vinnytsia, 21021, Ukraine). E-mail: radio@donnu.edu.ua. Scopus Author ID 12765904800, ResearcherID P-9022-2017, https://orcid.org/0000-0001-9808-0392

Lyudmyla I. Ardanova, Associate Professor at the Department of Biochemistry, Chemistry, and Geology, Minnesota State University, Mankato (241 Ford Hall, Mankato, Minnesota, 56001, USA). E-mail: lyudmyla.stackpool@mnsu.edu, lyuda111711@yahoo.com. Scopus Author ID 7801510561, https://orcid.org/0000-0002-8562-3113

Об авторах:

Гетьман Евгений Иванович, доктор химических наук, профессор кафедры неорганической, органической и аналитической химии факультета химии, биологии и биотехнологий Донецкого национального университета им. Васыля Стуса (Украина, 21021, Винница, ул. 600-летия, 21). E-mail: ie.getman@donnu.edu.ua, gtmn@i.ua. Scopus Author ID 6602738183, https://orcid.org/0000-0002-7665-556X

Олексий Юлия Анатольевна, магистрант, лаборант образовательно-научной лаборатории специальных методов исследования в аналитической химии факультета химии, биологии и биотехнологий Донецкого национального университета им. Васыля Стуса (Украина, 21021, Винница, ул. 600-летия, 21). E-mail: oleksii.i@donnu.edu.ua. https://orcid.org/0000-0002-7328-6674

Радио Сергей Викторович, кандидат химических наук, заведующий научно-исследовательской частью, доцент кафедры неорганической, органической и аналитической химии факультета химии, биологии и биотехнологий Донецкого национального университета им. Васыля Стуса (Украина, 21021, Винница, ул. 600-летия, 21). E-mail: radio@donnu.edu.ua. Scopus Author ID 12765904800, ResearcherID P-9022-2017, https://orcid.org/0000-0001-9808-0392

Арданова Людмила Ивановна, профессор кафедры химии и геологии, Государственный университет Миннесоты, Манкейто (США, 56001, Миннесота, Манкейто, Форд Холл, 241). E-mail: lyudmyla.stackpool@mnsu.edu, lyuda111711@yahoo.com. Scopus Author ID 7801510561, https://orcid.org/0000-0002-8562-3113

The text was submitted by the authors in English.
Edited for English language and spelling by Enago, an editing brand of Crimson Interactive Inc.

The article was submitted: October 09, 2020; approved after reviewing: October 19, 2020; accepted for publication: October 26, 2020.

MIREA – Russian Technological University
78, Vernadskogo pr., Moscow, 119454, Russian Federation.
Publication date *October 31, 2020.*
Not for sale

МИРЭА – Российский технологический университет
119454, РФ, Москва, пр-кт Вернадского, д. 78.
Дата опубликования *31.10.2020*
Не для продажи